DESIGN VERIFICATION OF A DIAPHRAGM WALL WITH STEEL PILES

by

Jeffrey Scott Sedey

Thesis submitted to the Faculty of the
Virginia Polytechnic Institute and State University
in partial fulfillment of the requirements for the degree of

MASTER OF SCIENCE

in

Civil Engineering

APPROVED:

R. M. Barker, Chairman

J. M. Duncan

D. A. Garst

January 1993
Blacksburg, Virginia

ABSTRACT

Design Verification of a Diaphragm Wall with Steel Piles

by

Jeffrey Scott Sedey

Committee Chairman: Richard M. Barker

Civil Engineering

(Abstract)

A study was conducted to verify the design of a diaphragm wall with steel piles. The original design was based on analysis performed on a soil-structure interaction program using soil parameters calibrated in a previous study. Original and "as-built" design models were compared to measured results of the constructed structure.

A second study was conducted to identify the sensitivity of moments and deflections to changes in wall stiffness and soil stiffness. A comparison of the effects of these changes was provided.

ACKNOWLEDGEMENTS

The author wishes to express his sincere gratitude to his advisor, Dr. Richard M. Barker, for his guidance during development of the thesis, and for his counsel throughout the year. Also, the author thanks Dr. J. M. Duncan and Prof. D. A. Garst for serving as thesis committee members.

The author appreciates the trust and confidence entrusted in him by the U.S. Army Corps of Engineers whose sponsorship for long-term training has made all of this possible.

Finally, the author wishes to give thanks to all of those who have contributed to his success, especially Mr. F. John Etzel for his continued support providing information necessary for the successful completion of this thesis. To Ms. Cathy Barker for her dedicated typing during a very compressed time period. And to my family and my friends, especially Ms. Carol Bendinelli, Mr. Bruce Queen, and Mr. Budi Widjaja for their friendship, support and wisdom. To all of you, thank you.

TABLE OF CONTENTS

LIST OF FIGURES

LIST OF TABLES

CHAPTER I

INTRODUCTION

1.1 Background

At the Bonneville Navigational Lock and Dam on the Columbia River near Portland, Oregon, the U.S. Army Corps of Engineers has designed both reinforced concrete and steel pile diaphragm walls for construction of a second navigational lock (Figure 1.1). Because of the close proximity to the Union Pacific Railroad's main transcontinental rail line, controlling lateral deflection and vertical settlement of the rail line is of primary importance. In an earlier construction phase of the project, a reinforced concrete diaphragm wall was constructed within 50 feet of the railroad. This temporary tieback wall is supported by steel strand tieback anchors and is keyed into bedrock at the base. It is instrumented to evaluate lateral deflections and internal stresses during all stages of excavation and installation of tiebacks.

A diaphragm wall is a reinforced concrete or concrete and steel pile retaining wall. It retains soils in the same manner as a soldier-pile wall, allowing excavation and installation of tiebacks on one side. However, diaphragm walls can develop

much higher strengths and stiffness than a soldier pile wall. They can also be watertight. It is for these reasons that a diaphragm wall was selected for use at the Bonneville project for the temporary tieback wall. Diaphragm walls will also be used at other sites on the project with similar requirements.

The loading chosen as the basis for the design of the temporary tieback wall was a combination of rectangular and triangular "at-rest" lateral pressure diagrams. The magnitude of the pressure diagram was based on NAVFAC D.M. 7.2 (1982). The wall was subsequently analyzed by a plane frame program. However, this analysis does not account for lateral deflections based on extension of the anchorage, nor for the stiffness properties of the soils. Therefore, a soil-structure interaction (SSI) analysis using non-linear Winkler spring supports was utilized and a parametric study performed to match the performance of the temporary tieback wall. A finite element analysis study was also performed to evaluate the design, and to support the soil-structure interaction model developed. This relatively simple soil-structure interaction model is to be used as a basis for the design of permanent walls in later phases of construction of the project.

The purpose of this research study is to verify the design of one of the permanent walls known as a guard wall. The guard wall is a tied-back concrete diaphragm wall with steel piles. Its design is based upon the soil-structure interaction model developed for the temporary tieback wall. Deflections and moments based

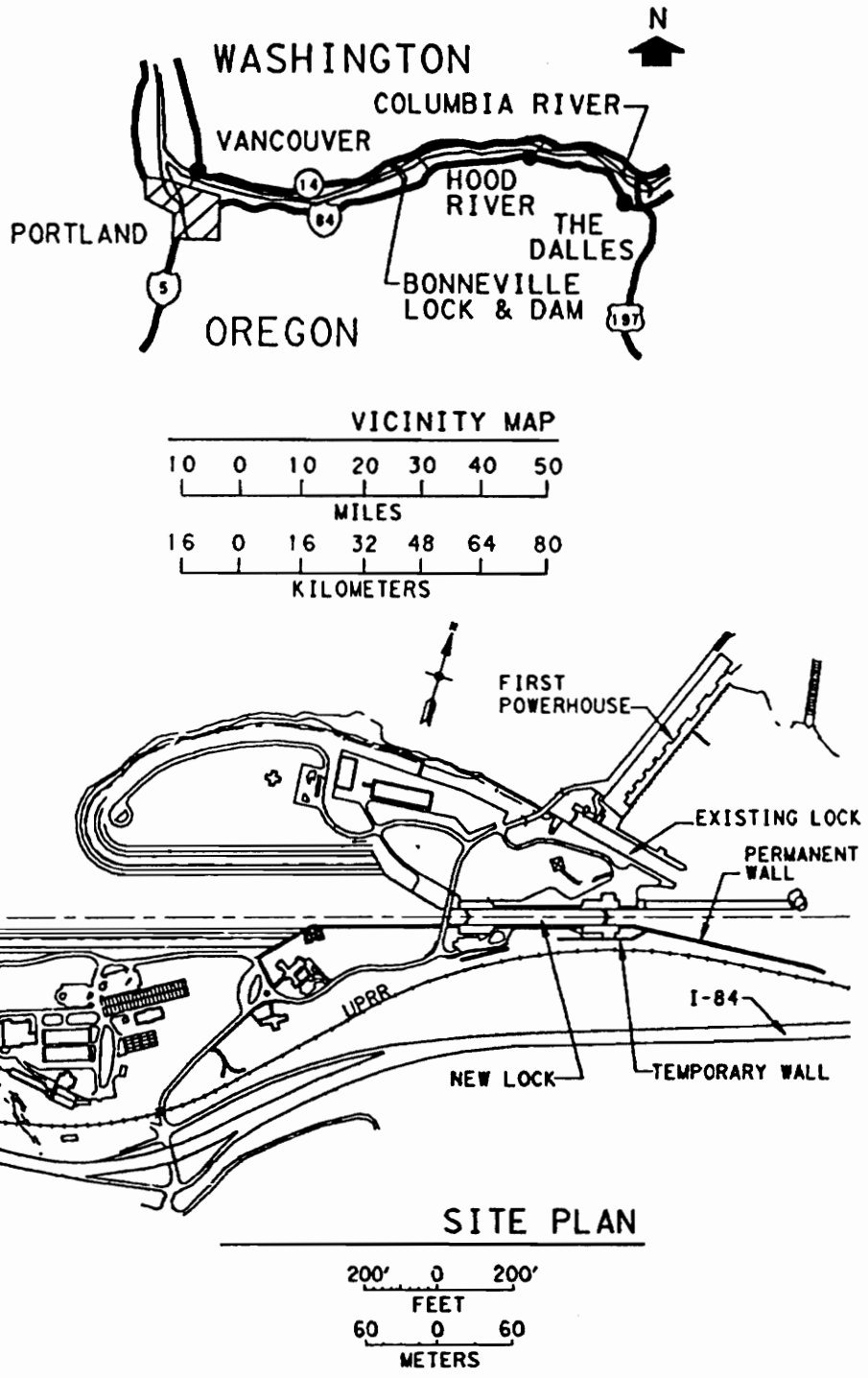

Figure 1.1 Vicinity Map and Site Plan (from Munger, Jones, and Johnson, 1990).

on instrumentation in the guard wall will be compared to the predicted values of the soil-structure interaction program.

A sensitivity study will also be conducted to identify the sensitivity of bending moments and deflections to changes in wall stiffness and soil stiffness.

1.2 Literature Review

Several performance evaluations of tied-back diaphragm walls have been published. Clough, Weber and Lamont (1972) used finite element analysis (FEA) to analyze the response of two diaphragm walls and a soldier-pile wall in overconsolidated clays proposed for a site in Seattle, Washington. Each analysis predicted a satisfactory performance of the wall, therefore the soldier-pile wall was selected based on economy. Although the actual performance of a diaphragm wall will not be known for that site the authors pointed out that the analysis of the stiffer diaphragm wall predicted a reduced lateral deflection from 2.0 inches to 1.5 inches. A post-construction analysis of the soldier-pile wall was performed to model as-constructed conditions. Comparison of the observed behavior with that predicted by analysis indicated a reasonable agreement.

Cunningham and Fernandes (1972) discussed measured ground movements of two diaphragm walls built in Chicago. However, no analysis technique was

mentioned. Caliendo, Anderson and Gordon (1990) performed a finite element analysis of a tied-back soldier pile wall using the computer program SOILSTRUCT. This analysis was compared with the observed performance of the soldier pile wall and good correlation was found between the analysis by SOILSTRUCT and the observed performance. However, this was not a diaphragm wall.

Kerr and Tamaro (1990) provide a parametric study of the effects of wall stiffness and subgrade modulus on bending moment and strut loads. They indicate that the wall stiffness, EI, appears to require adjustment for cracked moments of inertia, but that it was not as important for calculation of moments as originally thought. A summary of the results indicates that a reduction in EI by ½ caused an increase in maximum deflection by 48%, but a reduction of EI by ½ did not have a significant impact on moments. They also indicate very minor effects on moment when the soil stiffness and EI for the wall are analyzed at full value and compared to an analysis where both are reduced by ½. The increase in maximum moment was less than 2%. The increase in maximum deflection was 100%. When only the soil stiffness was reduced by ½, the moment increase was less than 4%, but the deflection increase was 22%. Their study did not compare predicted performances with measured performances of a diaphragm wall. The parametric study was conducted by a beam on elastic foundation approach. An analysis using an equivalent beam on rigid supports and an analysis using Terzaghi and Peck (1967) apparent pressure

diagrams were also conducted and moments and strut loads were compared to those evaluated in the parametric study. Neither of the latter two methods compared lateral deflections.

Munger, Jones and Johnson (1990) is one of only two published studies found that presents a parametric study and compares it with field performance of a diaphragm wall. The parametric study was performed on a soil-structure interaction beam-column analysis program known as CBEAMC. This program, developed for use by the U.S. Army Corps of Engineers, utilizes non-linear Winkler spring supports, and may be used to analyze beams on elastic foundations. The design of the guard wall that is to be verified in this thesis is based on this parametric study. Another parametric study on SOILSTRUCT was performed by Mosher and Knowles (1989) to confirm the results of the CBEAMC study. Both studies will be discussed in Chapter II.

1.3 Scope of Research

The purpose of this study is three-fold: (1) review and discuss the "design calibration" performed in 1988 by Munger, et al (1990) and supported by Mosher and Knowles (1989), (2) evaluate and compare the observed performance of the guard

wall with that of the predicted performance based on the calibrated model, and (3) perform a sensitivity study over a range of wall stiffness, EI.

The design calibration was based on the parameter study by Munger, et al (1990) for use in a soil-structure interaction beam-column analysis program. This established the basis on which the permanent diaphragm walls at the Bonneville project were analyzed and designed. The study by Munger, et al (1990) and the support study by finite element analysis methods by Mosher and Knowles 1989) will be reviewed and discussed in depth in Chapter II, Design Calibration.

The evaluation and comparison of predicted and observed performances is presented in Chapter III, Design Verification. During design of the guard wall, a doubling of the soil-stiffness was recommended. After a check of the worst load case, it was decided not to evaluate all load cases based on the increased soil modulus because the pile size would not change, and time would not permit evaluating non critical load cases. In this study, the soil stiffness will be matched to the recommended value and its prediction also compared to the observed performance.

In Chapter IV, the sensitivity of wall stiffness, EI, and its influence on predicting moments and deflections is evaluated. Finally, Chapter V provides conclusions and recommendations on the verification of the design of the diaphragm wall and for the sensitivity study.

CHAPTER II

DESIGN CALIBRATION

2.1 General

The new lock under construction at Bonneville was planned for construction in several stages or phases. Phase One moved the railroad line to the south of its existing alignment and out of the channel area of the new lock. Phase Two of construction was to excavate a major portion of the bedrock and overburden into which the lock structure itself was to be located. One part of Phase Two was to construct temporary tieback walls to retain soils supporting the realigned railroad. A diaphragm wall (the temporary tieback wall) was chosen for its strength and rigidity, and because it was not feasible to layback slopes to construct other types of retaining walls without interrupting rail service (Figure 2.1).

Phase Three is construction of the main lock structure itself, excavation of upstream and downstream entrance channels, and construction of the retaining structures supporting soils adjacent to these channels. One set of retaining walls adjacent to the upstream channel is known as the guard wall (Figure 2.2). On the

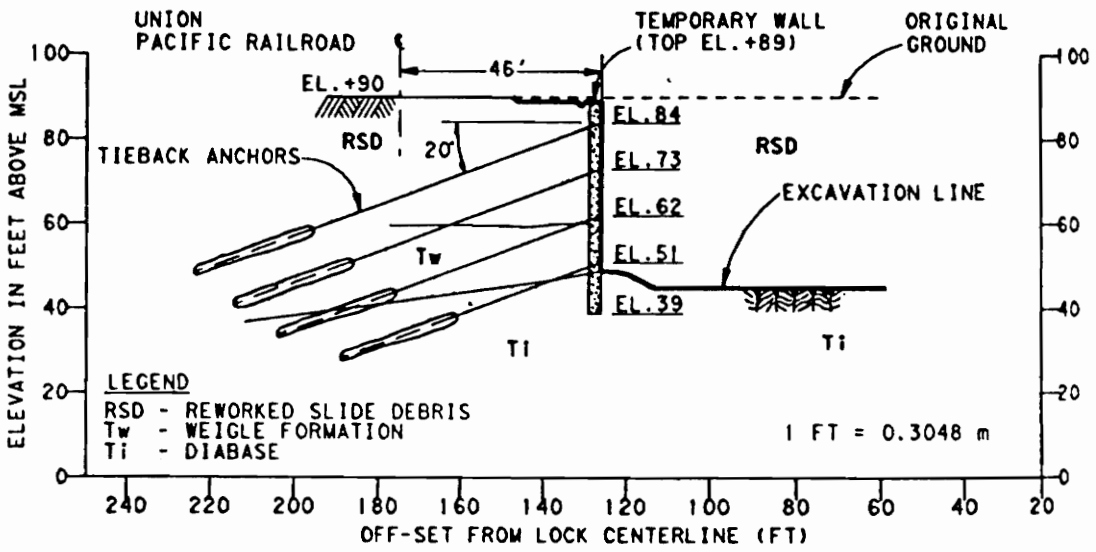

Figure 2.1 Temporary Tieback Wall Section (from Munger, Jones, and Johnson, 1990).

river side, the guard wall faces the lock channel with an "exposed" height of up to 70 feet. Most of this exposed wall is actually submerged below the river surface with only 3 to 10 feet above the water surface. For accessibility, only one row of permanent tieback anchors in the top of the guard wall was feasible. On the soil side of the wall, within as little as 50 feet, is the newly aligned railroad. Because of the location of the permanent tiebacks at the top and the height of the exposed face, the guard wall required a diaphragm wall using large steel piles closely spaced to develop the required strength and maintain lateral deflections.

The guard wall consists of approximately 108,000 ft^2 of slurry constructed wall for a length of approximately 1000 feet along the lock channel. This 1000 feet of wall is divided into five distinct areas for design based on changing geological conditions or on an increase of the exposed height due to deepening of the adjacent channel. Additionally, as many as eight different load cases for each section of wall needed consideration. Again, because of the close proximity of the railroad, lateral deflections of the guard wall was of concern during design. Therefore, it was decided that the analysis and design of the guard wall be based on a soil-structure interaction (SSI) program capable of estimating lateral deflections. One such soil-structure interaction beam-column analysis program was developed by W. P. Dawkins (1982) for the U.S. Army Corps of Engineers and is known as CBEAMC. CBEAMC is a one-dimensional SSI program for analyzing beams on elastic foundations utilizing

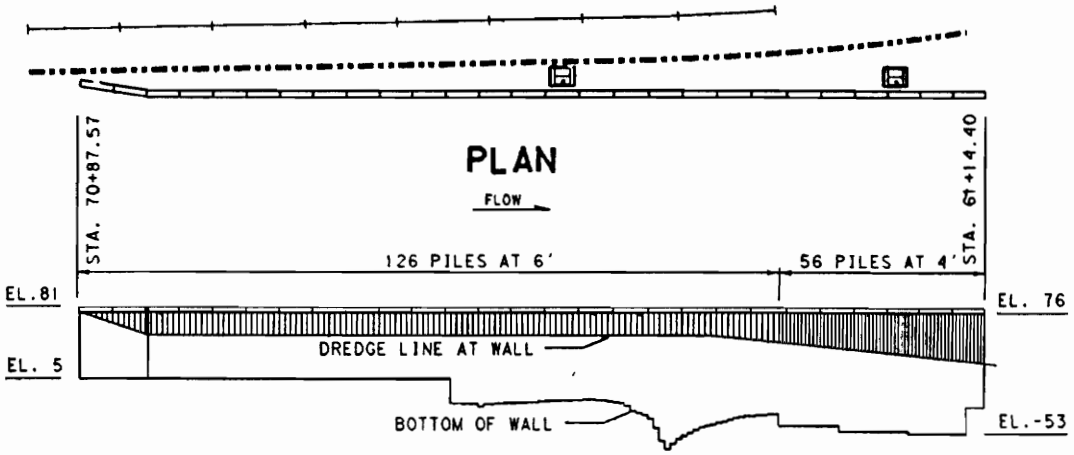

ELEVATION

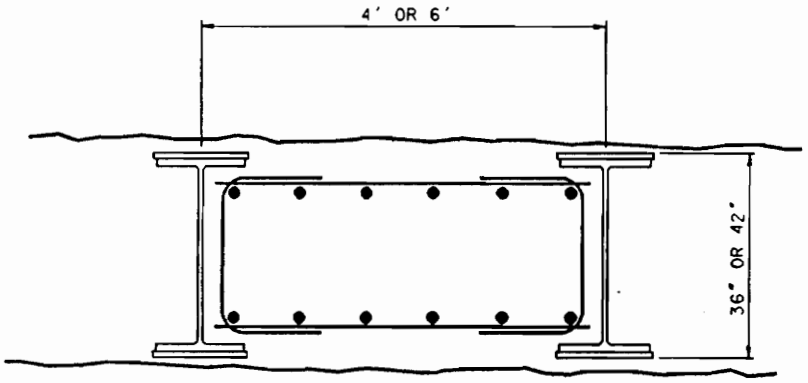

TYPICAL SECTION

(PILE WITH AND WITHOUT COVERPLATES)

Figure 2.2 Guard Wall Plan, Elevation, and Typical Section.

non-linear Winkler spring supports for modeling the soil load-deflection response. This program is relatively simple to use, making it preferred over a finite element analysis program which can be quite complex.

A CBEAMC analysis of the temporary tieback wall constructed in Phase Two was conducted to predict the response of that wall. Once constructed, a parametric study was performed to establish a CBEAMC model that would match the measured response. It was this model that would be the basis for analyzing and designing the guard wall.

In addition to the CBEAMC models, a finite element analysis (FEA) of the temporary tieback wall was performed using SOILSTRUCT by personnel of the Corps Waterways Experiment Station in Vicksburg, Ms. This analysis predicted the response of the temporary tieback wall, which was compared to the measured response, and then a parametric study was conducted to match the FEA model to the measured response. This study provides additional information for the design of the temporary tieback wall, indicating the amount of heave or settlement to be expected at the railroad. Also, the FEA parametric study verified the CBEAMC model developed for future guard wall analysis.

2.2 Temporary Tieback Wall

2.2.1 Description of Temporary Tieback Wall and Loads

The temporary tieback wall is a diaphragm wall approximately 180 feet in length, with a total wall area of approximately 3600 square feet (Figure 2.3). This wall was completed in February 1988 in Phase Two, the lock excavation contract. The wall is located at the upstream end of the lock chamber and retains soils supporting the Union Pacific Railroad rail line. The maximum height of the wall exposed in the excavation contract is 48 feet. The maximum exposed height of the temporary tieback wall will exceed 80 feet during the third stage of lock construction.

The temporary tieback wall was originally designed to be constructed of eleven, 20-foot panels, three-feet thick, with a maximum height of 90 feet. A value engineering study eliminated panels 1 and 2. Panels 6 and 11 were instrumented with panel 6 chosen for the CBEAMC parametric study. Panels 6 and 11 were both evaluated in the SOILSTRUCT study.

The wall soil loads consisted of a combination of rectangular and triangular at-rest soil pressures, plus a surcharge (Figure 2.4). The at-rest rectangular pressure distribution was derived from NAVFAC DM7.2. A

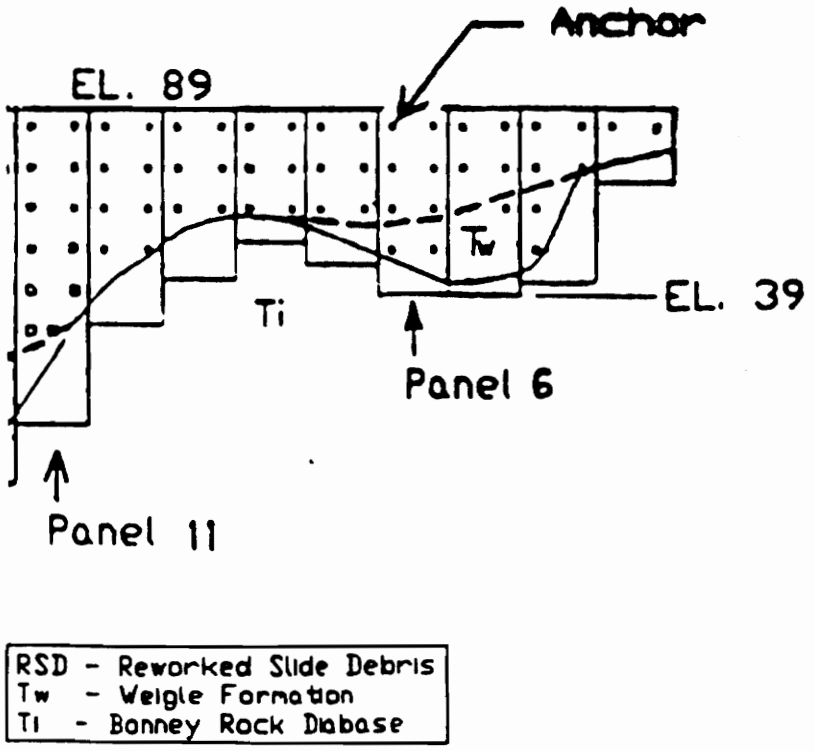

Figure 2.3 Temporary Tieback Wall Elevation (from Mosher and Knowles, 1989).

rectangular distribution is typical for braced walls in sand. The triangular diagram used allows for the possibility of upper anchors losing some load, and greater loads being transmitted to the lower anchors. The Jaky equation (Jaky 1944) was used to select the at-rest pressure coefficient, K_o.

$$K_o = 1 - \sin \phi \quad (1)$$

where ϕ is the soil friction angle. A surcharge was added representing a train and construction load. Hydrostatic pressure was eliminated by dewatering. The number, size, and spacing of the soil anchors was determined by a tributary area that limited an anchor load to a maximum of 358 kips.

2.2.2 Geology and Material Properties

Soil properties for design and for the CBEAMC study are shown in Table 2.1. The geology near the new lock consists of many slides. Much of the material in this area is unconsolidated slide debris (SD). Erosion and river work on the slide debris has produced a material known as reworked slide debris (RSD). RSD is a mixture of gravels, sands and silts, and boulder-size rocks. Below the slide debris lies the Weigle Formation (T_w). Weigle is often characterized as a "soft" rock, of volcanic origin consisting of mudstone, siltstone, and claystone. Another intact rock formation is the Bonney Rock

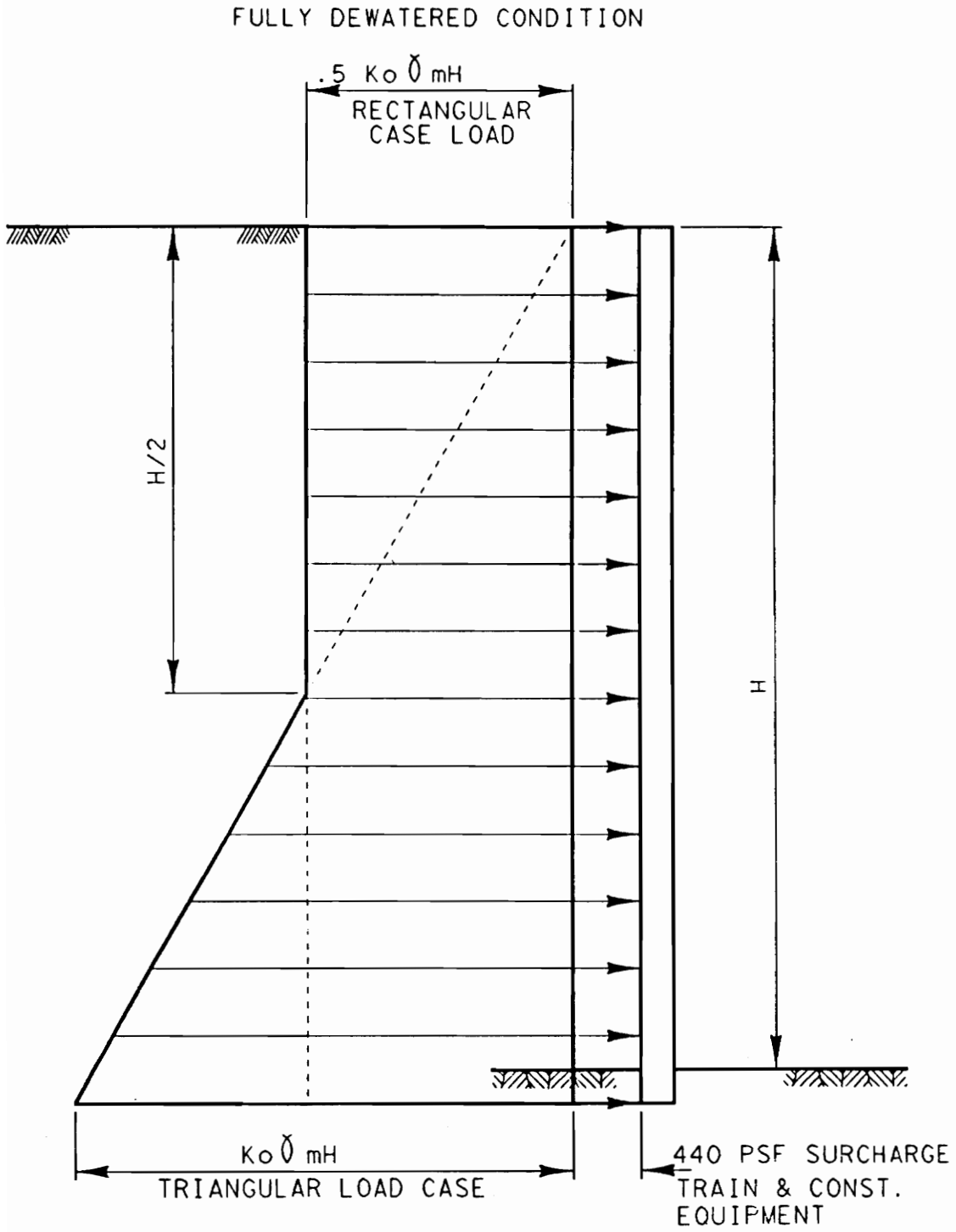

Figure 2.4 Earth Pressure Diagram for Temporary Tieback Wall.

Table 2.1 Soil Properties (From Munger, Jones, and Johnson 1990, and Mosher and Knowles 1989).

Parameter	RSD	T_w	T_i
Friction angle (deg)	30	30	0
Cohesion (psi)	0	10	16,000
Moist Unit Weight (pcf)	125[a]/118[b]	142.5[a]/130[b]	175
Saturated Unit Weight (pcf)	130	142.5	175
Constant of horizontal subgrade reaction l_h			
Moist (pci)	18	23	--
Submerged (pci)	13	23	--
Allowable Bond Stress	60	35	--

a. Unit weight used to develop earth pressure distribution for plane frame or hand analysis.

b. Unit weight used in CBEAMC analysis, changed due to accumulation of additional in-place density data.

Intrusive (T_i). Bonney rock is a large diabase rock intruded into the older Weigle formation. It is a basalt-like rock with high strength properties.

2.2.3 Wall Design

Design of the reinforcement for the temporary tieback wall utilized a plane frame analysis program developed for the Corps of Engineers by Hartman and Jobst (1983). This program, known as CFRAME, used load input modeled as previously described in Figure 2.4, and generates the moments, shears, and deflections necessary for design. The wall was modeled as 1 foot strips of vertical continuous beams spanning non-yielding supports at each row of tiebacks and at the base of the wall. A horizontal beam spanning between a pair of tiebacks provided the support to the vertical beams at each tieback row. Therefore, the soil pressure was applied to the vertical beams, the reactions of the vertical beams were carried as load by the horizontal beams, and the reaction of the horizontal beams was carried as the horizontal component of load in the tieback anchors (Figure 2.5). The horizontal component of tieback load was determined as the larger of either the reaction from the horizontal beams, or the load from the tributary area of the apparent pressure diagram.

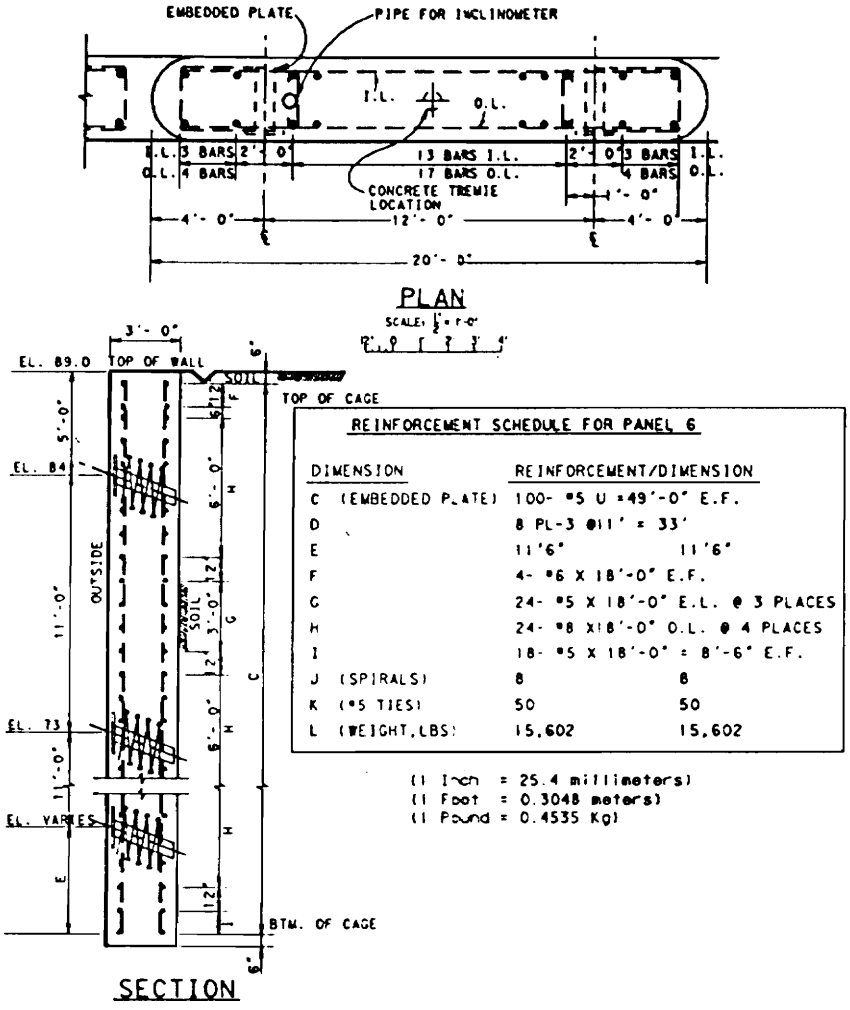

REINFORCEMENT SCHEDULE FOR PANEL 6

DIMENSION		REINFORCEMENT/DIMENSION	
C	(EMBEDDED PLATE)	100- #5 U =49'-0" E.F.	
D		8 PL-3 @11' = 33'	
E		11'6"	11'6"
F		4- #6 X 18'-0" E.F.	
G		24- #5 X 18'-0" E.L. @ 3 PLACES	
H		24- #8 X 18'-0" O.L. @ 4 PLACES	
I		18- #5 X 18'-0" = 8'-6" E.F.	
J	(SPIRALS)	8	8
K	(#5 TIES)	50	50
L	(WEIGHT, LBS)	15,602	15,602

(1 Inch = 25.4 millimeters)
(1 Foot = 0.3048 meters)
(1 Pound = 0.4535 Kg)

Figure 2.5 Wall Reinforcement for the Temporary Tieback Wall (from Munger, Jones and Johnson, 1990).

The tieback anchors consisted of grade 270 ksi, A416 low relaxation 7-wire strand tendons. The tendons were sized so that stress in the strands due to the design load was in accordance with ACI 318-83, but that the anchor test load was not to exceed 0.75 times the guaranteed ultimate tensile strength (GUTS) of the strands. The test load was either a proof or performance test load sized at 1.5 times the design load. Unbonded lengths were determined from slope stability analysis of the different panel heights and ranged from 27 feet to 83 feet. Bonded lengths were determined in an anchor test program completed in 1986. The test program demonstrated the feasibility of high capacity anchors with creep limited to 0.04 inches per log cycle. Allowable bond stresses, tabulated in Table 2.1, provided sufficient anchor to soil bond capacity in either Weigle or RSD. A minimum of 30 feet bonded length was required, later modified to 40 feet due to an anchor pullout failure. Forty feet was shown by the anchor test program to be the maximum bonded length acceptable.

The wall was instrumented in panels 6 and 11 with embedded slope inclinometers, strain gages on the reinforcement, and tieback anchor load cells. Other instruments added to the walls included one or more tiltmeters, horizontal extensometers, EDM survey targets, and alignment survey targets.

2.3 Calibration of CBEAMC

Munger, Jones and Johnson (1990) published their study as part of the proceedings of the Design and Performance of Earth Retaining Structures Conference at Cornell University held in June 1990. This conference was sponsored by the Geotechnical Engineering Division of the American Society of Civil Engineers. In their study, they evaluated a set of parameters to determine the effect of each in order to calibrate a CBEAMC model to better match the measured response of the temporary tieback wall. The response characteristics of concern were moments and deflections. The wall and site characteristics were described previously, with soils properties as given in Table 2.1.

2.3.1 CBEAMC Model

Because CBEAMC is unable to model construction sequencing, i.e. excavation, tieback installation and stressing, excavation to the next level, etc., it is what Munger called a "1-step construction model." The initial loads applied to the wall are at-rest loads with the tieback tendons stressed to the design loads. The computer analysis is then run and the deflections that satisfy equilibrium are determined. Therefore, analysis of the wall system

does not include strain energies and deflections that would be realized at every stage of construction sequencing. Construction sequencing is modeled by Mosher and Knowles (1989) on SOILSTRUCT and will be discussed later.

In order to develop the Winkler springs to represent soil stiffness, initial values of l_h, Terzaghi's (1955) "constant of horizontal subgrade reaction" were selected. Terzaghi has shown that deflections of retaining walls embedded in soils are sensitive to l_h, and that moments are less sensitive. Terzaghi has derived a set of values for l_h showing that deflection is inversely proportional to the fourth root of l_h. Letting RSD and T_w be assumed as cohesionless, Munger selected values of l_h from the higher end of Terzaghi's values because of the higher relative densities of the soils involved.

The stiffness of the soil springs in CBEAMC is a function of l_h. Terzaghi has called this stiffness, K_h, a "coefficient of subgrade reaction." Haliburton (1971) called this stiffness the "soil modulus" (E_s), where

$$E_s = l_h (X/D) \qquad (2)$$

and X is the equivalent depth of material for a given unit weight which will provide the actual effective overburden pressure at the elevation of interest. D is the contact area, assumed in the CBEAMC model as the average vertical distance between tieback anchors. E_s will then be the slope of the elastic portion of the nonlinear P-Y curve representing the soil springs (Figure 2.6a).

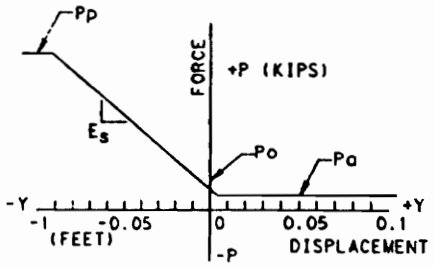

A) P-Y CURVE FOR SOIL ON THE LEFT SIDE OF WALL.

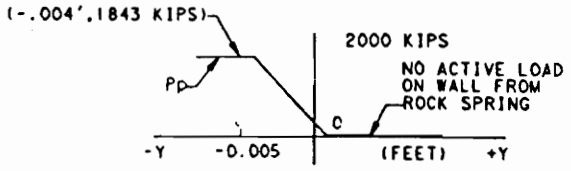

B) P-Y CURVE FOR ROCK OF LEFT SIDE OF WALL.

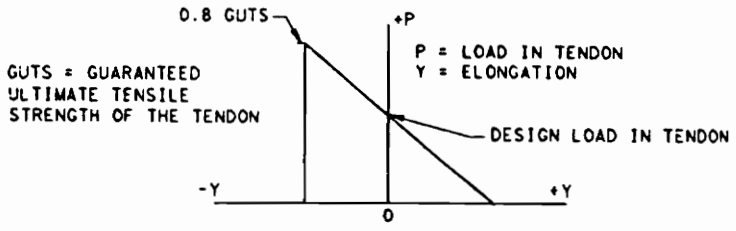

C) TENDON P-Y CURVE

Figure 2.6 Typical P-Y Curves Used in the CBEAMC Model (from Munger, Jones and Johnson 1990).

When the soil pressures P_a, P_o, and P_p have been determined for any particular elevation, Y_a and Y_p can be found by

$$Y_a = (P_o - P_a)/E_s \quad (3)$$

$$Y_p = (P_o - P_p)/E_s \quad (4)$$

establishing the location of the active and passive resistance on the P-Y curve. P_o will be located at $Y_o = 0$, since that is the deflection for at-rest pressure.

To develop what was called "rock springs," a P-Y curve modeled a one-foot square by two-foot long "rock strut." Only passive resistance can be developed by a rock spring (Figure 2.6b). For the maximum passive resistance, P_p = 0.8 times the unconfined compressive strength of the bedrock (Bonney Rock). The unconfined compressive strength of Bonney Rock is 16000 psi, and E_s = 6,040,000 psi per inch.

Figure 2.6c shows a typical P-Y curve representing "tendon springs" in the CBEAMC model. Each tendon was modeled with the length of the tendon equal to one half of the bonded length plus the unbonded length. At Y = 0, the initial load given by the tendon spring represented the design load applied at the tieback anchor, with its elongation. The CBEAMC model for tendon springs would exhibit tendon failure when 0.8 GUTS was exceeded by dropping the tendon load to zero as represented by the spring. The wall moment of inertia for a one-foot strip of wall was 2.25 ft^4/ft.

2.3.2 Predicted and Measured Performance

Because deflection is sensitive to l_h, a sensitivity study was performed to demonstrate the effects of changes of l_h. Munger examined initial values selected from Terzaghi of 18 pci and 23 pci for moist RSD and T_w, respectively. Also examined were 10 pci, 50 pci, and 100 pci for both soils, simultaneously. Figure 2.7 shows the results of the predicted moments and deflection together with those that were measured.

Inspection of the deflections show the predicted deflection at l_h equal to 100 pci nearly matching the measured deflections. All of the predicted and measured deflections were directed away from the excavations. The deflection predicted by the initial values for l_h was 0.05 feet at the top of the wall, five times greater than the measured deflection of 0.01 feet. The maximum deflection was observed at the top of the wall.

The predicted moments of the study were described as "approximately equal to the measured moments." As observed in Figure 2.7, at 35 feet from the top, with l_h = 100 pci, the maximum predicted positive moment is approximately 25 kip-feet. At l_h = 50 pci, 18/23 pci and 10 pci, the predicted positive moments were approximately 45 kip-feet, 65 kip-feet and 90 kip-feet, respectively. The apparent increase of moment is approximately four times

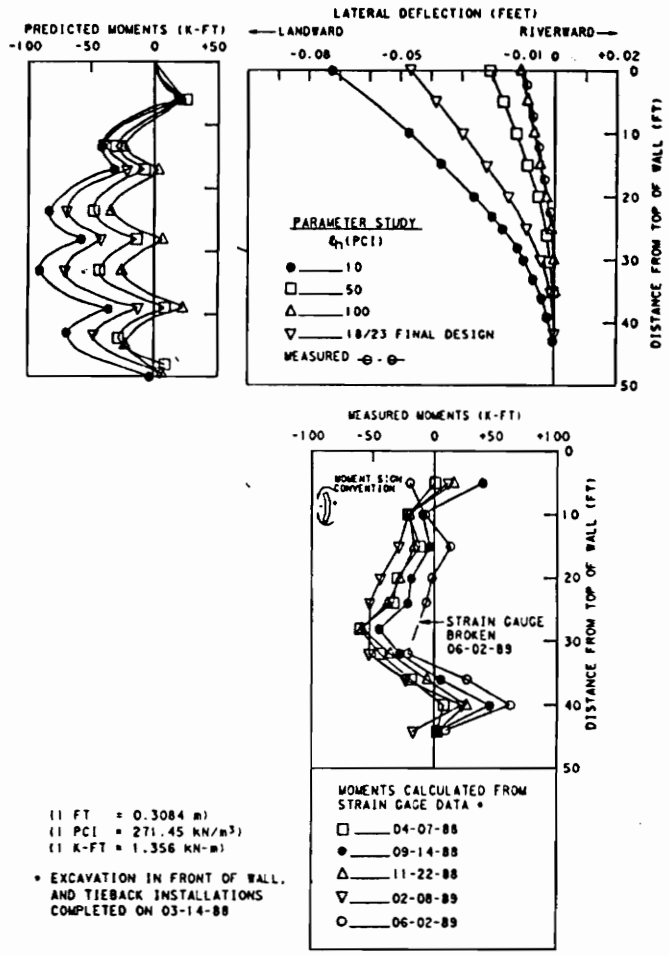

Figure 2.7 Predicted and Measured Performance (from Munger, Jones and Johnson 1990).

as l_h = 100 pci is decreased to l_h = 10 pci. The maximum measured negative moment is at 30 feet from the top at about 60 kip-feet. This closely approximates the predicted moment when values of l_h = 18 cpi and 23 pci are used.

Also described in the study was the observation that "the measured trends did not indicate the reduction in moments at the supports that were predicted by the CBEAMC analysis." As can be seen in Figure 2.7, CBEAMC indicates a tendency for significant reduction if not a reversal of moments at the support anchors. This trend was not supported by the measured moments.

Also indicated in the study was that back-calculation of the soil loads from the three upper load cells gave soil loads in the range of 2.2 to 2.3 kips per square foot. This closely matched the design loads of 2.1 to 2.4 kips per square foot derived from the pressure diagram of Figure 2.4, considering the change in height of panel 6. The initial design height of panel 6 was 54 feet and was assumed to be all RSD soil. Later excavation showed some T_w between Bonney rock and RSD. The completed wall height was 48 feet due to bedrock being higher than expected.

2.3.3 Design Calibration

The study indicated that the effect of increasing the soil friction angle was relatively minor compared to the effects of modifying l_h (Figure 2.8). Therefore, the study members chose to base the calibrated CBEAMC model on l_h. Although it was observed that the measured deflections were closely matched by selection of l_h = 100 pci, the selected value chosen for analysis of the permanent walls was l_h = 36 pci and 26 pci for moist RSD and saturated RSD, respectively. l_h for T_w was not changed. These values were recommended based on the "importance of the upstream walls, the lack of similar precedents from previous projects, and the likelihood of significant variability in materials at the site." Additional increases in l_h were not felt to be justified.

2.4 Finite Element Analysis of the Temporary Tieback Wall

Mosher and Knowles (1988) distributed the final draft report of their finite element analysis of the temporary tieback wall in 1988. The study had a number of goals. Primarily, it was to analyze the temporary tieback wall-soil system and the effects that may be felt at the railroad 50 feet away. Also, based on a comparison

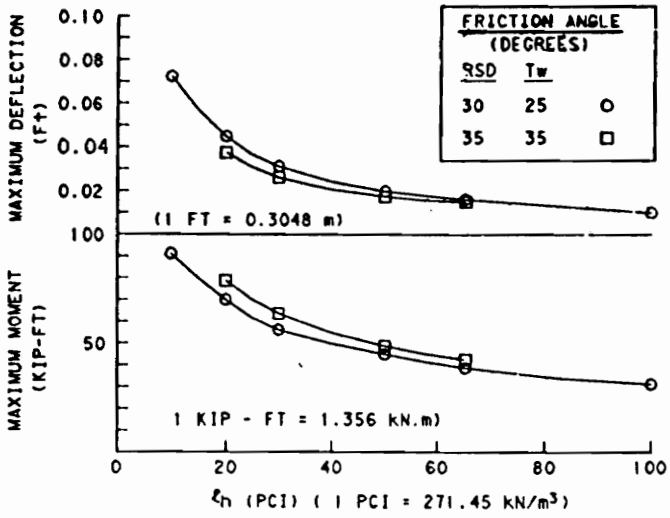

Figure 2.8 Comparison of Friction Angle and l_h on Deflection and Moments (from Munger, Jones and Johnson 1990).

of measured response and an analysis of panels 6 and 11, the study was to recommend a course of action on the design parameters which would assist the design of future walls.

The FEA study was divided into Parts I through IV. Part I described the FE model, confirmed the procedure used in the wall design, and predicted the behavior of the wall system based on panel 6 configuration. Part II assessed the sensitivity of the wall-soil system to a range in values of soil modeling parameters such as the soil stiffness constant. Part III conducted a study to establish a FEA model which better matched the measured response of panel 6. Based on Parts I, II and III, panel 11 was reanalyzed using increased soil stiffness. The results of that study were reported as Part IV. A description of pertinent information of each part will follow with any differences from the CBEAMC model identified.

2.4.1 Finite Element Analysis Model

The finite element analysis study was performed using computer program SOILSTRUCT. SOILSTRUCT was developed by G. W. Clough (1984) and others for modeling complex, soil-structure interaction problems through finite element analysis.

The finite element mesh developed to model panel 6 was extended well out beyond the wall to portray in-situ soil stress (Figure 2.9). The nodes at the sides were fixed horizontally. Nodes at the base were fixed in the horizontal and vertical directions, and all other nodes were free to displace horizontally and vertically.

The soil and wall were modeled by two-dimensional plane strain elements. The interface between the soil and the wall was modeled using a four-node, zero-thickness element. This element allows for controlled relative movements between materials with different properties. Bar elements (one-dimensional truss elements) modeled the anchors and were used to act as "strain gages" attached to the wall surface. The bar elements acting as strain gages are added to each exterior side of the wall elements and provide the means for determining moment in structural elements in a SOILSTRUCT analysis.

To model the soil characteristics, SOILSTRUCT uses a variation of the Duncan-Chang (1970) hyperbolic model. Initial values selected for the hyperbolic soil parameters were estimated based on data published by Duncan et al. (1980) and were lower bound values. For initial loading, soil response follows a non-linear hyperbolic curve (Figure 2.10). Upon unloading and reloading, the soil responds in a linear fashion. When reloading brings the

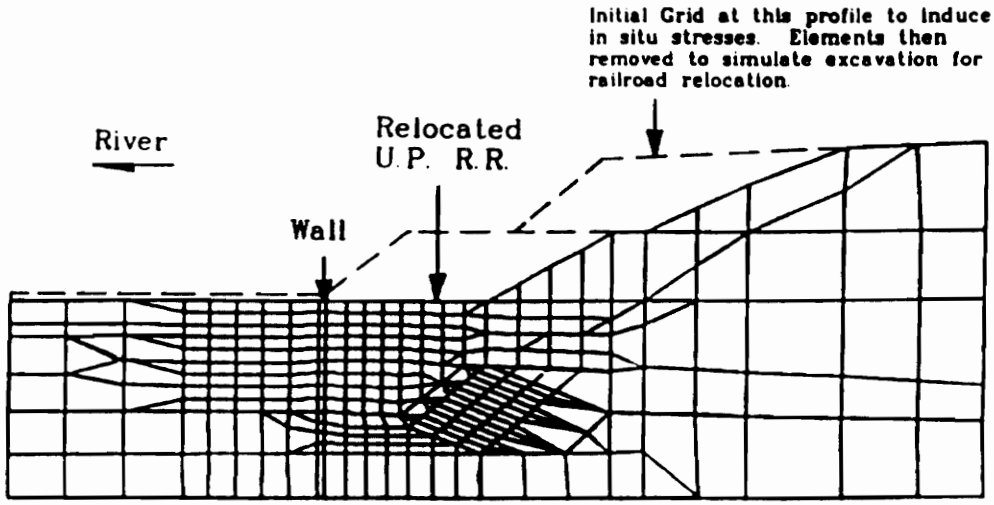

Figure 2.9 Finite Element Grid for Panel 6 Profile (from Mosher and Knowles 1988).

soil stress level to the stress level prior to unloading, additional loading beyond this point cause the soil response to follow the nonlinear hyperbolic curve. The soil modulus when initially loaded is identified as E_i. The unload-reload soil modulus is identified as E_{ur}. The hyperbolic equations demonstrated in figure 2.10 can be found by

$$E_i = p_a K_m (\sigma_3/p_a) \tag{5}$$

$$E_t = \left[1 - \frac{R_f(1-\sin\phi)(\sigma_1-\sigma_3)}{2c\cos\phi + 2\sigma_3\sin\phi}\right]^2 K_m p_a (\sigma_3/p_a)^n \tag{6}$$

$$E_{ur} = K_{ur} p_a (\sigma_3/p_a) \tag{7}$$

where:

E_i = initial modulus

E_t = tangent modulus

E_{ur} = unload-reload modulus

K_m and K_{ur} are the corresponding modulus numbers, σ_1 and σ_3 are the major and minor principle stresses, ϕ and c are Mohr-Coulomb soil strength parameters, p_a is the atmospheric pressure, and R_f is the ratio of the stress difference at failure to the asymptotic stress difference.

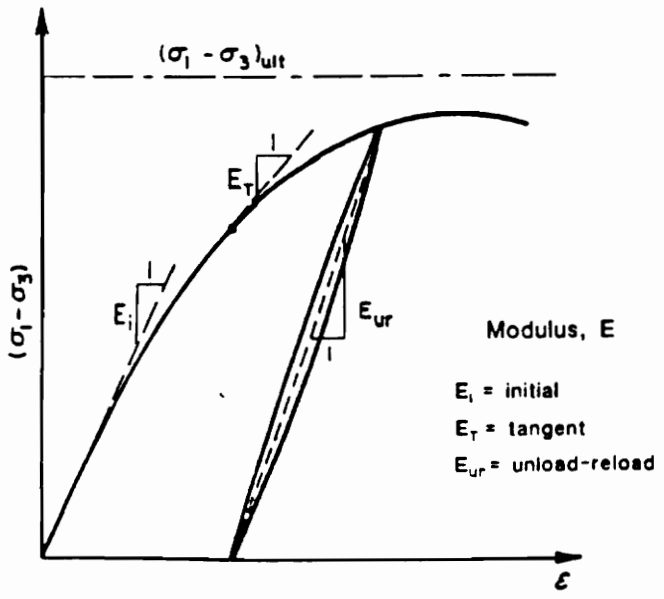

Figure 2.10 Hyperbolic Representation of Stress-Strain Curve (from Mosher and Knowles 1988).

Soil strength parameters selected follow Mohr-Coulomb criteria: using friction angle, ϕ, and cohesion, c. One ability of this program is to set the soil modulus to a very low value when stress in a soil element equals or exceeds those established by Mohr-Coulomb, so as not to take on any additional shear stresses.

The soil properties used in the finite element analysis are given in Table 2.2. Some differences exist in friction angles and cohesion from those selected for use in CBEAMC in Table 2.1.

The structural materials are assumed as linear elastic. Material properties are identified as: f'c equals 3000 psi, wall stiffness, EI, equals 1,013,000 kip-ft per foot, and the section modulus equals 1.5 feet cubed. Back calculation of the moment of inertia I, from EI, gives I equal to 2.25 ft^4 per ft. These properties match those for the CBEAMC model except the wall stiffness in CBEAMC was based on f'c = 3500 psi. The difference is negligible for the wall stiffness term E_c. The wall-soil interface was modeled as a "cohesionless surface of high shear stiffness, with a friction angle of 30 degrees."

SOILSTRUCT is designed to model the construction processes in the finite element analysis. SOILSTRUCT can emulate the steps during the construction process described as "initial stresses, fill placement, material

Table 2.2 Soil Properties and Parameters for Finite Element Analysis (from Mosher and Knowles 1989).

Material	Friction Angle (deg)	Cohesion (psf)	Unit Wieght (pcf)	Hyperbolic Parameters: Modulus Constant K	Hyperbolic Parameters: Strength Factor R	Hyperbolic Parameters: Modulus Exponent n
RSD, SD and Fill	34	0	125	300	0.7	0.3
SB	32	750	130	200	0.7	0.6
$T_{(w)}$	30	20,000	130	2000	0.7	0.5
$T_{(i)}$	0	200,000	175	200,000	0.7	0.5

excavation, dewatering, and placement of structural materials in a series of incremental loading steps." Stresses and displacements are analyzed for each step in the loading and unloading of the soil and the wall-soil system. Some of these steps include placement of fill for a nearby highway, removal of the fill and additional overburden to realign the railroad, placement of the wall (displacements then reset to zero), dewatering, and finally, excavation and installation of tiebacks. Table 2.3 shows the sixteen loading steps used in the finite element analysis model. Figure 2.11 shows the excavation and tieback installation models used.

2.4.2 Predicted and Measured Performance

Part I

In Part I, the goals were to confirm the procedure used in the wall design, and to predict the response of the wall-soil system during the construction process. Moment diagrams were developed for each step in the excavation and installation process and, except for the first excavation step, retain the same shape throughout all of the process. At the first excavation step, the wall deflected towards the excavation, developing negative moments. (The sign convention is positive moment produces tension on the riverward

Table 2.3 Loading Steps in Finite Element Analysis (from Mosher and Knowles 1988).

Step Number	Description
1	Build natural slope - first increment
2	Build natural slope - second increment
3	Build natural slope - third increment
4	Build natural slope to pre-excavation profile
5	Excavate for R.R. relocation (current profile)
6	Build wall
7	Excavate El. 78.5 (in front of wall)
8	Prestress first tieback, El. 84 (150% design load)
9	Excavate to El. 67.5, lockoff first tie at field load
10	Prestress second tieback, El. 73
11	Excavate to El. 56.5, lockoff second tie
12	Prestress third tieback, El. 62
13	Excavate to El. 45, lockoff third tie
14	Prestress fourth tieback, El. 51
15	Excavate to bottom of wall, El. 39, lockoff fourth tie
16	Release top anchor in failure simulation analysis

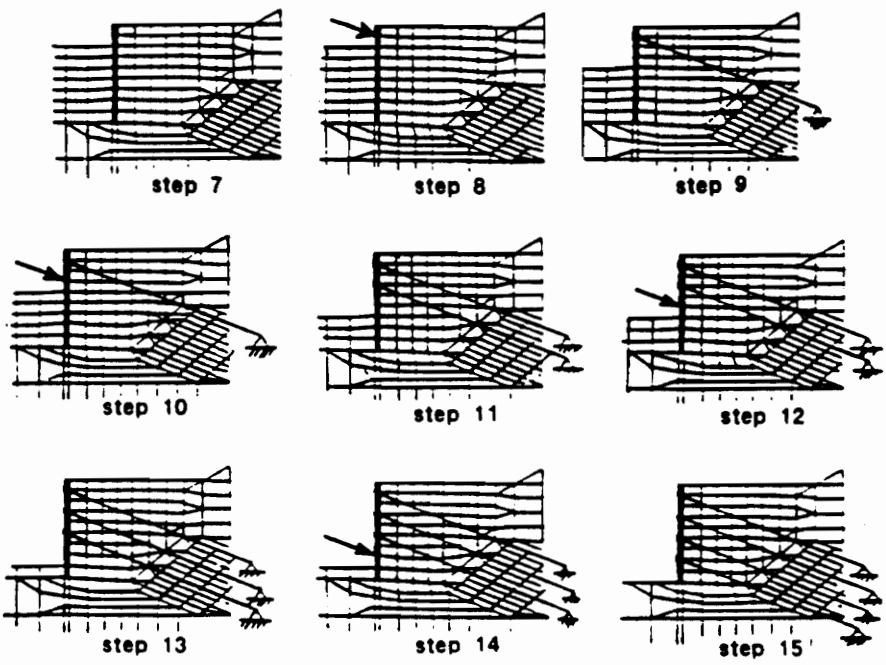

Figure 2.11 Loading Sequence Modeling Construction Operations (from Mosher and Knowles 1988).

side.) After the first tieback was installed, the moment diagram for the following steps in the process generally showed the top ⅓ of the wall with negative moments, the bottom ⅔ showing positive moments (Figure 2.12). The maximum observed moment was less than the design moment of 191 kip-feet by 44%. Since in Part I of the study, conservative soil modeling parameters were selected, then the conclusion would be that the original design was satisfactory for structural considerations.

The response of the wall-soil system to the construction process was as much a qualitative question as well as quantitative. The observed lateral deflection for the wall was toward the excavation 0.5 inches. The first tieback pulled the wall back into the retained soils 0.78 inches past vertical. After that, it was observed that little change occurred in deflections for the remaining construction steps. Generally, the wall would deflect outward slightly when excavated and pull inward slightly when a tieback was stressed. The final end of construction results showed a deflection with respect to wall height of 0.11% which compared well with observations of other wall systems. The other walls realized a range from 0.11% to 0.38%. This would indicate that the finite element model was reasonable and could be used for predicting the response of the wall-soil system with changes in parameters.

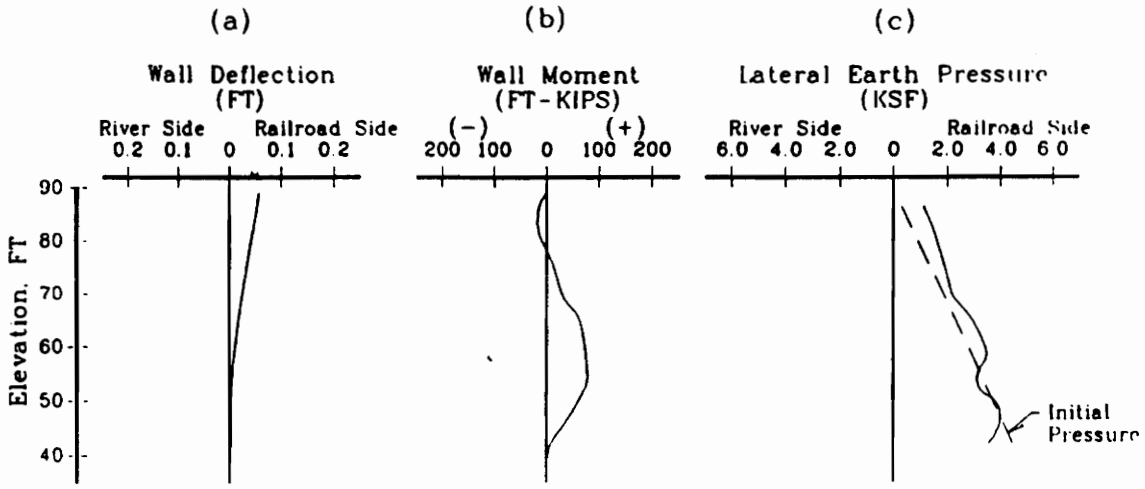

Figure 2.12 Final Excavation to EL.39', Lockoff Fourth Anchor (from Mosher and Knowles 1988).

Three other considerations were discussed in Part I which are not directly pertinent to the design verification study, but worth noting. The first is that soil pressures were also plotted with each stage of the excavation sequence. The final pressure, plotted with the initial and the design pressure are shown in Figure 2.13. The observation was made that the final pressure was more triangular than rectangular. It is seen in Figure 2.13 that the bottom ⅔ of the final pressure is outside of the design pressure as calculated from NAVFAC DM 7.2.

Second, the final anchor loads for the four rows of anchors, after some variation with each construction stage, had nearly the same value as the initial loads. Finally, surface deflections due to wall movement towards the railroad reached a maximum of 0.2 inches approximately 10 feet from the wall, and 0.1 inches at the tracks 50 feet from the wall.

Part II

The goal of Part II was to access the sensitivity of the wall-soil system in response to changes in selected parameters. The changes would be made to three different sets of parameters: 1) two sets of anchor loads of different magnitudes, 2) reduced capacity and failure of the top anchor, and 3) reduced

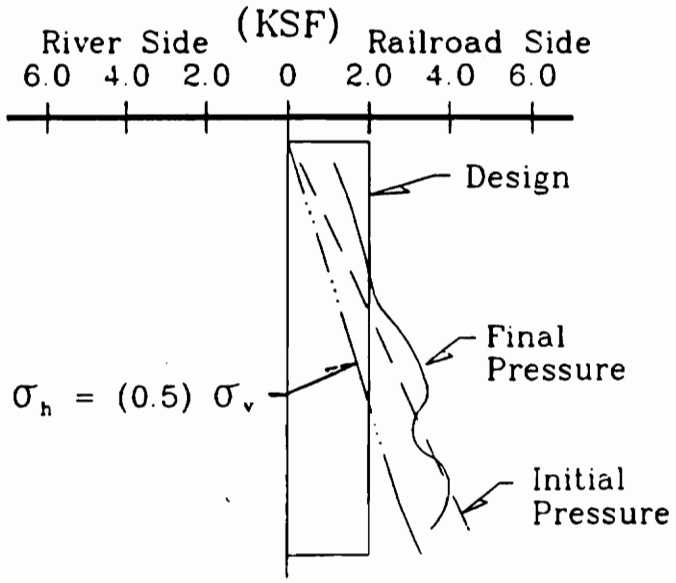

Figure 2.13 Earth Pressures on the Tieback Wall (from Mosher and Knowles 1988).

stiffness parameter of all soils. For the purpose of the design verification study, only the reduction of the soil stiffness parameter is directly pertinent to this study. The other two sets of parameters were not a part of the CBEAMC calibration, but are worthy of discussion. Considering the soil stiffness parameter study, the soil stiffness was reduced by ½ by reducing the modulus constant, K_m, by ½. K_m determines the initial tangent modulus value representing the stiffness of the soil (Figure 2.10). The analysis of the "softer" soil is compared to that of the original analysis, and is shown in Figure 2.14. The results as indicated in the study show deflections increase about 65% and moments increase about 40% when the softer soil is used. Ground surface deflection increased as well, with a maximum heave of 0.16 inches at the rail line, or a 60% increase.

The other two parameters studied were the differing anchor load sets, and a reduced or failed top anchor. The differing anchor load sets were: 1) as constructed, 2) 110% as constructed, and 3) approximately double the as-constructed loads. The results showed the deflections, moments and soil pressures to be proportional to the increase in loads.

When the top anchor was assumed failed, the top of the wall moved 0.78 inches past vertical out into the excavation. Also, moment reversal occurred towards the top of the wall, producing a maximum negative moment

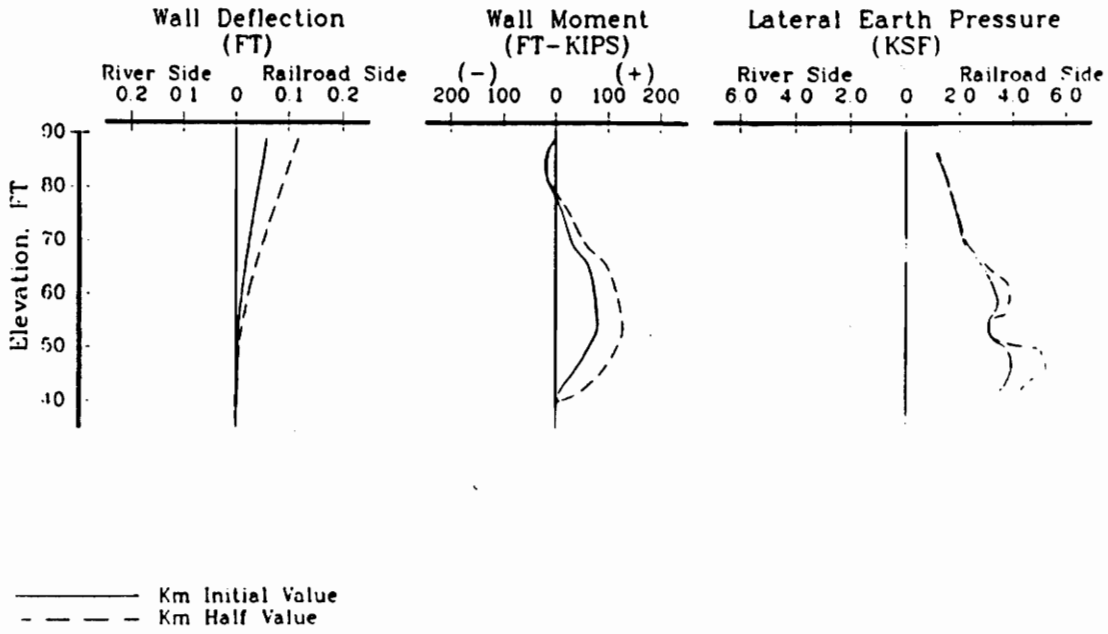

Figure 2.14 Wall Behavior with Reduced Soil Stiffness (end of construction) (from Mosher and Knowles 1988).

of 115 kip-feet. Interestingly, only 13.5% of the failed anchor's load was transferred to the remaining anchors. The remaining load was transferred to bending in the wall.

Part III

In Part III, a parametric study is performed to match the predicted wall-soil system response to the measured response observed on panel 6. The instrumented results of panel 6 are plotted with the original FEA results in Figure 2.15. Changes in parametric values studied were the at-rest pressure coefficient, K_o, the modulus constant, K_m, and the unload-reload modulus constant, K_{ur}.

In the original FEA, K_o was selected as 0.5 for RSD, Weigle and Bonney rock. However, since the soils were overconsolidated due to the fill, values for K_o could have been higher. Two analyses were conducted, one with K_o equal to 1.0, another with K_o increased to 2.0. The study indicated as the value of K_o increased, the wall tended to bulge towards the excavation and

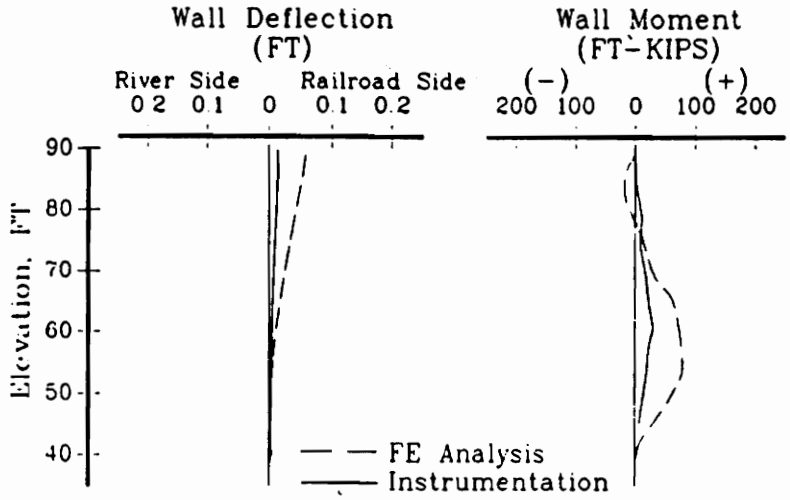

Figure 2.15 Instrumentation and F.E.A. Analysis Results for Panel 6 at End of Construction (from Mosher and Knowles 1988).

had corresponding increases in moments. As K_o increased, the deflection took on a "shape" less like the measured deflection and correspondence appeared to be divergent. Moments increased well beyond the measured values.

K_m and K_{ur} were evaluated separately, yet since they are interrelated, their responses were compared with each other as well as with the measured responses. First K_m was varied and evaluated. K_m is used in the non-linear hyperbolic model representing the soil response. As K_m is the soil modulus stiffness constant, it is directly proportional to the soil modulus, E_i. When K_m was doubled and tripled, the corresponding predicted deflections and moments approached the measured responses (Figure 2.16).

K_{ur} is similar to K_m during initial loading. However, the tieback wall would experience several occasions of unloading and reloading the retained soils during the construction stages. K_{ur}, the unload-reload modulus constant, better describes the soil response while unloading and reloading the wall. K_{ur} is directly proportional to the unload-reload soil modulus, E_{ur}. Previously, when K_m was varied, K_{ur} was also varied. However, Duncan et al. (1980) showed that the unload-reload modulus could be as much as three times the initial modulus. Therefore, an analysis was performed in which only K_{ur} was tripled, and was compared to the analysis of K_m (thus, K_{ur} too) being tripled.

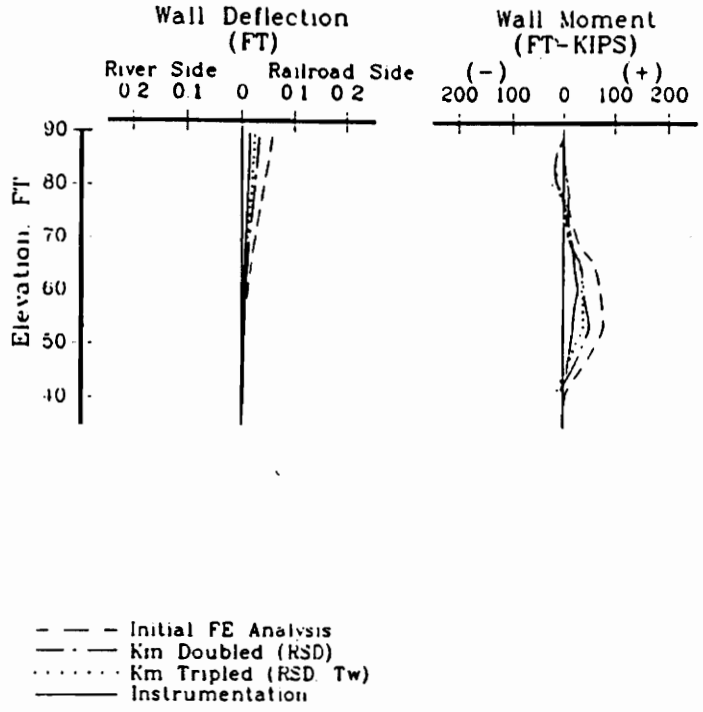

Figure 2.16 Wall Behavior with K_m Increased (from Mosher and Knowles 1988).

The results showed that the unload-reload modulus was more responsible for the soil response than the initial modulus. The study continued using K_{ur} for predicting the wall system response compared to the measured response for all stages of construction. Figure 2.17 shows the results at the end of construction for the measured response, the initial FEA, and the K_{ur} tripled FEA.

A final analysis tried increasing both K_m and K_{ur} by six times the original values, and increasing only K_{ur} by six times the original value. The comparison showed that both analysis "overshoot" the measured wall response, and that the K_m times six overshoots more than the K_{ur} times six analysis.

Conclusions developed by Mosher and Knowles based on Parts I to III indicate that variation of K_m and K_{ur} most closely match the measured wall responses. They indicated the best FE model would probably consist of variations of both K_m and K_{ur}, but by differing amounts. Most importantly, they concluded that the soil stiffness could be increased from the original values selected.

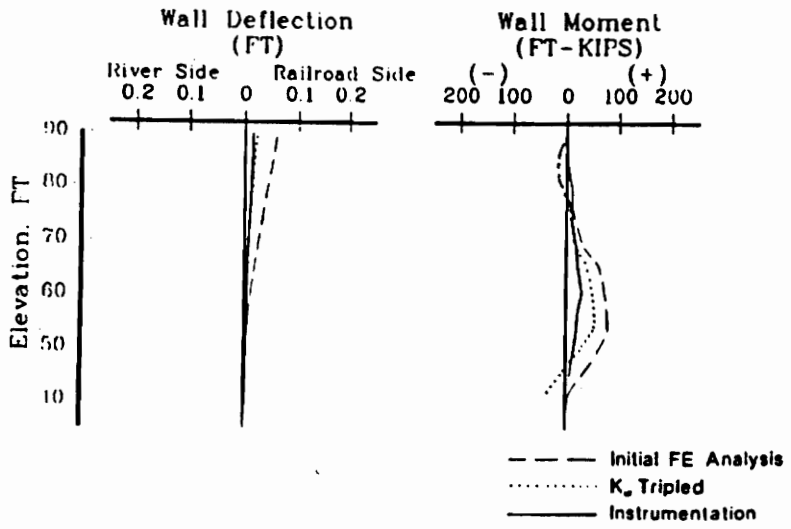

Figure 2.17 Results from Instrumentation, Stiffened K_{ur}, and Initial Analysis (from Mosher and Knowles 1988).

Part IV

In Part IV, panel 11 of the temporary tieback wall was analyzed with parameters of the original FEA and with increases of three times and six times K_{ur}. Panel 11 differs from panel 6 in that it is taller and "stepped" at the base. The stepped base was necessary due to the steeply sloping Bonney rock. Therefore, the right half of panel 11 is 65 feet high and the left half stepping down increased the height to 82 feet. Because of the greater height, panel 11 has six rows of tieback anchors instead of four rows. The design, construction and excavation staging are all similar to panel 6. The geology showed that panel 11 retained all RSD above Bonney rock.

The analysis procedure was performed in a similar manner and the results were shown to nearly mirror those of panel 6. The difference being that the results for panel 11 were just a larger scale than those of panel 6. Panel 11 did not have instrumented results with which to compare, but the study indicated that the panel 6 measured results will reflect the expected results from panel 11.

2.5 Conclusions of Calibration

(1) The material properties for concrete for both studies used an f'c of 3000 psi to 3500 psi. The E_c for 3500 psi is 500,000 kips/ft^2. The measured 28-day strength of concrete samples for panel 6 was 10,320 psi (Memorandum, Jan. 13, 1988), for which E_c = 834,000 kips/ft^2. The effect of doubling the wall stiffness would be a decrease in wall deflections, possibly by ½. This will be evaluated further in Chapter IV.

(2) The selection of l_h = 36 pci and 26 pci for moist RSD and saturated RSD would indicate a predicted moment of approximately 50 to 55 kip-feet which would closely match the measured moment of 55 to 60 kip-feet (Figure 2.7). The predicted deflections would be about 2.5 times the measured deflection.

(3) Munger concluded moments experienced little sensitivity to changes in soil stiffness, whereas Mosher concluded moments were sensitive to changes in soil stiffness. Both concluded that wall deflections were sensitive to changes in soil stiffness. A possible increase of up to three

or four times the original l_h was considered possible, but not recommended without a precedence. A possible increase between three to six times was considered possible for the soil stiffness parameters used in SOILSTRUCT. A combination of increases on K_m and K_{ur} was considered most likely.

(4) Neither study correlated the relative stiffness of E_s used in CBEAMC to E_i and E_{ur} in SOILSTRUCT to determine if the two studies began with the same approximate soil stiffness. The selected values for the CBEAMC study began with upper end values derived by Terzaghi (1955). The selected values for the SOILSTRUCT study began with lower end values published by Duncan et al. (1980).

CHAPTER III

DESIGN VERIFICATION

3.1 General

In February 1989, the Corps of Engineers contracted with S. J. Groves and Sons to construct the diaphragm walls. S. J. Groves, later bought out and renamed Torno America, was to build as a part of their contract four walls by the slurry construction process. Of the four walls, the largest was the permanent wall known as the guard wall (Figure 1.1).

Design of the guard wall was based on two analyses. The first analysis was a limit state equilibrium analysis (hand analysis) to size the primary members of the wall system using Rankine-based active and passive pressures. After preliminary selection of the structural members was complete, a soil-structure interaction (SSI) analysis was conducted to complete a final design based on established structural and deflection criteria.

The SSI analysis was to be conducted on CBEAMC using typical parameters to describe the structural elements in the wall model. Soil stiffness parameters were initially selected based on values derived by Terzaghi (1955). However, a later parametric study conducted by Munger, Jones and Johnson (1990) concluded that the Terzaghi values could be safely doubled, possibly resulting in reduced sizes for some

of the steel pile members. The final design was completed and in some cases, the doubled soil modulus was able to reduce steel pile sizes. In other areas of the guard wall, the analysis with the doubled soil modulus did not result in a change in pile sizes.

In this chapter, a particular panel of the guard wall will be evaluated and the predicted results compared to the measured response. Preceding the comparison will be a description of the guard wall, which demonstrates its similarities and differences with relation to the temporary tieback wall of the CBEAMC calibration. A description of the slurry construction process given next will provide insight into the making of a diaphragm wall. The CBEAMC models consist of the one used in the actual design and a model which better represents the as-built conditions.

The verification of the design evaluates the reasonableness of the CBEAMC model based on soil stiffness parameters recommended by Munger, Jones and Johnson. The evaluation will be a comparison of predicted and measured moments and deflections for the selected panel.

3.2 Guard Wall Description

3.2.1 Description of Guard Wall

The guard wall is a permanent diaphragm wall on the upstream channel of the main lock structure (Figure 1.1). It retains the soils on the landward (south) side of the channel. The exposed height of the wall, once all construction is complete, may be up to 70 feet at the dredge line of the wall.

The guard wall consists of 36-inch and 42-inch diaphragm walls with steel piles as the primary structural elements (Figure 3.1). These piles, spaced 4 feet and 6 feet on center, utilize reinforced concrete tremied between the piles as lagging. In the vertical direction, the concrete was considered as composite with the steel piles to include the additional stiffness to the wall system provided by the concrete. All permanent tiebacks are located at a single level above the maximum normal pool. A continuous steel girder is attached to the top of all of the piles. This cap girder is encased in a reinforced concrete cap beam. The cap beam provides corrosion protection for the cap girder, pile tops, and tieback anchorage assembly (Figure 3.2). Should a tieback fail, the cap beam will transfer the load to adjacent ties without exceeding the allowable stresses on the tendons. Tieback replacement procedures may then be carried out.

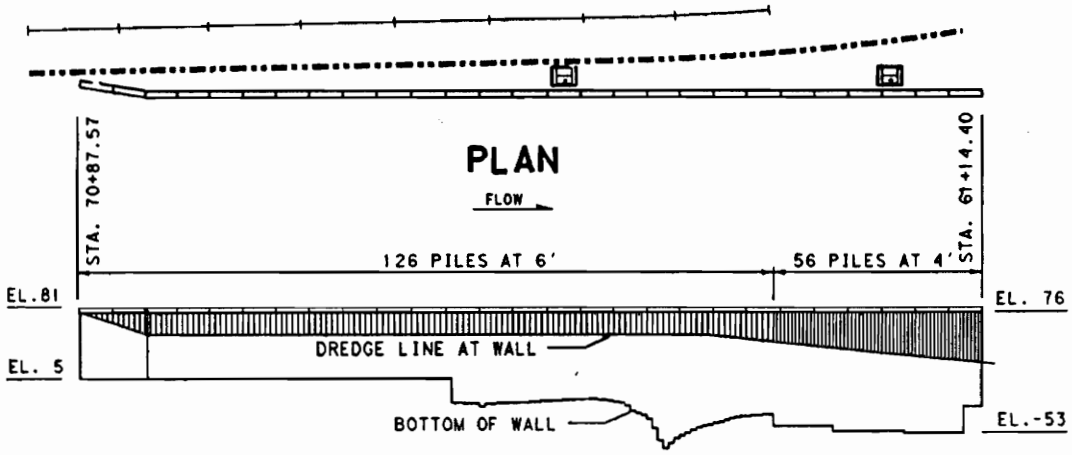

ELEVATION

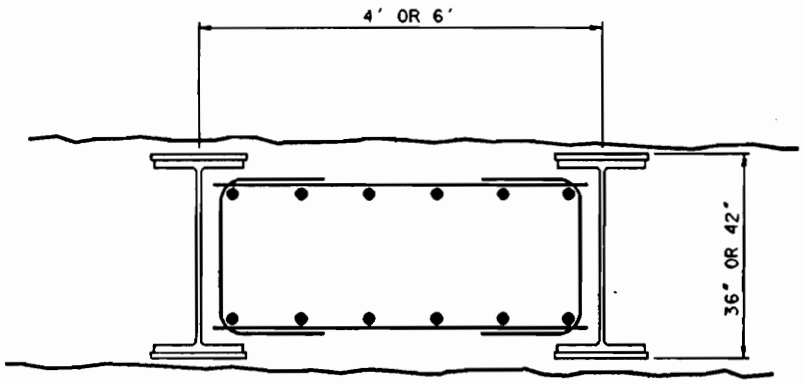

TYPICAL SECTION

(PILE WITH AND WITHOUT COVERPLATES)

Figure 3.1 Guard Wall Plan, Elevation, and Typical Section.

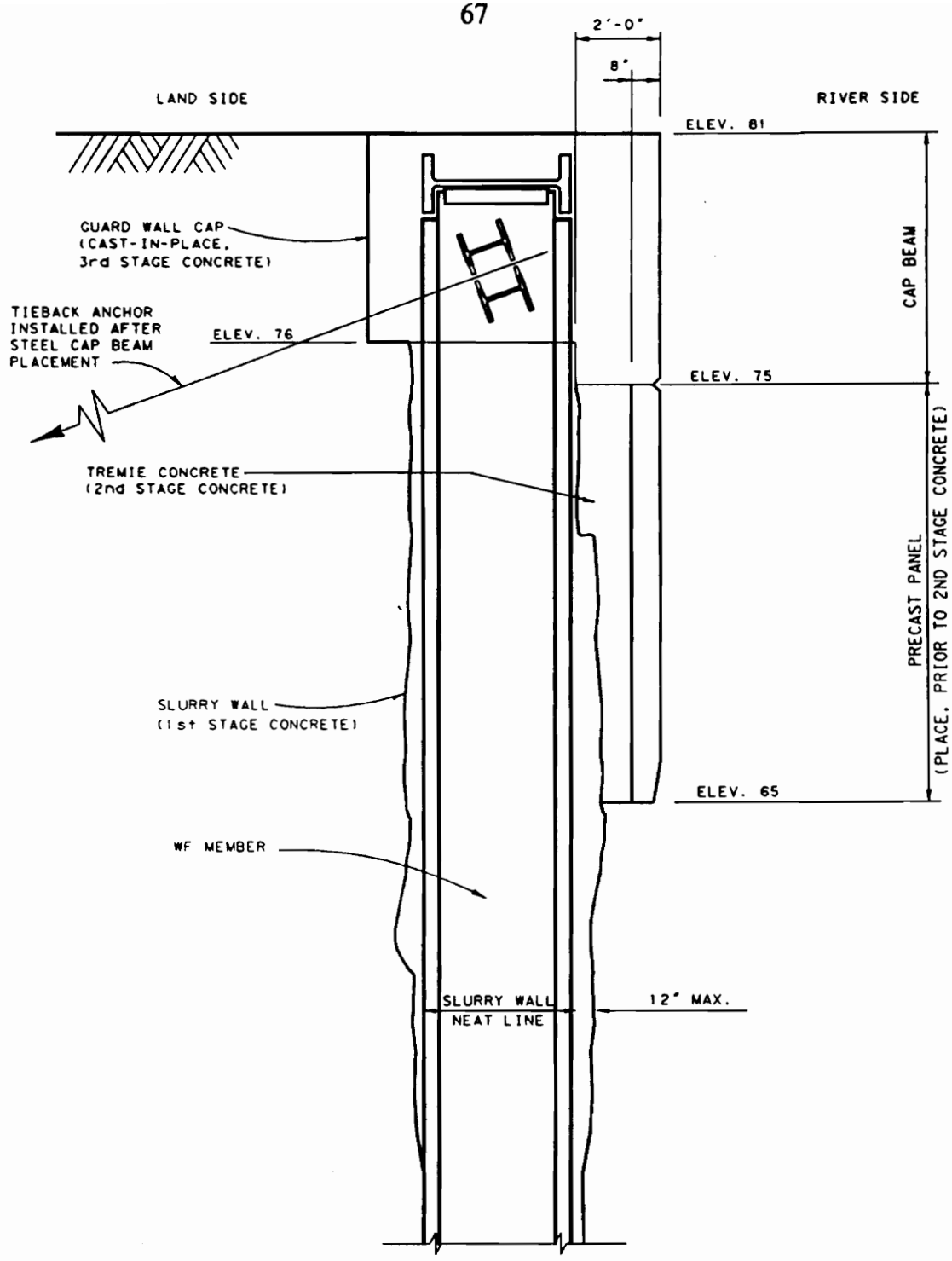

Figure 3.2 Typical Guard Wall Section (from U.S. Army Corps of Engineers, July 1988)

The vertical steel piles range in size from a W36 x 195 to a W36 x 300 with cover plates attached. The largest pile matches the section modulus of a W36 x 848.

The depth of embedment of the guard wall was established either by wall stability or seepage cutoff. For purposes of seepage cutoff, the guard wall was required to be embedded into Bonney rock, Weigle foundation, or large slide blocks derived from the Weigle formation and determined to be "tight." For this reason, much of the guard wall goes to great depths relative to the exposed height and follows an irregular profile at the base.

The permanent tieback anchors are high capacity strand tendons utilizing a double corrosion protection system. The maximum number of strands per tendon is limited to 11-0.6 inch diameter grade 270 strands due to the anchor bond capacity of the Weigle foundation. To minimize losses, ASTM A416 low-relaxation strands were specified. Forty foot bonded lengths were required by the specifications to begin a minimum of 10 feet beyond the critical slip-failure plane.

For protection of navigation traffic, precast panels were installed on the outboard face of all but the furthest downstream portions of the guard wall (Figure 3.2). Abrupt protrusions of concrete extending from the face of a diaphragm wall occurs when rocks or boulders have been torn from the sidewalls during panel excavation. Therefore, line drilling at the wall face to remove excess

concrete, plus installation of the panels, insure a smooth surface should any traffic run alongside the wall.

The landward side of the guard wall will have the water table drawn down to elevation 40 or below. This will be accomplished by a drainage system consisting of two concrete-lined, vertical shafts, 14 foot inside diameter, an array of 500 foot horizontal drain lines emanating radially from the shafts in two layers, and an 18-inch drain pipe to carry the water away from the shafts to the downstream end of the navigation lock. The purpose of this drainage system is two-fold: (1) to provide a stabilizing influence to counteract the potentially de-stabilizing channel excavation, and 2) to reduce the hydrostatic loads from the landward side of the guard wall.

A great deal of instrumentation is monitoring the guard wall; however, only the specifics relating to Panel 178 will be discussed. That discussion will be a part of section 3.2.4, Guard Wall Panel 178 Details.

3.2.2 Geology

The geology along the guard wall alignment is very similar to that of the temporary tieback wall. The guard wall intersects many known slides derived of the same types of materials retained by the tieback wall. Again, these materials

are slide debris (SD), reworked slide debris (RSD), Weigle formation (T_w), Bonney rock intrusive (T_i), and one other known as Slide Block (SB_w). Slide block is primarily large, essentially unmixed, competent Weigle formation displaced to its present position as a large block unit. It may be fractured, but generally is considered to have a low permeability.

Table 3.1 presents the soil parameters used in the design of the guard wall. Two other materials unique to the guard wall are river deposit (RD) and fill. The fill material consists largely of diabase rock approximately 1 foot to 3 feet in size and larger. It was placed at the toe of one slide unit in the 1940s to stop its movement.

3.2.3 Design Assumptions and Criteria

Two sets of criteria were established for the design of the guard wall: (1) deflection criteria, and (2) structural criteria.

The deflection criteria was based on keeping the risk of initiating a landslide a minimum and to control settlement of the Union Pacific's rail line. Deflection necessary for the soils to reduce to residual strength levels, thus potentially initiating a landslide, was considered to be on the order of 10 inches. Wall movements should be kept well below this amount to ensure that sliding does not

Table 3.1 Guard Wall Soil Parameters (From U.S. Army Corps of Engineers, July 1988)

Parameter	RSD/RD/Fill	SB_w/SD	T_w	T_i
Friction angle (degree)	30	25	30	50
Cohesion (psi)	0	0	10	10
Moist Unit Weight (PCF)	118	131	142.5	170
Saturated Unit Weight (PCF)	121	139	142.5	170
Constant of Subgrade modulus, moist (TCF)	18/36[a]	23	23	Rock Springs
Constant of Subgrade modulus, saturated (TCF)	13/26[a]	23	23	Rock Springs

LEGEND: RSD - reworked slide debris; RD - river deposit; SB_w - Weigle slide block; SD - slide debris; T_w - Weigle bedrock; T_i - diabase bedrock

a. The constants of subgrade modulus 36 TCF and 26 TCF were not from the above reference, but were added to reflect the recommendations for final design as put forth by Munger, Jones and Johnson (1990).

occur. Therefore, guard wall deflections were limited to what was necessary to minimize settlements at the railroad. Deflections and resultant settlements would likely occur over long reaches parallel to the guard wall due to the rigid, continuous cap beam. One rule-of-thumb used for the amount of settlement and the distance affected behind the wall is that the settlement would be equal to 0.7 times the deflection and this would affect a distance behind the wall 0.7 times the wall's structural height. The existing railroad line fell within that distance at only a few specific locations. However, the alignment for a second rail line is almost entirely within that reach.

The allowable wall deflection considered acceptable was established as follows:

1) 0.2 feet, riverward at all points on the wall for normal load cases.
2) 0.3 feet, riverward at all points on the wall for extreme load cases.

At locations where deflections exceeded the above requirements, judgment was used to consider acceptability. Load case descriptions will follow in later paragraphs.

Deflection estimates were to be based on CBEAMC, the soil-structure interaction program. The accuracy of the calculations of deflection based on this method has been considered questionable; however, based on the soil parameters selected, it was believed to be conservative.

Structural criteria reflects design procedures accepted by the Corps of Engineers for hydraulic structures and non-hydraulic structures. Hydraulic design criteria for Corps projects seeks to minimize cracking in the concrete structures, and to extend the service life of all concrete and steel elements of a structure. To summarize some of the essentials of hydraulic design criteria for concrete, the following requirements were considered from U.S. Army Corps of Engineers, Engineering Technical Letter ETL 1110-2-312 (1988) (superseded after completion of the guard wall by Engineering Circular EC 1110-2-26):

1) applied load factors were 1.5 and 1.9 (vs 1.4 and 1.7 in ACI 318-83),
2) strain was limited to 0.0015 at the extreme compression fiber,
3) a design stress limit of f_y = 48,000 psi was applied to ASTM A615 Grade 60 reinforcement.

Other design requirements were also applied in accordance with the above ETL.

Hydraulic design criteria for structural steel, as applied to the guard wall, limit the allowable design stress to 0.85 times AISC allowables.

Three types of load cases were applied to the design of the guard wall: (1) normal, (2) extreme, and (3) construction (wall exposed in the dry for a significant height). For the normal load case, full hydraulic design criteria were applied. For extreme load cases, a modified hydraulic design criteria applied. The nominal bending strength of reinforced concrete was based on f_y = 60,000 psi for grade 60

reinforcement. Additionally, a 50% overstress on the steel piles was allowed. For the construction load case, only ACI and AISC design criteria were applied since hydraulic conditions would not exist. Although temporary, the construction load case could exist for up to two years. The following load cases were considered:

1) normal load case,
2) extreme load case,
   a) drains failed,
   b) seismic
   c) lock gate failure, pool drawdown,
3) construction load case.

Each of the normal and extreme load cases (except 2c) was considered with maximum and minimum pool elevations, doubling the analysis effort.

Based on the above criteria, the factor of safety for the guard wall piles are as follows:

1) normal load case:

$$F.S. = \frac{F_y}{(0.85)(0.66)F_y} = 1.78 \quad (8)$$

2) extreme load case:

$$F.S. = \frac{F_y}{(1.5)(0.85)(0.66)F_y} = 1.19 \quad (9)$$

3) construction load case:

$$F.S. = \frac{F_y}{(0.66)F_y} = 1.52 \quad (10)$$

Normal calculation of the effective moment of inertia follows ACI Code equation 9-7:

$$I_e = (M_{cr}/M_a)^3 I_g + [1-(M_{cr}/M_a)^3] I_{cr} \quad (11)$$

where:

I_e = effective moment of inertia

M_{cr} = cracking moment of concrete

M_a = maximum moment in member at stage deflection is computed

I_g = moment of inertia of gross concrete section

I_{cr} = moment of inertia of cracked section

Because of variations with regard to tremie concrete and the variation in moment with height of wall, the determination of a correct effective moment of inertia (I_e) for the concrete is uncertain. Therefore, the design of the guard wall was evaluated for strength and deflection separately.

The analysis of the guard wall for strength purposes is based on a composite moment of inertia of

$$I = I_s + I_{e(tr)} \quad (12)$$

with $I_{e(tr)} = I_{g(tr)}$

where:

I = composite moment of inertia

I_s = moment of inertia for steel pile

$I_{e(tr)}$ = effective moment of inertia transformed to steel

$I_{g(tr)}$ = moment of inertia of gross concrete section transformed to steel

Since a stiffer wall will attract higher moments, and determination of the actual effective moment of inertia is uncertain, a conservative assumption was to set $I_{e(tr)}$ equal to $I_{g(tr)}$. The results of this analysis were the basis for sizing the steel piles. The strength of the guard wall is based solely on the capacity of the steel piles.

The analysis of the guard wall for deflection is based on a composite moment of inertia of

$$I = I_s + I_{e(tr)} \tag{12}$$

with $$I_{e(tr)} = I_{cr(tr)}$$

where:

$I_{cr(tr)}$ = moment of inertia of cracked section transformed to steel

This approach allowed minimum credit to the concrete for contribution to wall stiffness to resist deflection. The results of this analysis were the basis for determining if predicted wall deflections would be within the given criteria.

Design of the Area V panels as a tied-back wall assumed $I_{e(tr)}$ = zero, in effect ignoring the concrete in the original design models. This will be considered

during this study by comparing bending moments in the steel piles. Deflections will be addressed in the section on results.

3.2.4 Guard Wall Panel 178 Details

For this design verification, only Panel 178 in the guard wall will be studied. It was chosen since it is in the only area of the guard wall that has had sufficient excavation to date. All other locations along the guard wall will not have complete excavation until 1992-1993.

Panel 178 is located near the downstream end of the guard wall. In Figure 3.3, Guard Wall Design Regions, Panel 178 is located in Area V at the corner where the base of the wall jumps up. This is seen again in Figure 3.4, Area V Elevation, with bedrock, panels, and piles identified. Area V, like all of the guard wall, was designed based on a single row of permanent tiebacks located within the cap beam. However, the greatest exposed height of the guard wall, when all of the lock construction is complete, occurs at Panel 181 at the downstream end of Area V. The exposed height at Panel 181 will be 69 feet, from elevation 81 to elevation 12. Because the channel continues to deepen away from the wall towards the channel centerline, a concrete monolith was selected to span the channel and support the base of the retaining walls on each side. At the guard

wall, the base of this structure is at elevation -13 at its lowest point along the wall. A cofferdam upstream of the monolith permits construction of that structure in the dry.

To support the guard wall during construction of the monolith at the base, a temporary tieback wall design was required. Loads for the design were initially based on the pressure diagram of Figure 2.4. Tiebacks were located by using a tributary area of the pressure diagram to equal the maximum carrying capacity of an 11-strand tendon. The horizontal spacing of tiebacks was set at 8 feet, coordinating with a 4 foot spacing of the piles. The vertical spacing between rows of tiebacks varied with the pressure diagram. Table 3.2 shows the elevation of the rows of tiebacks. The final pile size was selected based on the final design condition of only one tieback row at the top and support from the monolith at the base.

Concrete reinforcement for the horizontal direction was considered based on the concrete acting as lagging. However, the size of the reinforcement selected was controlled by temperature and shrinkage requirements. The vertical reinforcement was designed only for temperature and shrinkage. Figure 3.5 shows the reinforcement details for all Area V panels, including Panel 178.

Piles B178 and B179 were installed to a final depth of elevation -38.7 which is 5 feet into Bonney rock. All Area V piles were W33 x 241 with cover plates to

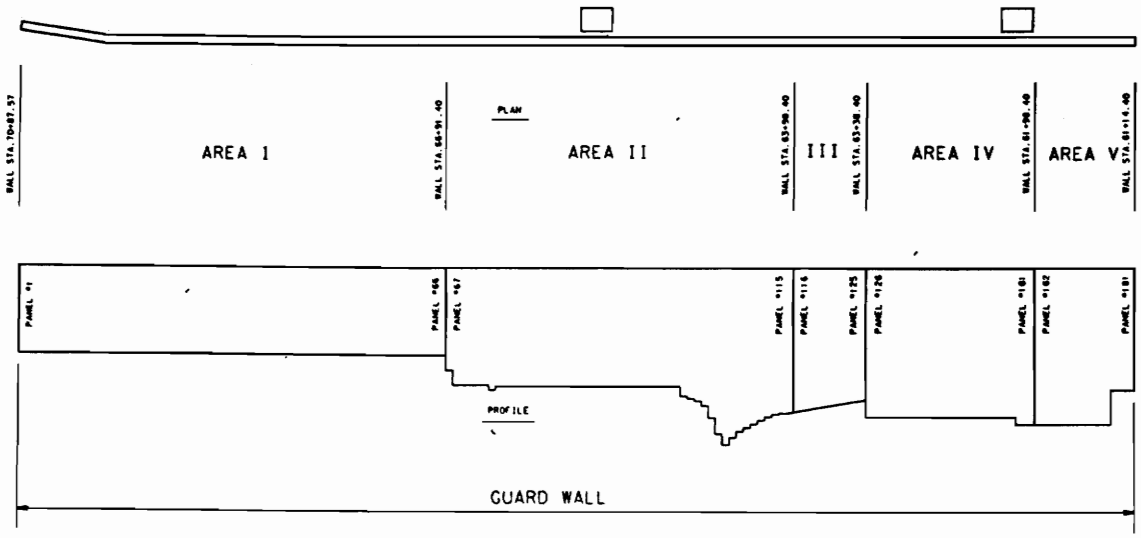

Figure 3.3 Guard Wall Design Regions.

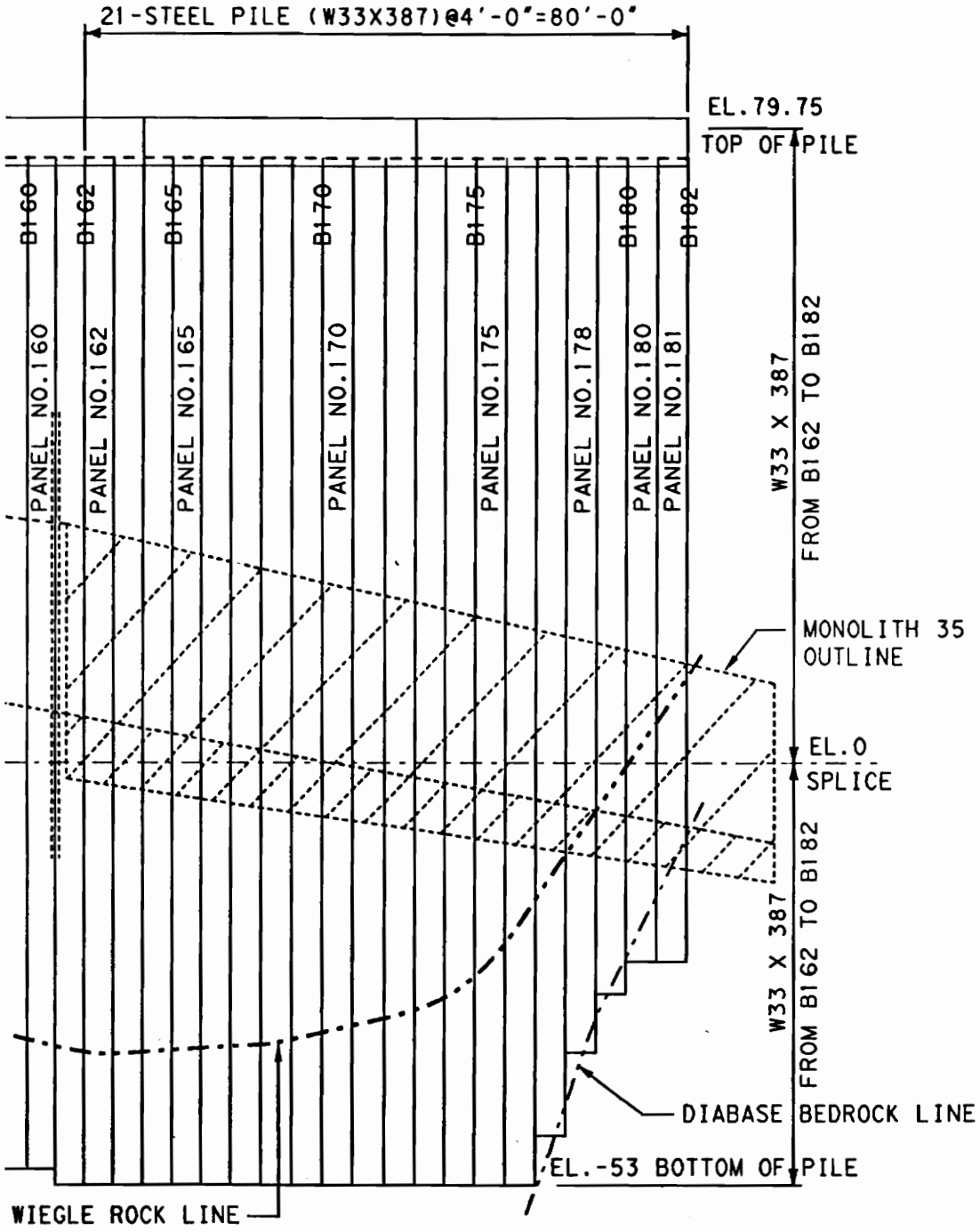

Figure 3.4 Area V Panel Arrangements.

Table 3.2 Tieback and Corresponding Strain Gage Elevations.

Tieback Elevation (ft)	Tieback Lockoff Date	As-Built Strain Gage Elevation (ft)
79	5/17/90	
		73.2
69	7/20/90	67.2
		62.2
59	9/11/90	57.2
		52.2
49	10/29/90	47.2
		42.2
39	12/5/90	37.2
		32.2
30	1/15/91	28.2
		24.2
22	1/30/91	20.2
		16.2
14	2/20/91	12.2
		8.7
7	3/8/91	5.2
		2.2
1	3/18/91	- 0.8
		- 3.8
-5	3/27/91	- 6.8
		- 9.8
-11	4/9/91	-12.8

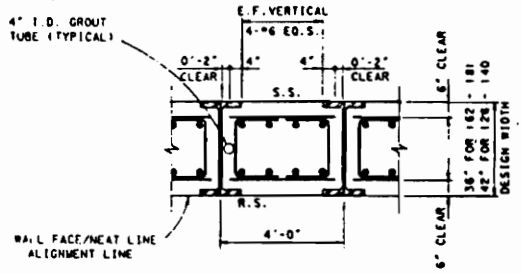

SECTION OF PANELS
126 - 140 & 162 - 181
NOTE: FOR PANEL 178 BLOCKOUT DETAILS, SEE DWG. BDN-2-2/47.

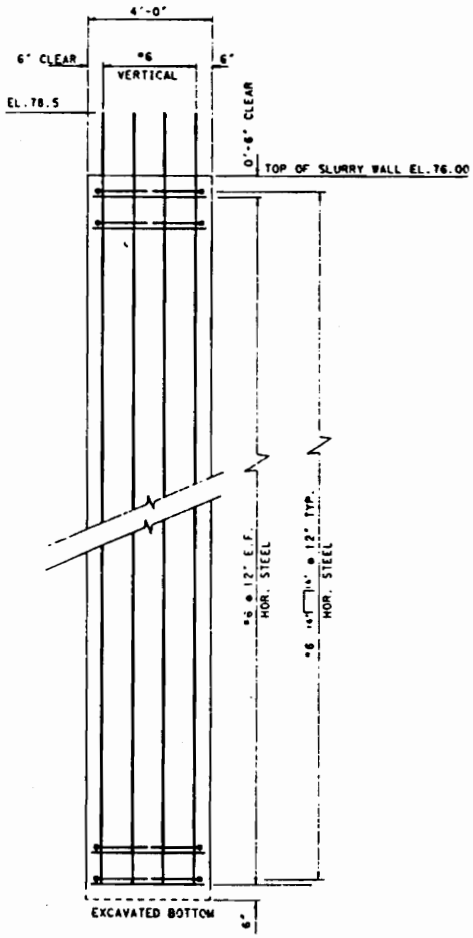

CAGE ELEVATION

Figure 3.5 Panel 178 Reinforcement Details

provide an equivalent section modulus of a W33 x 387.

Instrumentation was selected for a number of panels to monitor the activities of the guard wall. Panel 178 was selected because of the relatively large exposed height of Area V panels, and because it is away from influences that might be imposed on panels at the end of the guard wall by other structures. Those instruments associated with monitoring the guard wall at or near Panel 178 include: (1) a triaxial borehole transducer, (2) an EDM survey target, (3) two open-tube piezometers, (4) a slope inclinometer, and (5) a wall strain gage system. Data from the slope inclinometer will be interpreted to determine lateral displacements of Panel 178. Vibrating wire strain gages have been located on the inner face of both flanges of pile B178. The strain gages were located to correlate with the tieback anchor locations. One pair of strain gages (one on each flange) was located at the same elevation as each tieback anchor. Another pair was located midway between tiebacks. This was to capture the maximum and minimum flexural stresses experienced by the steel pile. The as-built location of the strain gage elevation are tabulated with the corresponding tiebacks in Table 3.1. The as-built locations indicate that pile B178 was placed 1.8 feet lower than the intended design elevations for the strain gages. The significance of the strain gages being 1.8 feet lower than was intended is not well known. This is partly

because the waler supports also spread the tieback load over the face of the pile approximately 2.75 feet.

The two piezometers located near Panel 178 are Z-40 (40 feet south) and Z-29 (65 feet south). Piezometer Z-40 was inadvertently grouted in mid-November 1990. Z-29 was destroyed on 30 January 1989. The last readings from Z-40 indicated the water table was approximately elevation 30 and dropping. This places the hydrostatic load to Panel 178 well below the excavation level at that time. During excavation, weep holes were drilled through Area V panels of the guard wall to ensure that hydrostatic pressures were not present. The weep holes act as a backup to the dewatering plan for the tieback walls.

3.3 Slurry Construction Process

During preliminary engineering of the upstream approach to the new Bonneville Navigation Lock, at least two major problems were apparent. One was the close proximity of the Union Pacific Railroad, and the other was the geologic conditions at the site. Because the railroad is so close to the wall alignment (even after being relocated), laying back the slope and construction of conventional buttress walls or gravity monoliths were not viable options. Further, the abundance of boulders and cobbles precluded the use of sheetpile cells. In one area, where a slide had been

creeping (known as the Railroad Slide), the local soil was removed and replaced by rock fill in the 1940s. One option that did look viable was the slurry construction method used to build structural bearing and retaining walls.

Most slurry wall construction in the United States is for seepage cutoff purposes. This method is to be used again in creating a cofferdam from in-situ soils in a limited space at the upstream end of the new Bonneville Navigation Lock. However, it is the use of slurry "diaphragm" walls that made possible the channel alignment at the upstream end of the navigation lock. A slurry diaphragm wall is a structural wall designed for bearing or for retaining soils. The structural characteristics are what distinguishes diaphragm walls from slurry "cutoff" walls which control seepage and may or may not contain concrete.

The construction process for a diaphragm wall (see Figure 3.6) can have many variations, but typically it is as described below. Guide walls (not shown) are constructed for guiding the alignment of the "clamshell bucket" to be used. The clamshell will excavate a vertical slot known as a "panel" (Figure 3.6A). As the clamshell excavation proceeds downward, the panel is maintained open by a bentonite water slurry. This slurry, kept at a level a few feet above the local water table, and having a unit weight somewhat greater than water, provides a positive hydrostatic pressure on the side walls of the panel. Stop end tubes (Figure 3.6B) are placed at one or both ends of the panel to form guides for the clamshell for

excavating adjacent panels, and to provide interlocks between completed panels. Once the panel has been excavated to its designated depth, a reinforcement cage is lowered into the slot and dogged off into place (Figure 3.6C). A tremie pipe is then directed to the bottom of the panel and concrete placement begins (Figure 3.7D).

The concrete must have high flowability and a set-up time sufficient to allow the placement to be completed. It is important that the set time is extended to avoid problems with delayed fresh concrete mixing with already-placed concrete. As concrete is tremied into place, the slurry is displaced and is removed at the surface. The tremie pipe is always to remain embedded well below the surface of the concrete to insure vertical flow of an even surface. It is important that the stop end tubes are not removed too early or too late. It is not required that the panel concrete placement be completely finished prior to pulling of the stop end tubes; however, the tubes must always be at a depth below where the concrete is still fluid. Therefore, pulling of the stop end tube part way to keep the bottom from becoming stuck with the hardening concrete, while the top still retains fluid concrete, is common practice. Pulling the stop end tube too soon will allow concrete to slump into the cavity left by the tube. Pull it too late, and the tube may become stuck, requiring hydraulic jacks to remove it.

After the first panel is complete, the remainder of the wall is completed by excavating every other panel, termed primaries, and then completing the panels

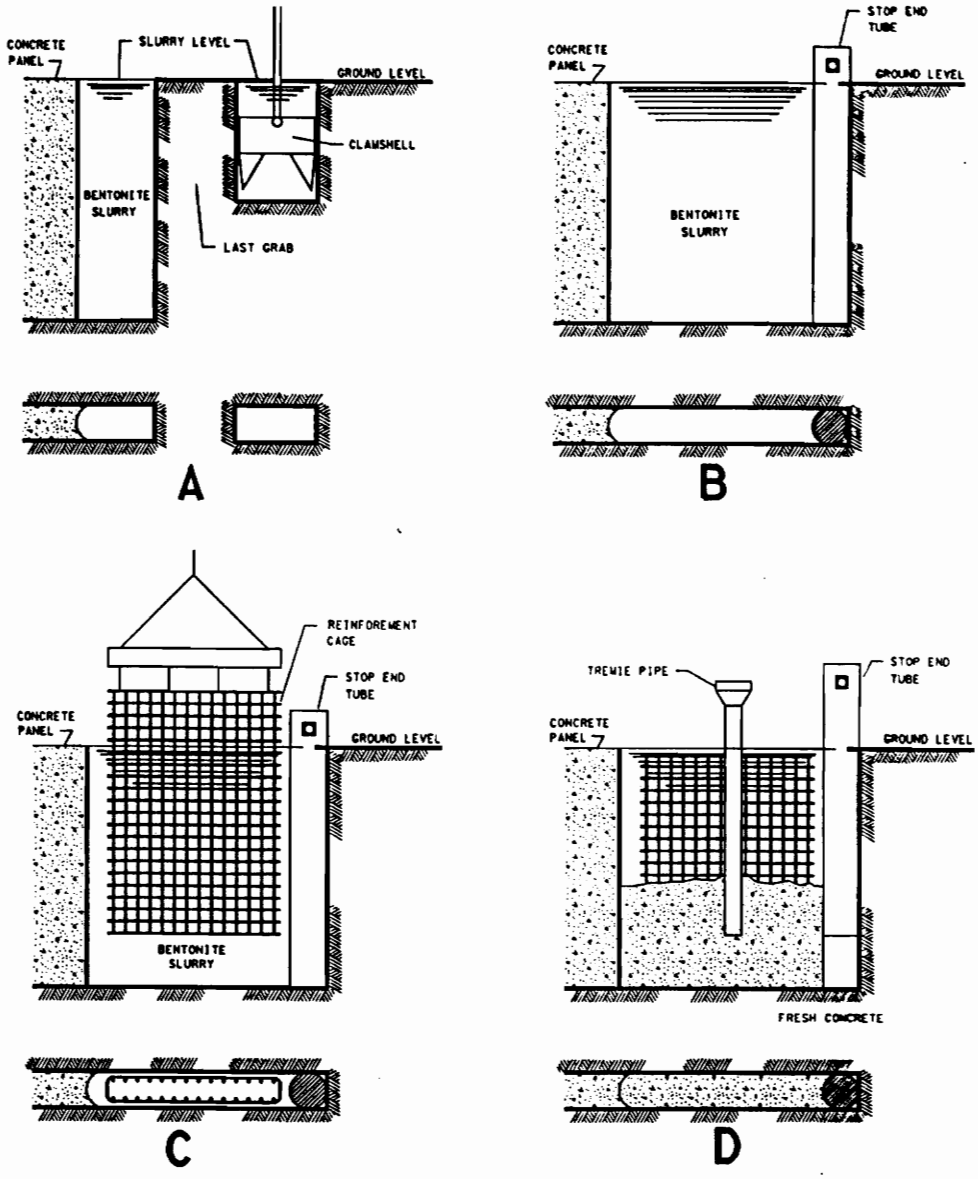

Figure 3.6 Construction Process for a Diaphragm Wall.

between the primaries, termed secondaries. The round formed ends of the primaries, due to the stop end tubes, are used as guides for the clamshells while excavating secondaries. An alternative and commonly used procedure is to construct the first primary and then construct adjacent panels sequentially using the previous panel as the guide. An alternative to a reinforced concrete wall is to use steel piles lowered singly or in pairs into the excavated slurry trench. The concrete tremied in place between the piles serves as lagging. The flanges of the piles also serve as guides for the clamshell excavating secondaries, thus eliminating the need for stop end tubes. This type of wall was used at Bonneville for the guard wall. (See Figure 3.7).

For design of slurry diaphragm walls at Bonneville, certain recommendations have been followed (Xanthakos, 1979). In general, the recommendations are conservative when dealing with the uncertainties of slurry concrete walls. First of all, a 15-percent reduction was taken for the design strength of the concrete. Secondly, generous lap lengths of 1.5 to 2.0 times the normal splice lengths are recommended for concrete reinforcement. The laps for this project were increased by a factor of 1.8, which was applied to the development length.

Other recommendations concern the constructability of slurry wall panels. Because concrete must flow through and around reinforcement and displace the bentonite slurry, it is important that the flow not be restricted or the restrictions be minimized. Therefore, spacing of reinforcement should be maximized. For vertical

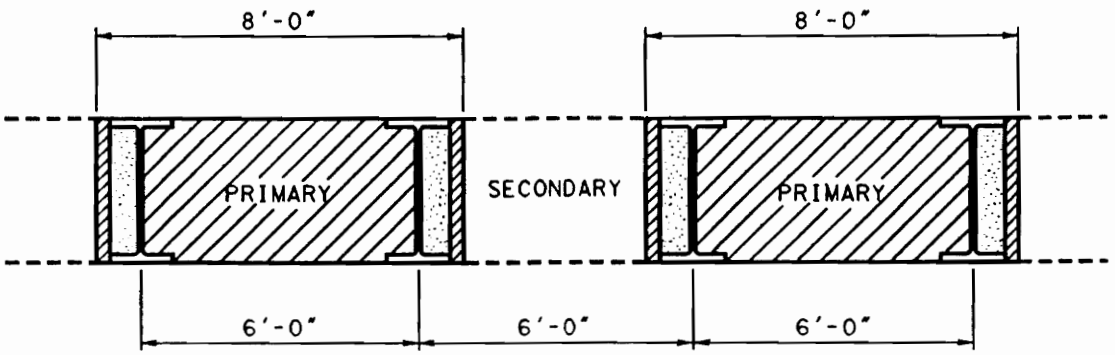

Figure 3.7 Steel Pile Alternative for Diaphragm Walls.

reinforcement, the minimum spacing recommended is 6 inches and preferably 9 inches. For horizontal bars, the minimum spacing recommended is 12 inches. In addition to good bar spacing is the flowability of the concrete. One measure of flowability is its slump. A slump of 7 to 8 inches minimum is recommended. Slumps of 9 to 10 inches were measured during concrete placement in the Diaphragm Walls contract. Spacing of the reinforcement also must allow for insertion of a 6- to 10-inch tremie pipe between bars. Some contractors have said joints on the tremie pipe may be oversized and may require up to 14 inches of space, but this was not observed.

3.4 Description of CBEAMC Models, Panel 178

Two CBEAMC models were considered for the study presented here. The first model was the original design model representing the perceived conditions at the time. The second model represents the as-built conditions of Panel 178.

As discussed in Section 2.3.1, CBEAMC Model, P-Y curves representing soil springs, concentrated springs for the tieback anchors, and rock springs were developed for each of the models.

Both models represent specific stages of excavation and tieback installation for the guard wall as a tieback wall. The original design model will be used to compare the

predicted results for four stages with the measured results. The as-built model will then be compared with the original design model and the measured results at one stage only. This stage, Stage 6, represents the stage at which the greatest amount of excavation was complete for which instrument data was available. The as-built model will then have the soil modulus modified by l_h x 2 and l_h x 3 to compare the results of increases in the soil stiffness to the measured results. This is similar to the calibration procedure conducted on the temporary tieback wall.

The comparisons should indicate the validity of the original design calibration and verify the adequacy of the present structure.

3.4.1 Original Design Model

After examining several variations of load conditions, soil profiles, and pile depths that represented different parts of Area V, one design configuration was selected as the controlling design load case. For the original design model, Figure 3.8 shows the pile embedded to elevation -25. The soil behind the wall is RSD to elevation +4, changing to Weigle (T_w). Both sides of the wall are dewatered to the top of the Weigle formation. Therefore, the wall was primarily loaded by moist RSD, similar to Panel 6 in the CBEAMC calibration.

Deflections of the Area V panels, while supported as a tieback wall, were not expected to exceed the deflections when supported by a single tieback at elevation +79 and the monolith at elevation +10. Therefore, analyses were run ignoring the composite effects of the concrete with the piles.

3.4.2 As-Built Model

The "as-constructed" Panel 178 is embedded to elevation -38.7. From excavation records, Weigle is estimated to be from elevation -29 to -37 where the panel embeds approximately 2 feet into Bonney rock (Figure 3.9). The original wall design specified W33 x 387 piles spaced at 4 foot centers with 4000 psi concrete. The as-built wall contains W33 x 241 with 1" x 17" cover plates and 7000 psi concrete. This model also accounts for the concrete which will affect the predicted moments and deflections. A composite strength due to the steel pile and the concrete was iterated to an effective moment of inertia when bending moments exceeded the cracking strength of the concrete.

Being an as-built model, the predicted characteristics of Panel 178 should better represent the actual performance and should more closely match the measured results.

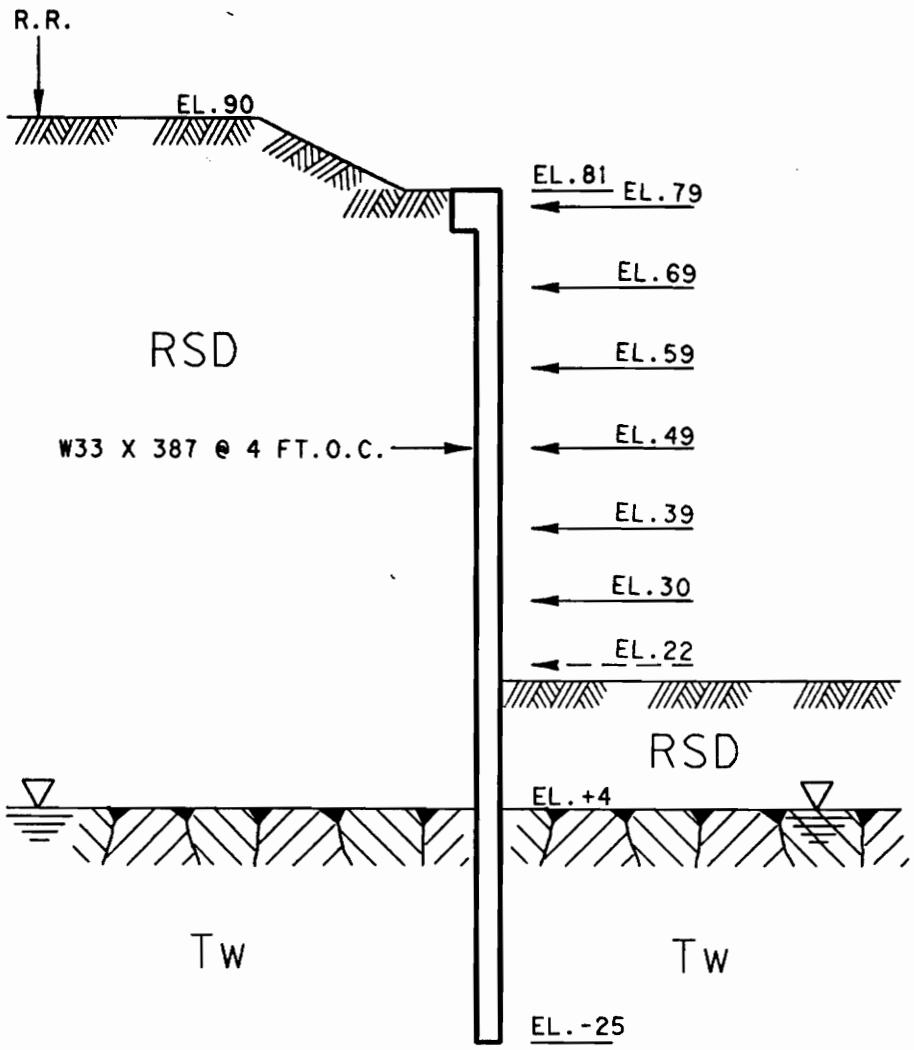

Figure 3.8 Original Design Model, Stage 6.

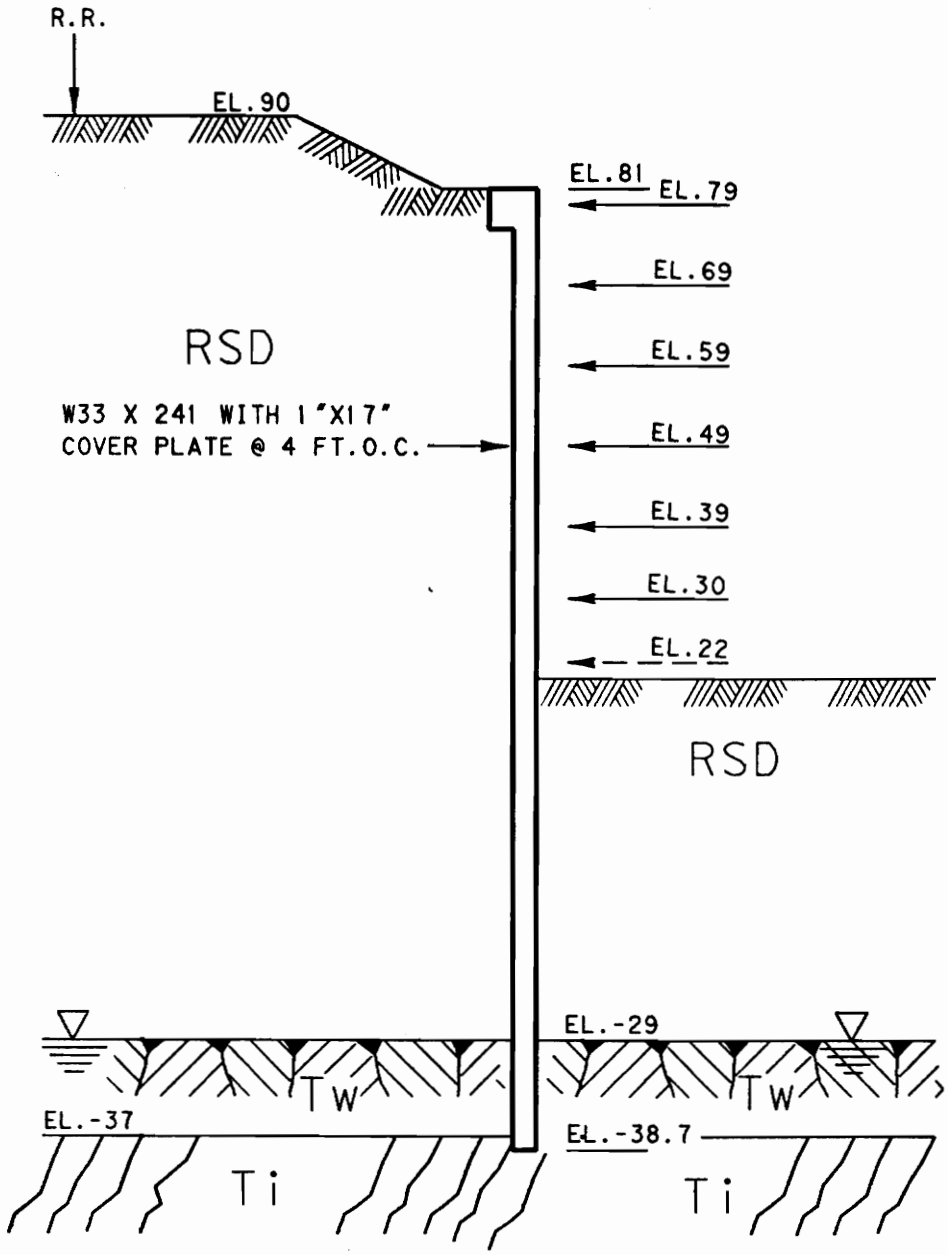

Figure 3.9 Panel 178, As-built Model, Stage 6.

3.4.3 Construction Stages

As excavation proceeded in front of the guard wall, rows of tieback anchors were installed at regular intervals. Excavation was specified to proceed no more than 2 feet below the next row of tiebacks to be installed. As shown in Figures 3.8 and 3.9, a tieback at elevation +22 is next to be installed. Therefore, excavation stopped at elevation +20. It is during this waiting period for a tieback to be installed that the greatest unsupported height exists. This occurs for each row of tiebacks installed and is identified as a "construction stage." Table 3.3 shows the four stages studied, with the last tieback row installed for that stage identified. Also shown is the elevation of excavation, the file names of the CBEAMC files modeling each stage, and the date of reading of the instruments best representing that stage.

Shown in the as-built column are files SQ6NE, SQ6DE, and SQ6TE, all modeling Stage 6. SQ6NE is the as-built model with l_h = 18 pci, (l_h x 1), the same as used in the original design models. SQ6DE uses a doubled soil stiffness, l_h x 2, and SQ6TE uses a tripled soil stiffness, l_h x 3.

Table 3.3 Construction Stages.

Stage	Excavation Elevation	Last Tieback Installed	Original Design File Name	As-built File Name
3	+ 47	+ 59	SEQ3	-----
4	+ 37	+ 49	SEQ4	-----
5	+ 28	+ 39	SEQ5	-----
6	+ 20	+ 30	SEQ6	SQ6NE, SQ6DE, & SQ6TE

	Strain Gage Reading Date	Slope Inclinometer Reading Date
3	20 Sep 90	24 Oct 90
4	26 Nov 90	27 Nov 90
5	07 Jan 91	14 Jan 91
6	15 Jan 91	30 Jan 91

3.5 Verification Results

The initial review of the predicted results from the original design models was concerned with determining if the models were reasonable. Likewise, the review of the measured results should consider if they make sense or if the results follow an unexpected pattern. In review of the graphed results, bars with elevations were added at the elevation of the rows of tieback anchors. They aid the reviewer to see responses in the graphs, and where the influence of each tieback acts in that response to make sure the results make sense.

All of the measured moments are moments calculated from the measured strains in the piles. Because composite action will exist between the piles and the concrete, it can be reasonably assumed that the concrete will also carry flexural stresses. Also, if the concrete and piles strain together, as they should, then the moment carried by the concrete could easily be calculated as long as it remained uncracked. If the concrete remains uncracked, then calculations show that the concrete carries 55% of the moment in the composite member, and the steel piles carry 45%. For direct comparisons, only the proportion of moments carried by the steel piles will be considered. This is necessary since the original design models do not assume composite action. The as-built models are analyzed with the composite wall stiffness

and the proportion of moment attributed to the steel piles graphed for comparison with the measured and original design model.

3.5.1 Original Model Results

Figure 3.10 shows the deflections predicted by the original design models, SEQ3 through SEQ6. SEQ3 represents Stage 3 of the wall excavated to elevation +47 with tiebacks installed at elevations +79, +69, and +59 (Table 3.3). SEQ4 represents Stage 4, SEQ5 represents Stage 5, and SEQ6 represents Stage 6 with excavation to elevation +20 and tiebacks installed from elevations +79 to +30. The deflections for Stages 3, 4, and 5 show a gradual increase which could be expected with the increasing exposed wall height. However, SEQ6 indicates a slight decrease in deflection. Another general observation is that a significant deflection into the retained soil occurs in the upper ⅓ of the wall. It appears the upper portion of the wall has been forced into the retained soil by the tiebacks imposing pressures greater than at-rest soil pressures on the wall. The ratio of deflection to excavated height predicted by the model is approximately 1"/60' or 1"/720". This is 0.139% and is comparable to ratios mentioned by Mosher and Knowles.

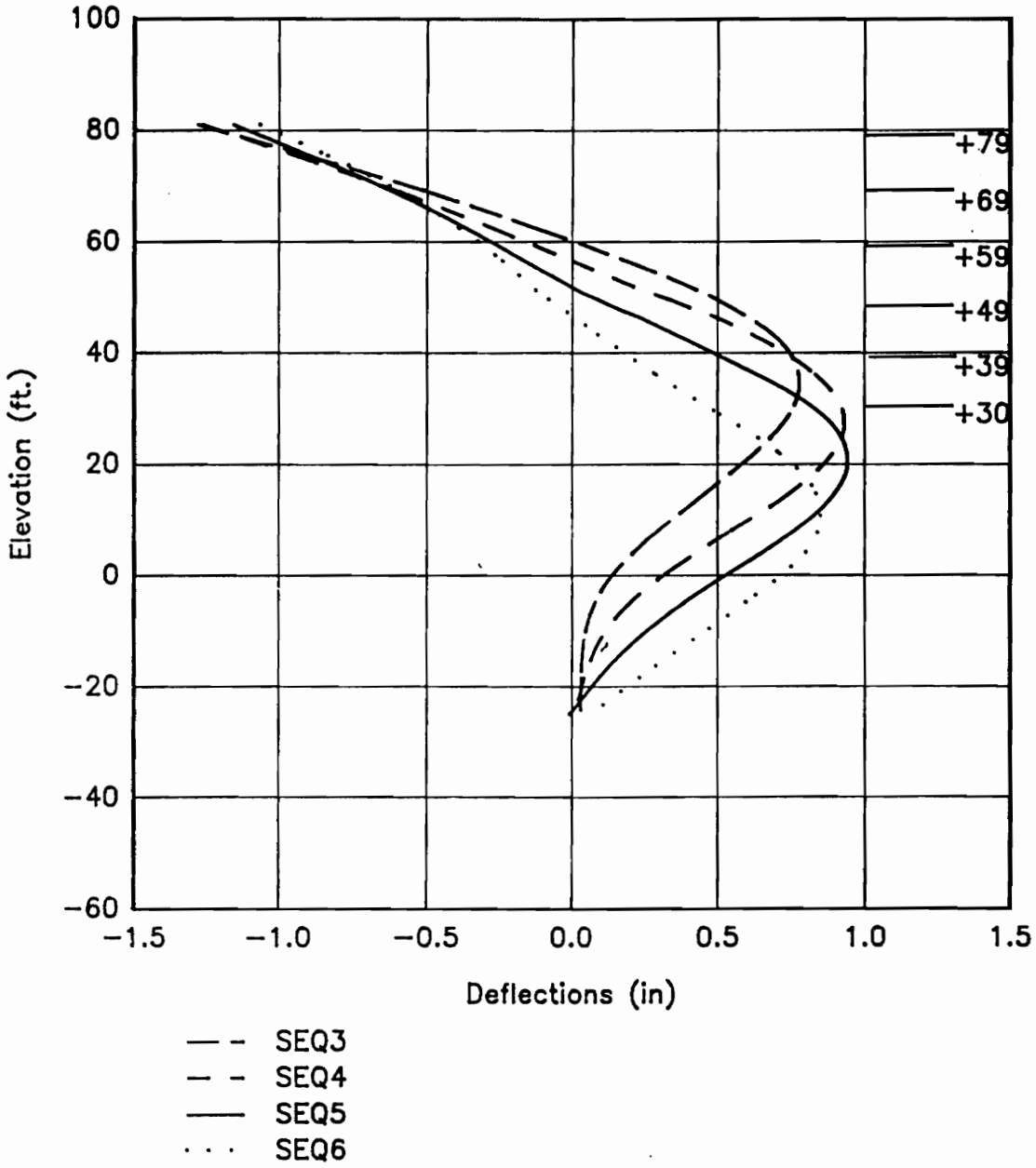

Figure 3.10 Pile B178 Original Design Deflections.

Figure 3.11 shows the measured deflections. The trends of the measured deflections correlate well with the original design models (indicated in parenthesis). As indicated in SEQ3, SEQ4, and SEQ5, lateral deflections trend toward the excavation. Then, as predicted in SEQ6, the lateral movement is away from the excavation slightly. Two differences between the predicted movements and the measured movements exist. First, the measured movements do not have the same negative deflection in the top ⅓ of the wall. Only the top 5 feet of the wall exhibited any negative deflections. Second, the magnitude of the overall deflections are about one-fifth those predicted.

The predicted moments for the original design models are shown in Figure 3.12. The predicted moments follow a distinct pattern as excavation progresses from stage to stage. Three distinct characteristics of these patterns can be identified. First, for each stage below the last tieback installed, the wall experiences a large, negative moment of almost 300 foot-kips, followed by a smaller, positive moment. Second, for all stages, the top 20 feet experienced negative moments on the order of 50 to 100 foot-kips. Finally, as each tieback anchor is installed, the wall experiences localized jumps towards the positive at the tiebacks.

In Figure 3.13, the measured moments share two characteristics observed in the predicted moments. First, the top 20 feet experienced measured negative

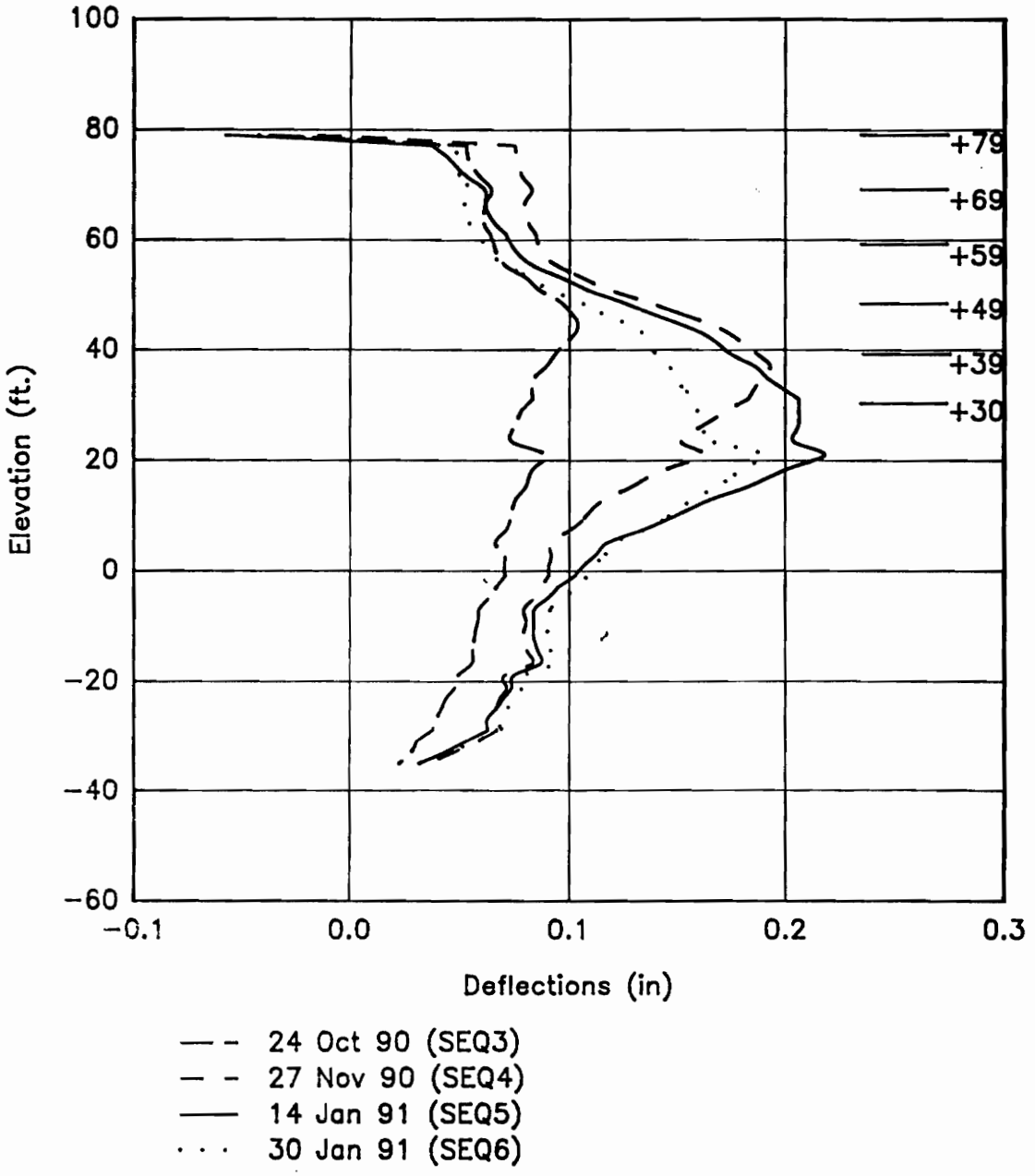

Figure 3.11 Pile B178 Measured Deflections.

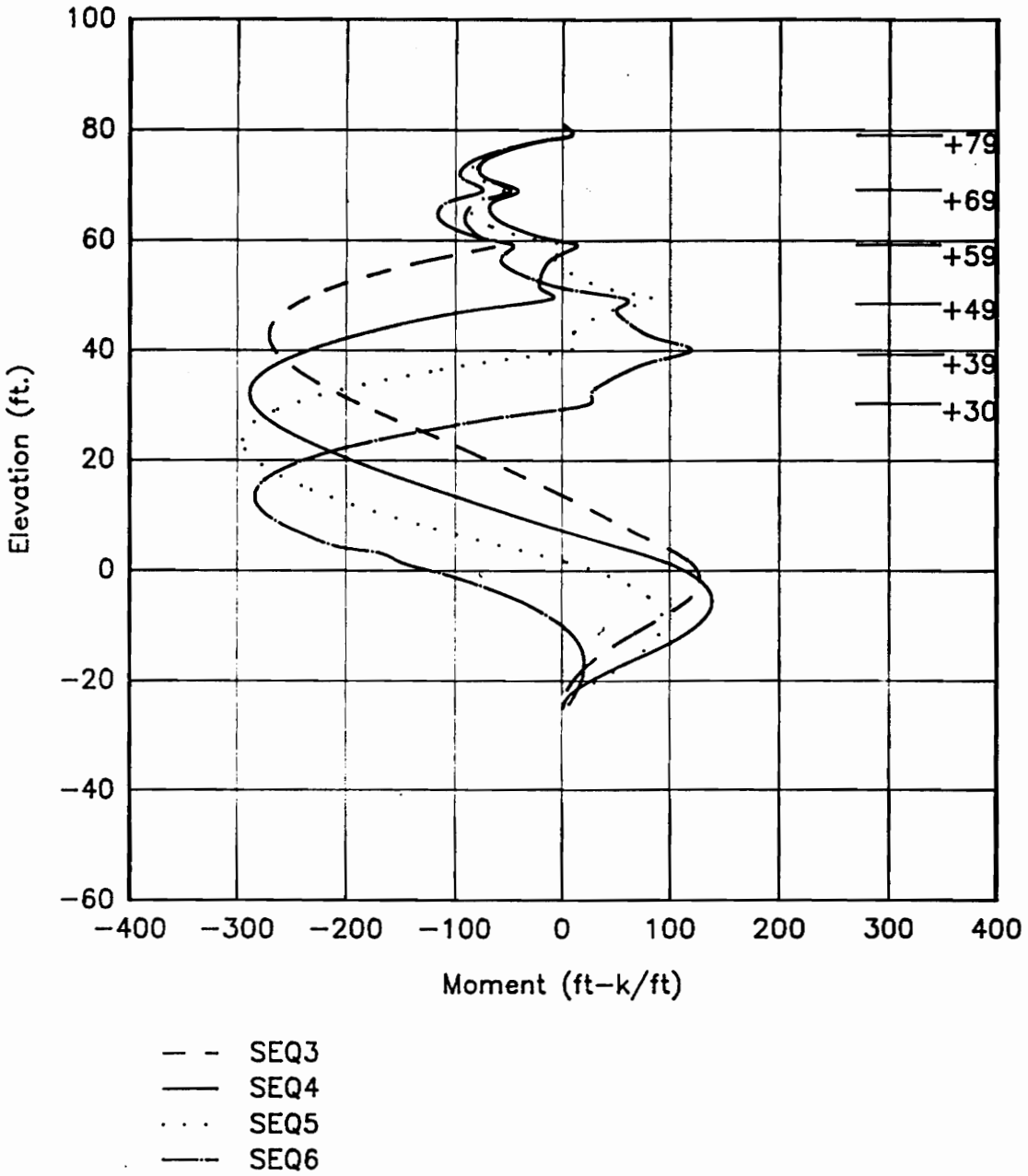

Figure 3.12 Pile B178 Original Design Moments.

moments which agree with the predicted values of 50 to 100 foot-kips. Secondly, the wall is shown to experience jumps towards the positive at the locations of tiebacks.

The most significant observation in Figure 3.13 is the lack of a tendency for a large negative moment as predicted in the original design models. In fact, below the excavation level, very little trend is exhibited. Stages 4, 5, and 6 had small positive moments measured from elevation +20 to -5, but these measurements are not consistent with the predictions.

Although the moment comparisons seem inconclusive at this point, the deflections seem to correlate fairly well, and the original design model is reasonable.

3.5.2 As-built Model Results

The as-built model is established based on actual field conditions, the actual wall dimensions, material characteristics, etc., and Stage 6 excavation for simulation of the greatest exposed wall height. Figure 3.14 compares the deflection results of the as-built model with the original design model and the measured deflection. The shape of the results of the as-built model is very much like the original design model. However, rather than more closely matching the

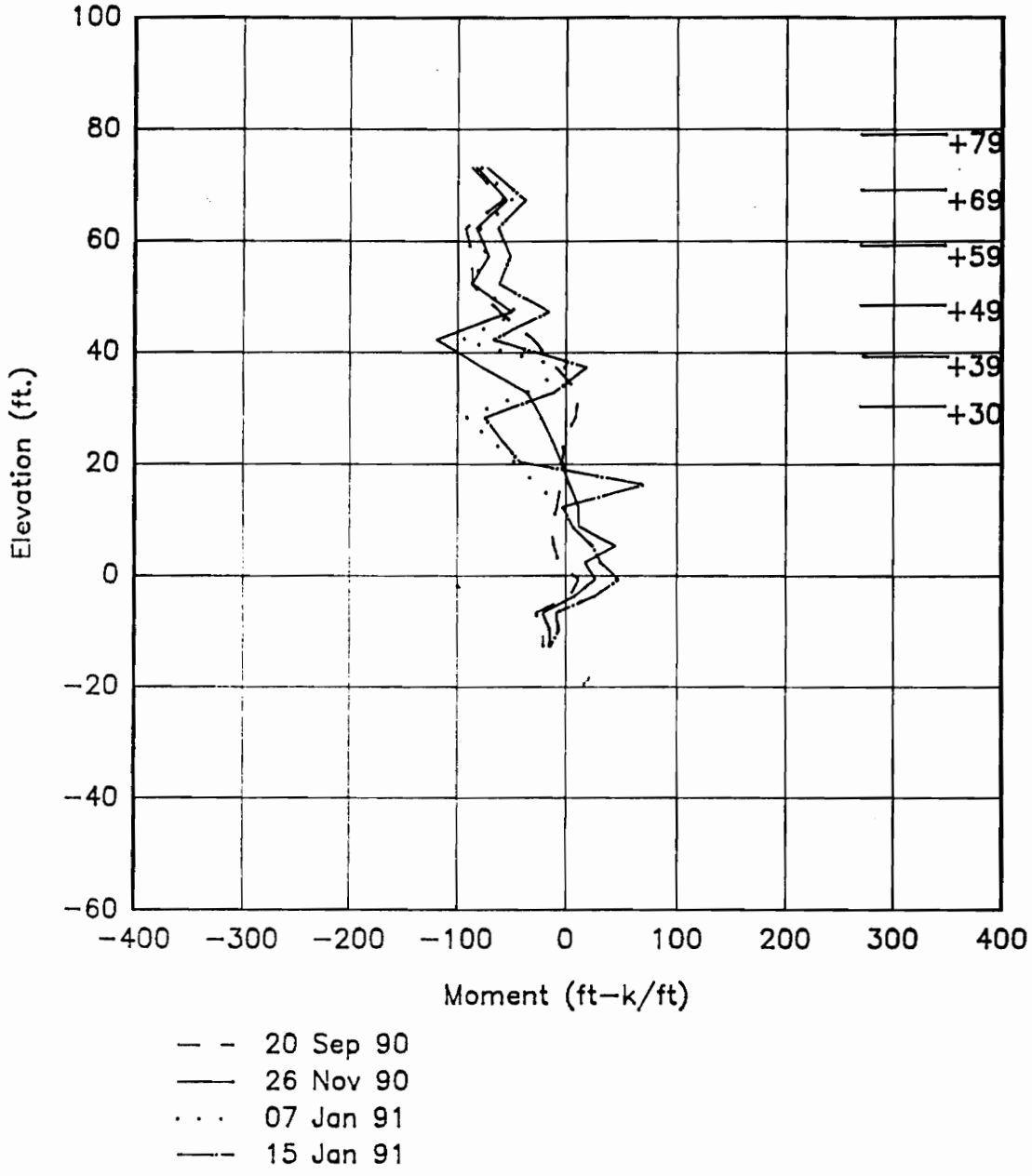

Figure 3.13 Pile B178 Moments, Based on Measured Strains.

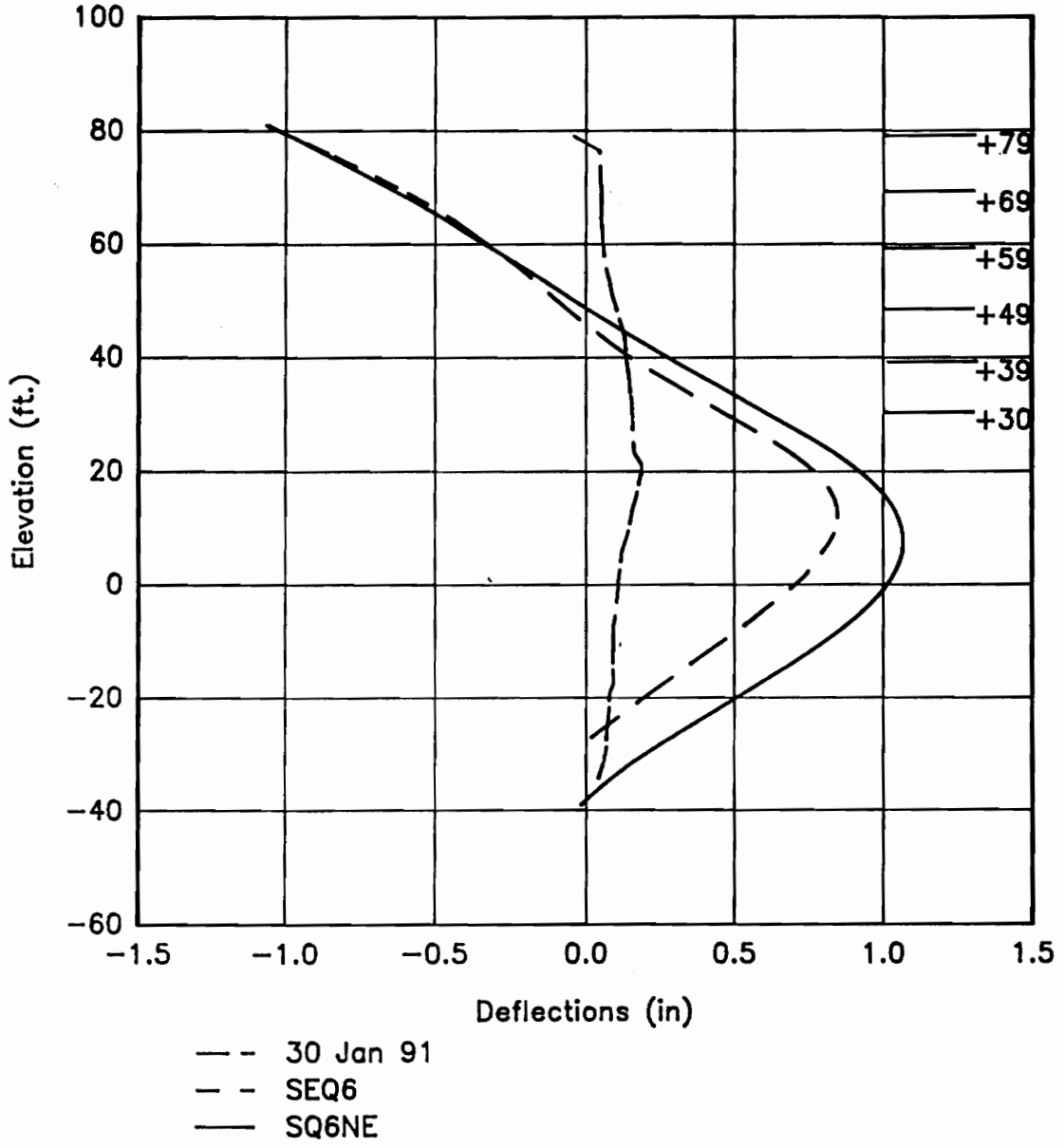

Figure 3.14 Pile B178 Stage 6 Deflections.

measured results, the as-built model actually shows more overall deflection towards the excavation. The top ⅓ of the wall nearly mirrors the original design model prediction. The most probable reason for the increase in predicted deflection in the lower ⅔ of the wall by the as-built model is that the Weigle bedrock is founded at elevation -29 rather than at +4. Also, the as-built pile length is 120 feet instead of the 106 feet used in the original design model. Deflections typically are proportional to the third power of length for a simply supported beam with a triangular loading, which may be what the wall is similar to below the last row of tiebacks.

Both SEQ6, the original design model, and SQ6NE, the as-built model, use l_h = 18 pci (l_h x 1) for modeling the soil stiffness. Deflection towards the excavation predicted by SEQ6 is approximately four times the measured deflections. Deflection predicted by SQ6NE is approximately five times the measured deflection.

Figure 3.15 more clearly demonstrates the differences between the predicted moments and the measured moments. The top 20 feet of the wall show similarity between measured and predicted results. Response to the tieback anchors correlates well between the measured and predicted results. However, below approximately 25 feet from the top of the wall, the measured results differ in both magnitude and sign from the predicted results.

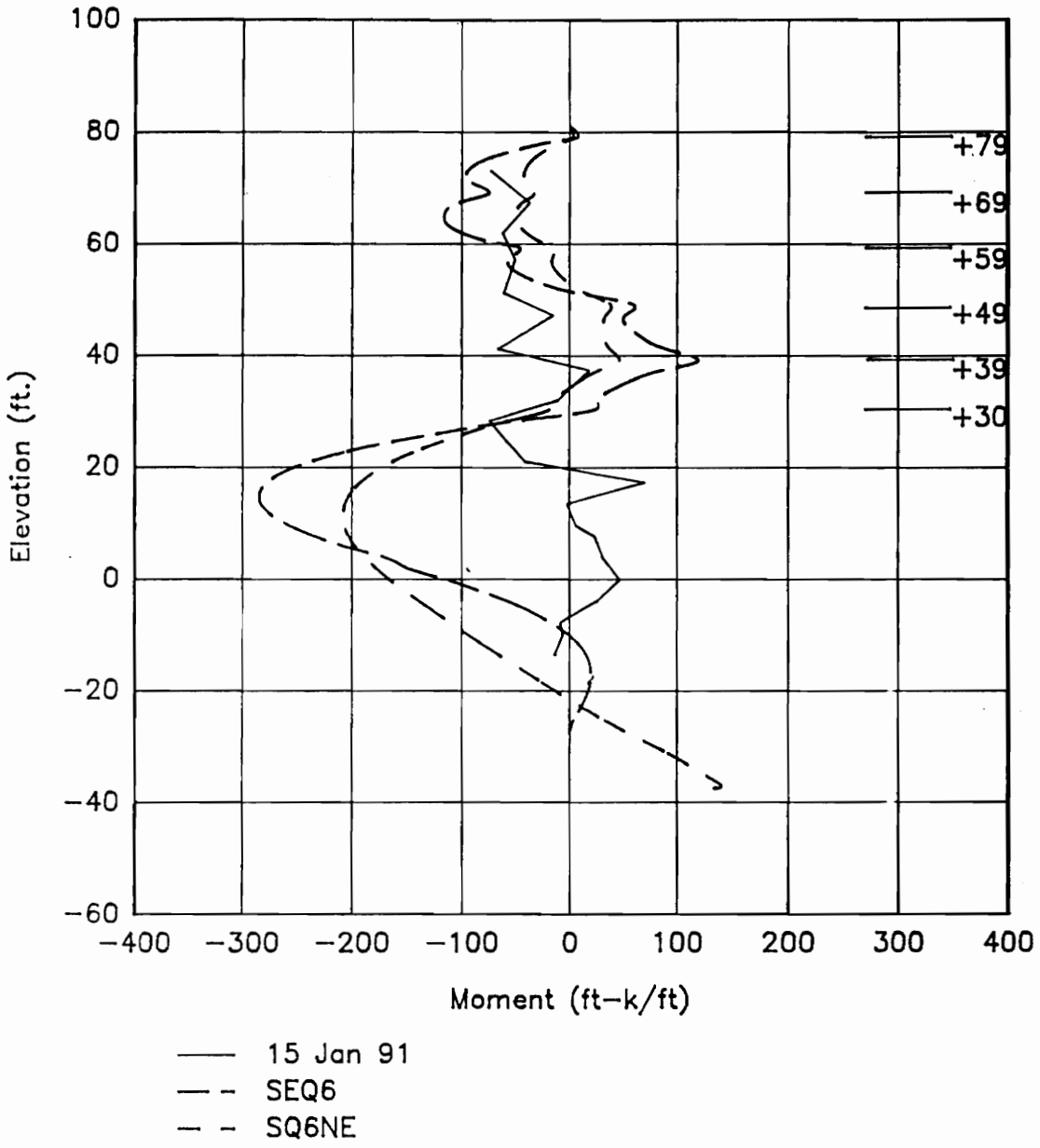

Figure 3.15 Pile B178 Stage 6 Moments.

The as-built model compares well with the original design model. SQ6NE incorporates the composite wall stiffness into the analysis, and the proportion of moment carried by the steel piles is plotted to compare with SEQ6 and the measured results. Even with the stiffer wall, the steel pile of the as-built model carries less moment than the original design model. The reduced moment in the as-built model is consistent throughout the height of the wall.

As was done by Munger, Jones and Johnson, and by Mosher and Knowles, the soil stiffness was increased for this study. The recommended soil stiffness for the design of the guard wall was originally l_h = 18 pci for moist RSD. After the CBEAMC calibration study was complete, a new recommended value for soil stiffness was l_h = 36 pci (l_h x 2). An increase to l_h = 54 pci (l_h x 3) was considered but not used. For the construction stage analysis of Area V panels, the tieback wall design did not control the final design; therefore, l_h = 18 pci had not been changed in any SEQ files.

Figure 3.16 shows a comparison of deflections of the as-built model with l_h x 1, l_h x 2, and l_h x 3, soil stiffness increases. Also, the measured deflection is plotted to indicate how closely the predicted deflections match the real. The tripled soil stiffness reduced deflections to approximately 0.5 inch. This is roughly twice the measured deflection. Twice the magnitude would seem still to be a large difference. However, 0.5 inch predicted deflection compared to 0.2 inch

measured deflection in a 60-foot exposed wall height is a good comparison. The ratio of deflection to excavated wall height for the measured results is 0.026%. The ratios for the predicted results are 0.147%, 0.093%, and 0.069% for no increase in soil stiffness, doubled soil stiffness, and tripled soil stiffness, respectively.

Figure 3.17 shows a comparison of the predicted moments for increased soil stiffness, and the measured moments. The doubled soil stiffness indicates a reduction in maximum moments by 29%. The tripled soil stiffness indicates a reduction in maximum moment by 42% from the original soil stiffness model. As expected, the shapes of the predicted moment diagrams were similar.

3.6 Conclusions

(1) The design of Panel 178 as a tied-back wall is based on the original design model. Of the stages of construction for which instrumentation data was available during this study, stage 5 (SEQ5) of the original design model predicted the highest bending moment of 296 foot-kips. The largest moment based on strain in the steel piles is 110 foot-kips, slightly more than ⅓ the predicted amount. The greatest deflection was also found during stage 5 measured at slightly more than 0.2 inch into the excavation. This is far less

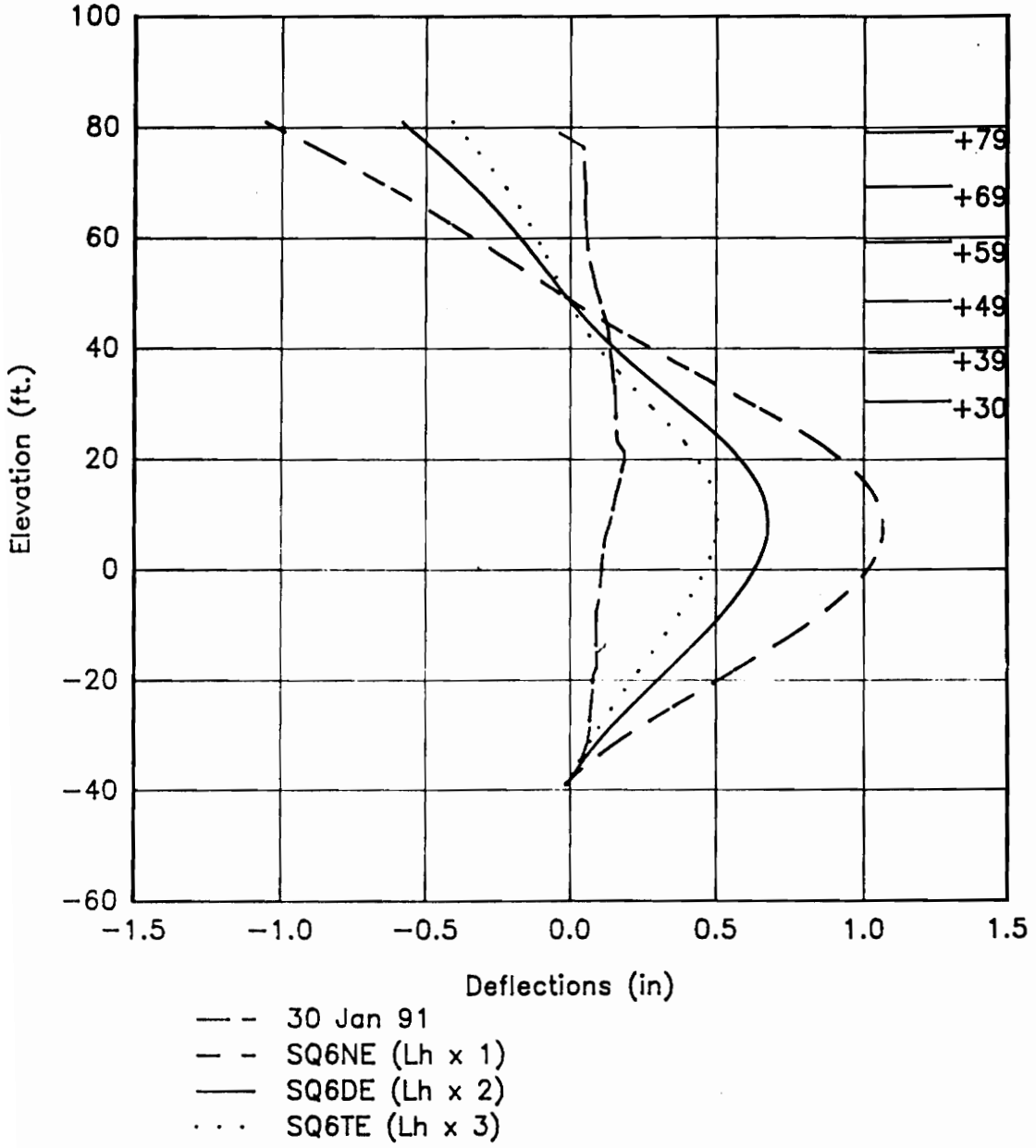

Figure 3.16 Pile B178 Deflection vs Soil Stiffness.

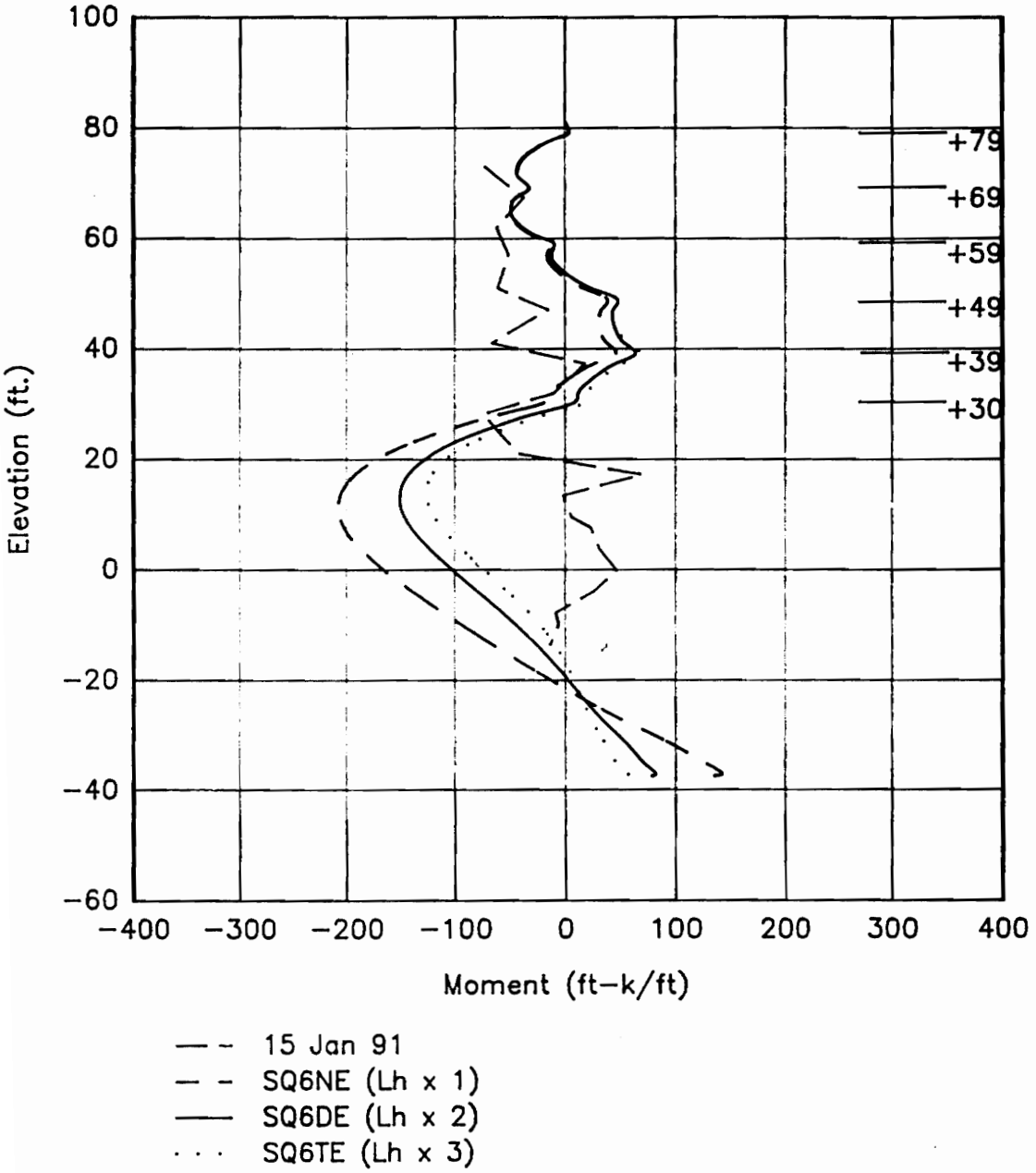

Figure 3.17 Pile B178 Moment vs Soil Stiffness.

than the 0.2 foot (2.4 inches) maximum allowed. Based on the results of this study the design of the guard wall at Panel 178 using the applied original design model is structurally adequate.

(2) The trends indicated by comparing deflections of the original design models (Figure 3.10) with the measured deflections (Figure 3.11), and the relatively small difference in magnitude of deflections between the as-built model with l_h x 3 and the measured deflections (Figure 3.16) indicate the CBEAMC models are reasonable. In terms of deflection, the final design for AREA V panels as a tieback wall could have been based on CBEAMC using l_h x 3 or higher as indicated by Munger, Jones and Johnson.

(3) The slight decrease in deflection at stage 6 of excavation was probably due to the decrease in vertical spacing of tiebacks beginning with the elevation +30 tiebacks. Also, less excavation was performed in preparation for the +22 tieback. Both model and measured deflections realized this decrease in deflection demonstrating proper correlation.

(4) Agreement between the predicted and measured results for moments is difficult to identify. However, some conclusions can be arrived at considering the studied wall.

Moments in the existing wall are based on measured strains in the steel piles. For direct comparison with the predicting models only the moments carried by the steel piles were considered (see paragraph 3.5). Moments in the top 20 feet of the wall agreed fairly well with the predicting models. By back-calculation, those moments in the top 20 feet of the existing wall, as well as the rest of the wall below, indicate the concrete did not exceed the cracking moment of M_{cr} = 135 k-ft/ft. Therefore, proportioning the moment to the steel pile (45%) and the concrete (55%) to analyze the fully composite existing structure is a reasonable approach.

(5) Moments predicted in the as-built models exceeded the cracking moment and therefore required an iterative process to determine the correct composite moment of inertia. A trial and error method of assuming an effective moment of inertia for the concrete, transforming and combining it with the moment of inertia of the steel pile for a composite moment of inertia, running the CBEAMC program for the resulting moments, and calculating an effective moment of inertia for the concrete based on the resulting moments was used.

Once the assumed moment of inertia agreed with the calculated value then the moments could be proportioned to the concrete and steel pile based on the ratio of transformed moments of inertia. The resulting moments carried by the steel pile and deflections carried by the composite member were then used in the comparisons. This method is simple and effective for this type of modeling, although a number of computer runs per model are required to iterate to a solution.

(6) Considering the erratic results of moments calculated from measured strains in the steel pile below the excavation level, the verification study appears inconclusive when the moments from predicted results are compared with the measured results. The predicted moments follow what appear to be reasonable patterns. The measured results agree in the top 20 feet in sign and magnitude, and always show the expected response at the tiebacks. But below the top 20 feet, the measured results are opposite in sign and follow no identifiable trend below the excavation level.

There may be many reasons for the inconsistencies below the excavation level, but primarily, the loads anticipated to cause the stresses expected did not develop sufficient displacement below grade to cause those stresses. Either the expected magnitude of loads did not exist, the movement caused by those

loads are even smaller than a soil stiffness of l_h x 3 would indicate, or possibly, a combination. But those possibilities do not explain the erratic nature of the measurements below the excavation levels for Figure 3.13.

CHAPTER IV

SENSITIVITY STUDY

4.1 General

This chapter reports the results of a sensitivity study considering the effects of changes in wall stiffness and soil stiffness. The literature reviewed does not find a widely accepted view on the effects of changing wall stiffness and soil stiffness on predicted moments. Three studies reviewed, Kerr and Tamaro (1990); Munger, Jones and Johnson (1990); and Mosher and Knowles (1989) indicate different sensitivities of moments to changes in wall stiffness and soil stiffness.

Kerr and Tamaro considered a range of wall and soil stiffnesses from an uncracked wall with doubled soil stiffness to a fully cracked wall with ½ soil stiffness. Their conclusions indicate that moments are not greatly affected by changes in stiffness parameters, although deflections are. Cases not considered were a stiff wall with a low soil stiffness, and a fully cracked modulus with a high soil stiffness.

Munger, Jones and Johnson had concluded for the wall they studied that a five-fold increase in the soil stiffness resulted in a five-fold decrease in deflections, with predicted moments staying within the range of measured moments. No consideration was given to any affect a change in the wall stiffness may have on the results.

The wall stiffness for their study was based on f'c = 3000 psi. The quality assurance report for the Temporary Tieback wall indicates the concrete strength is at least f'c = 10,300 psi. Based on ACI-318, section 8.5.1:

$$Ec = 57{,}000(f'c)^{1/2} \text{ psi} \quad (13)$$

Therefore, as-built, Panel 6 has an Ec = 833,000 ksf, 1.9 times that used in the CBEAMC calibration study (450,000 ksf). Either an increase in wall stiffness or an increase in soil stiffness will result in a decrease in wall deflections. When Munger, et al calibrated CBEAMC to a measured deflection, they did not account for a possible increase in wall stiffness and may have overestimated the effective stiffness of the soil.

With the same wall stiffness as used for the CBEAMC calibration, but using hyperbolic soil parameters, Mosher and Knowles found that a reduction by ½ in the initial tangent soil modulus resulted in an increase of 65% in deflections and 40% in moments. All three studies agreed on the significance of soil stiffness and its effects on deflections. However, Mosher and Knowles also indicate moments are affected by changes in soil stiffness. The effects of wall stiffness were not considered in their study.

Clough, Weber and Lamont (1972) indicated in their FEA study of a diaphragm wall and a soldier-pile wall that the stiffness of the diaphragm wall resulted in reduced predicted deflections. The diaphragm wall, with 10 times more stiffness than

the soldier-pile wall, showed a deflection of 1.5 inches compared 2 inches for the soldier-pile wall. No further discussion was pursued by the authors.

Timoshenko (1956) showed a method of practicle use for beams on elastic foundations (BOEF) originally developed by Winkler (1867). In this development, the relationships between wall stiffness, soil stiffness, deflections, moments, and shear forces are demonstrated.

The sensitivity study in this chapter will consider variations in both soil stiffness and wall stiffness. The effects of these variations will be viewed by studying the results of CBEAMC analysis. Also, predictions by use of Timoshenko's methods will be provided.

4.2 Study Model

All three previous studies discussed were based on multiple row tieback walls. For that reason, this study chose Stage 6 of Panel 178, a multiple row tieback wall, as the model for analysis. The values for the wall stiffness and the soil stiffness are then selected from a range of representative values for wall sizes and soil stiffnesses that can reasonably be expected.

Five values were selected for wall stiffness and are tabulated in Table 4.1. In the column titled "Wall Type," representatives of types of walls that may be used are

Table 4.1 Selected Wall Stiffnesses

Data Point	Wall Type	f'c (psi)	Pile	EI (k-ft^2/ft)
1	30 in. uncracked reinforced concrete	3,000	---	585,000
2	36 in. uncracked reinforced concrete	3,000	---	1,012,000
3	steel pile, non-composite on 4-foot centers	---	W33x241 with 1"x17" cover plates	1,244,000
4	36 in. uncracked reinforced concrete	10,000	---	1,847,000
5	steel pile on 4-foot centers, and 36 in. composite concrete, uncracked	7,000	W33x241 with 1"x17" cover plates	2,790,000

shown. The emphasis is on the wall stiffness in this study and not the wall type, since several different wall types may produce the same wall stiffness. However, the wall types shown will give a feel for the size of structures being considered when designing diaphragm walls.

Initially, the analysis of the different wall stiffnesses was conducted at a soil stiffness of l_h = 18 pci (l_h x 1). Then to determine the relative effect of the soil stiffness, l_h was varied by l_h x 2 and l_h x 3.

The results of deflection and moment calculations by Timoshenko's methods represent the maximum deflection and the maximum bending moment occurring at the origin of concentrated forces. Dimensions of force and length are applied without applying units such as inch or foot. The trends to be developed in this aspect of the study will be relative trends in deflections and moments, and will be demonstrated in percentages for comparison with the CBEAMC aspect of the study. From Timoshenko, the maximum deflection and maximum bending moment occurring at the origin are, respectively,

$$y_{(x=0)} = P\beta/2k \tag{14}$$

$$M_{(x=0)} = P/4\beta \tag{15}$$

where:

P = concentrated force

$\beta = [k/4EI]^{1/4}$

k = soil stiffness

EI = wall stiffness

By keeping P constant then deflection and moment are simply functions of the soil and wall stiffnesses,

$$y_{(x=0)} \propto \beta/k \tag{16}$$

$$M_{(x=0)} \propto 1/\beta \tag{17}$$

4.3 Results

4.3.1 Moments in the Wall

Figure 4.1 shows a plot of the effect of changing wall stiffness on the resulting maximum negative moments as analyzed by CBEAMC. The largest moment indicated by the analysis is a negative moment found below the level of excavation (see Figure 3.17). The plot indicates that wall stiffness does indeed affect the moments. It also shows that the relative effect of wall stiffness on moments

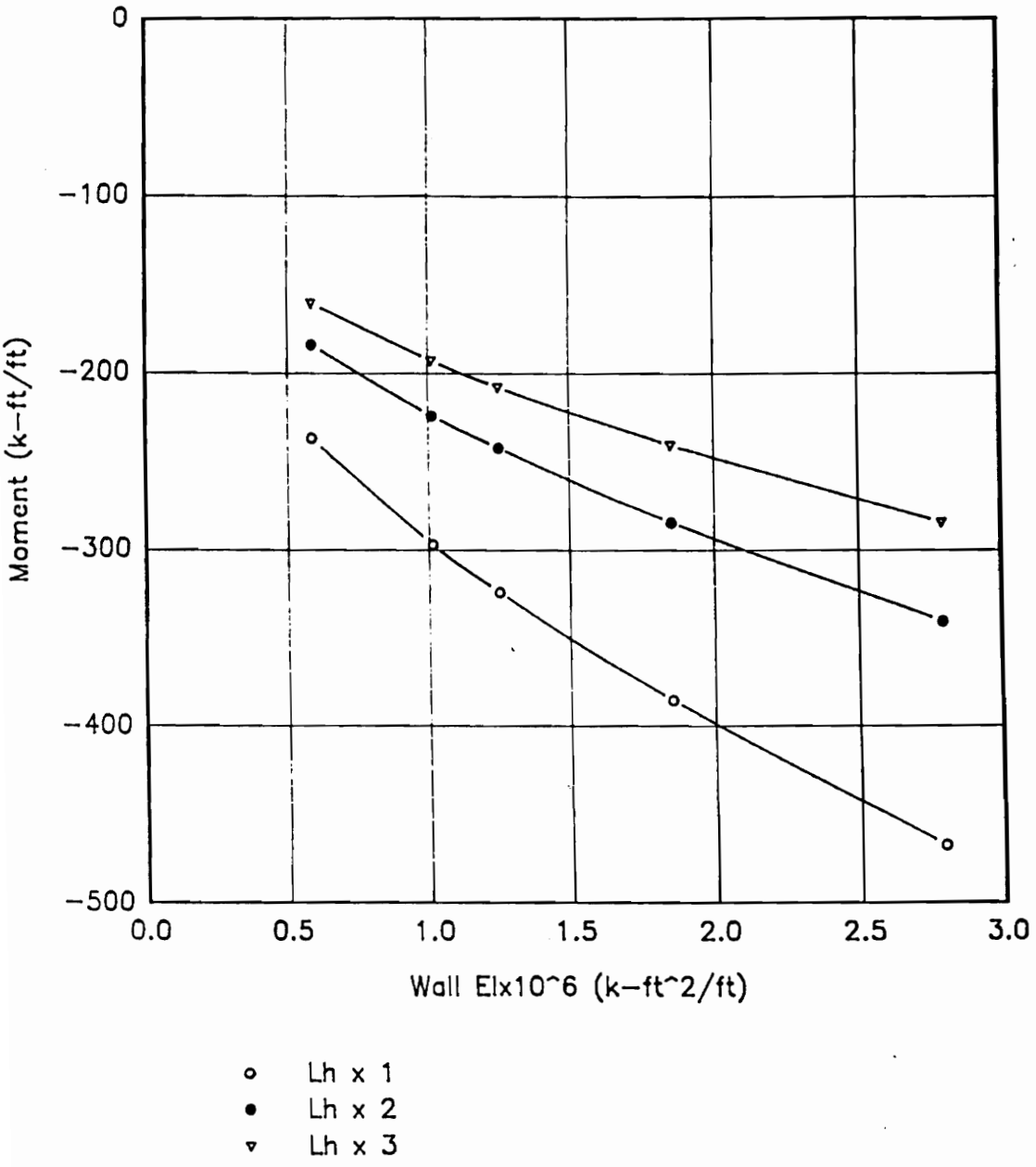

Figure 4.1 Sensitivity of Maximum Moment to Wall Stiffness.

decreases as the soil stiffness increases.

CBEAMC results in Table 4.2 indicate a bending moment increase for an increase in wall stiffness from the least rigid wall to the most rigid wall (a increase by a factor of 4.77, to be used in BOEF analysis). The degree of increase in bending moment varied and the amount of increase tended to reduce as soil stiffness increased. The beam on elastic foundation results in Table 4.2 demonstrate that increasing the wall stiffness also results in higher bending moments. An increase in the soil stiffness had no effect on the percent of increase in moments due to an increased wall stiffness. This can be seen in equation (17) that at any given soil stiffness, k, the effects on bending moment are only a function of the change in wall stiffness, EI. The results shown in Figure 4.1 and Table 4.2 verify that an increase in wall stiffness does indeed cause an increase in bending moments.

More interesting are the results shown in Table 4.3. CBEAMC results in Table 4.3 demonstrate that increasing the wall stiffness has nearly the same percentage of increase in bending moments as decreasing the soil stiffness. For instance, a doubling of the wall stiffness is equivalent to reducing the soil stiffness by ½. The effects of wall stiffness on induced moments is inversely proportional to the effects of the soil stiffness. Also, there is no net change in moments when wall stiffness and soil stiffness are both increased or decreased equal amounts.

Table 4.2 Percent Change in Moment Due to Increase in Wall Stiffness.

CBEAMC Results:

EI	l_h x 1	l_h x 2	l_h x 3
(k-ft^2/ft)			
585,000	-237.2	-184.0	-160.6
2,790,000	-467.5	-340.7	-284.7
Change in Moment (%)	97.1	85.2	77.3

BOEF Results:

EI	k = 1	k = 2	k = 3
1	1.41	1.19	1.07
4.77	2.09	1.76	1.59
Change in Moment (%)	47.8	47.8	47.8

Table 4.3 Percent Change in Moments, Comparison of Wall Stiffness Effect vs Soil Stiffness Effect.

CBEAMC: EI x 10^6 ($k\text{-}ft^2/ft$)	Moment (k-ft/ft) l_h x 2	l_h x 1	Change in moment (%)
1.0	-224	-295	+31.7
2.0	-293	-398	+35.8
Change in Moment (%)	+30.8	+34.9	
	l_h x 3	l_h x 1	
0.75	-173	-260	+50.3
2.25	-260	-422	+62.3
Change in Moment (%)	+50.3	+62.3	
BOEF:	k = 2	k = 1	
1.0	1.19	1.41	+18.9
2.0	1.41	1.68	+18.9
Change in Moment (%)	+18.9	+18.9	
	k = 3	k = 1	
1.0	1.07	1.41	+31.6
3.0	1.41	1.86	+31.6
Change in Moment (%)	+31.6	+31.6	

For example, increasing both the wall stiffness and soil stiffness by a factor of three results in the same moment, -260 k-ft/ft. The results as determined by the beam on elastic foundation method verify those found by the CBEAMC analysis.

4.3.2 Deflections of the Wall

Figure 4.2 shows a plot of the effects of changing wall stiffness on the largest positive deflection. As expected, deflections are sensitive to changes in the wall stiffness, decreasing with increases in wall stiffness. They also show a sensitivity to the soil stiffness, which the three mentioned studies indicated.

CBEAMC results in Table 4.4 show that increasing the wall stiffness decreases the deflection, and interestingly enough, by nearly equal percentages regardless of the soil stiffness. The beam on elastic foundation results in Table 4.4 also show equal an percentage of decrease in deflection regardless of the given soil stiffness. The results shown in Figure 4.2 and Table 4.4 verify that an increase in wall stiffness does indeed cause an decrease in deflections.

Results from both CBEAMC and BOEF analysis provided in Table 4.5 also shows that the effect on deflections by changes in wall stiffness is virtually independent of the soil stiffness. However, Table 4.5 also shows that changes in the soil stiffness has more of an effect on deflections than changes in wall stiffness.

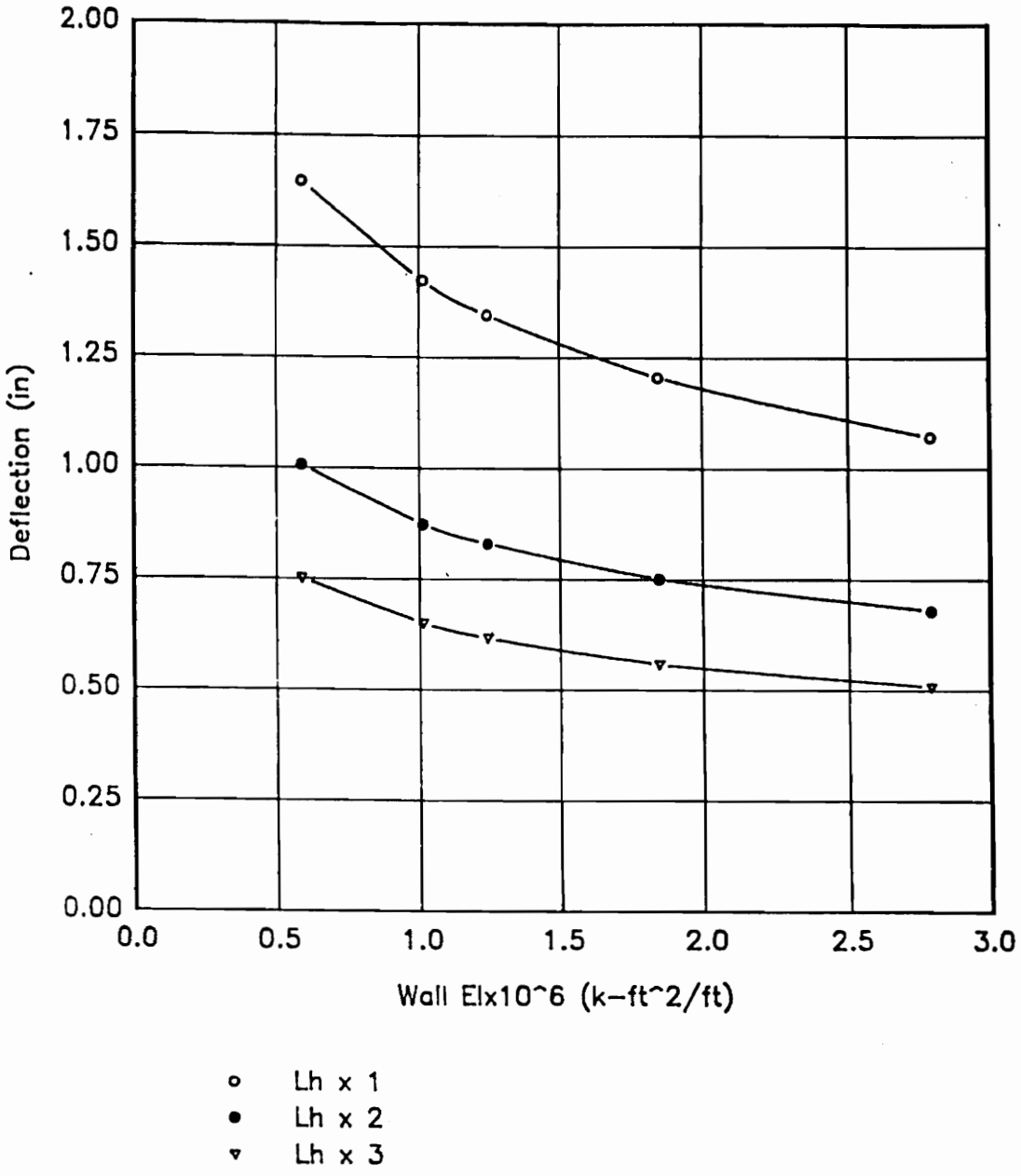

Figure 4.2 Sensitivity of Outward Deflections to Wall Stiffness.

Table 4.4 Percent Change in Deflection Due to Increase in Wall Stiffness.

CBEAMC Results:

EI	Deflection (in) l_n x 1	l_n x 2	l_n x 3
(k-ft^2/ft)			
585,000	1.65	1.01	0.75
2,790,000	1.07	0.68	0.51
Deflection Decrease (%)	-35.2	-32.7	-32.0

BOEF Results:

EI	k = 1	k = 2	k = 3
1	0.71	0.42	0.31
4.77	0.48	0.28	0.21
Deflection Decrease (%)	-32.3	-32.3	-32.3

Table 4.5 Percent Change in Deflections, Comparison of Wall Stiffness Effect vs Soil Stiffness Effect.

EI x 10^6 ($k\text{-}ft^2/ft$)	Deflection (in)		Deflection Decrease (%)
	l_n x 1	l_n x 2	
1.0	1.43	0.88	-38.5
2.0	1.18	0.74	-37.3
Deflection Decrease (%)	-17.5	-15.9	
	l_n x 1	l_n x 3	
0.75	1.56	0.71	-54.5
2.25	1.09	0.54	-50.5
Deflection Decrease (%)	-30.1	-23.9	
BOEF:	k = 1	k = 2	
1.0	0.71	0.42	-40.5
2.0	0.59	0.35	-40.5
Deflection Decrease (%)	-15.9	-15.9	
	k = 1	k = 3	
1.0	0.71	0.31	-56.1
3.0	0.54	0.24	-56.1
Deflection Decrease (%)	-24.0	-24.0	

For example, tripling the wall stiffness results in a decrease in deflections by 20 to 30 percent. Whereas tripling the soil stiffness reduces deflections by 50 to 55 percent, nearly double. This ratio of effectiveness is consistent throughout the table, with the effect of wall stiffness on deflection equal to about ½ the effect of soil stiffness.

4.4 Conclusions

(1) For a tieback wall, such as Panel 178 at Stage 6 of excavation, the effects on moments from changes to the wall stiffness and the soil stiffness were considered. The results indicate that changes to wall stiffness have an inversely proportional effect on moment compared to changes in soil stiffness. Doubling a wall stiffness will have the same effect as reducing the soil stiffness by ½.

(2) For the same tieback wall, a change in soil stiffness has approximately double the effect on deflections as a change in wall stiffness.

(3) Based on these results, if a need for a reduction in lateral deflection presents itself, the more effective approach to the problem is to first consider increases in the soil stiffness are possible, and then increases to the wall stiffness (other solutions aside). An increase in soil stiffness will more effectively reduce the

deflection while reducing flexural stresses. Increases in wall stiffness will reduce deflections at a slower rate while increasing flexural stresses.

(4) Even though the above conclusions are drawn based on the CBEAMC analysis, each conclusion is verified by BOEF analysis as developed by Timoshenko.

CHAPTER V

Summary, Conclusions, and Recommendations

5.1 Summary

Two studies were conducted in this research. One was to verify the design of a diaphragm wall based on a calibrated soil-structure interaction program. The deflections and calculated moments based on measured strains were compared to the original design models and then to as-built models. The comparison was first to establish that the original design models were reasonable by comparing trends in moments and deflections for different stages of excavation with the measured results. The measured results were next compared to an as-built model. Finally, the as-built model had refinements made to the soil stiffness to try to better match the measured results. This procedure was similar to the original calibration of the soil structure interaction model.

The second study, performed on CBEAMC, considered the influence that changes in wall stiffness and soil stiffness might have on moments and deflections in a multiple row tieback diaphragm wall. Five wall stiffnesses were selected which represented a reasonable range of stiffnesses that can be found in diaphragm walls. Three soil stiffnesses were used for comparing the sensitivity of moments and

deflections on changes in wall stiffness to changes in soil stiffness. Analysis using a beam on elastic foundation method demonstrated by Timoshenko was also performed for comparison with the CBEAMC results.

5.2 Conclusions

5.2.1 Design Verification

Conclusions drawn from this study are:

(1) The stresses calculated from measured strains are well below the predicted and allowable stress. Therefore, the design for Area V panels is structurally adequate.

(2) Trends indicated by predicted and measured deflections show that the original design models, and subsequent models based on them, are reasonable for predicting deflections. A careful selection of a soil stiffness is essential. If possible, a selected soil stiffness can be rationalized based on previous experience with the subject soils.

(3) The deflections for these walls could have been better predicted by using a soil stiffness of l_h = 54 pci, three times the original stiffness, or even higher.

This agrees with results indicated by the CBEAMC calibration study by Munger, Jones and Johnson.

(4) Below the top 20 feet of Panel 178, the moments based on measured strains were not consistent with the predicted results, except for the localized response at tieback locations. Below the excavation level, the measured moments did not appear to follow any rational trend. These results made the study inconclusive for verifying moments predicted with actual results.

5.2.2 Sensitivity Study

Conclusions drawn from this study are:

(1) For a multiple row tieback diaphragm wall, moments are sensitive to changes in wall stiffness and soil stiffness. The effects of changes in wall stiffness are inversely proportional to changes in soil stiffness.

(2) Deflections are also sensitive to changes in wall stiffness. But changes in soil stiffness have approximately twice the effect as changes in wall stiffness.

(3) Based on the results of this study, if a need for a reduction in lateral deflection presents itself, the more effective approach is to first consider if increases in the soil stiffness are possible, and then increases to the wall stiffness.

5.3 Recommendations

5.3.1 Design Verification

The application of a soil-structure interaction (SSI) program utilizing non-linear Winkler springs supports is a relatively simple approach to analyzing diaphragm walls. The solution to accurately predicting deflections based on this approach is achievable, but more study must be conducted on determining rational values for l_h, the constant of horizontal subgrade reaction, to be used.

The results of this study indicate that l_h has a significant influence on predicted deflections and bending moments . But the influence l_h has on the moments is not well defined when the measured results were unable to support them. Therefore, more study is necessary to rationalize the selection of l_h, to achieve safe designs with reasonable predictions of deflections through SSI analysis. The finding of a correlation of l_h for use on diaphragm walls, to better known soil parameters such as soil density, Mohr-Coulomb soil strength parameters, etc., may well serve the purpose.

Finding an appropriate l_h may go beyond studying multiple row tieback diaphragm wall designs, but should consider different support configurations such as cantilever walls and walls with a single tieback. These types of structures result

in more deflections, may show better defined trends in moments and deflections, and indicate correlations more directly. Several locations in the guard wall at the new Bonneville Navigation Lock are well instrumented and may well serve the purpose of further study.

5.3.2. **Sensitivity Study**

The selection of a diaphragm wall for use as a retaining wall may be based on minimizing lateral deflections. This is accomplished by taking advantage of the high wall stiffness. However, as indicated by the sensitivity study, deflections in a multiple row tieback wall are sensitive to changes in wall stiffness, but nearly twice as sensitive to changes in soil stiffness.

The study also indicated a sensitivity of moments to changes in wall stiffness and soil stiffness. These sensitivities, both deflections and moments, should be studied for other support configurations to determine if the same correlations found in this study apply for all configurations.

LITERATURE CITED

1. Clough, G. W., "User Manual for Program SOILSTRUCT," Virginia Polytechnic Institute, Blacksburg, Va., 1984.

2. Dawkins, W. P., "USERS Guide: Computer Program for Analysis of Beam-Column Structures with Nonlinear Supports (CBEAMC)", **Instruction Report K-82-6**, U.S. Army Engineers Waterways Experiment Station, Vicksburg, Ms., June 1982. 90 p.

3. Duncan, J. M., Chang, C. Y., "Nonlinear Analysis of Stress and Strain in Soils," **Journal of the Soil Mechanics and Foundations Division, Proceedings of the American Society of Civil Engineers, Vol. 96, No. SM5**, September, 1970.

4. Duncan, J. M., Byrne, P., Wong, K. S. and Mabry, P. "Strength Stress-Strain and Bulk Modulus Parameters for Finite Element Analyses of Stress and Movements in Soil Masses," **Report No. UCB/GT/80-01**, University of California, Berkeley, California, 1980.

5. Haliburton, T. A., "Soil Structure Interaction: Numerical Analysis of Beams and Beam-Columns," **Technical Publication No. 14**, School of Civil Engineering, Oklahoma State University, Stillwater, Ok., 1971, 179 p.

6. Hartman, J. P. and Jobst, J. J., "Users Guide: Computer Program with Interactive Graphics for Analysis of Plane Frame Structures (CFRAME)," **Instruction Report K-83-1**, U.S. Army Engineer Waterways Experiment Station, Vicksburg, Ms., Jan. 1973, 62 p.

7. Jaky, J., "The Coefficient of Earth Pressure at Rest," **Journal of the Society of Hungarian Architects and Engineers**, 1944, 355-358.

8. Mosher, R. and Knowles, V., "Finite Element Study of Tieback Wall for Bonneville Navigation Lock," **Draft Technical Report ITL-89-**, Information Technology Laboratory, Dept. of the Army, Waterways Experiment Station, Vicksburg, Ms. 1988.

9. **NAVFAC Design Manual 7.2**, "Foundations and Earth Structures", Department of the Navy, Naval Facilities Engineering Command, Alexandria, Va., May 1982. Chapter 3.

10. Terzaghi, K., "Evaluation of Coefficients of Subgrade Reaction," **Geotechnique, Vol. 5**, Dec. 1955, 297-326.

11. Timoshenko, S., "Chapter I, Beams on Elastic Foundations", **Strength of Materials**, Part II, D. Van Nostrand Co. Inc., Princeton, N.Y.,Third Edition, 1956

12. U.S. Army Corps of Engineers, **Bonneville Navigation Lock Technical Design Report No. 13, Diaphragm Walls**, Portland District, Portland, Or., July 1988.

13. U.S. Army Corps of Engineers, "Strength and Design Criteria for Reinforced Concrete Hydraulic Structures," **Engineering Technical Letter 1110-2-312,** 10 March 1988.

14. U.S. Army Corps of Engineers, "Report of Quality Assurance Tests on Production Tremie Concrete", **Memorandum CENPD-EN-G-L (1110-1-8100C) W. O. #88-C-519**, Jan. 13, 1988.

15. Xanthakos, P. P. "Slurry Walls," McGraw-Hill, New York, 1979.

16. Winkler, E., **Die Lehre von der Elastizitat und Festigkeit**, Prague, 1867

APPENDICES

Appendix A

Calculation of Wall Parameters

Wall Stiffness: Per Foot of Wall

As-Built Conditions: Piles @ 4 ft on center

$f'c = 7000$ psi

$E_c = 57{,}000(7000)^{1/2}/1000 = 4{,}770$ ksi

$f_y = 63{,}750$ psi

$E_s = 29{,}000$ ksi

$n = E_s/E_c = 6.08 \Rightarrow 6$

Steel Pile:

I_s: W 33 X 241 with 1 X 17 inch cover plates

$I_s = 14{,}200 \text{ in}^4 + 17(36.18^3 - 34.18^3)/12 \text{ in}^4$

$I_s = 24{,}722.70 \text{ in}^4 = 1.19 \text{ ft}^4$

Per Foot: $I_s = 1.19 \text{ ft}^4/4 \text{ ft} = 0.298 \text{ ft}^4/\text{ft}$

A_s: $A_s = 70.9 \text{ in}^2 + 2(1)(17) \text{ in}^2 = 104.9 \text{ in}^2$

$A_s = 104.9 \text{ in}^2 = 0.73 \text{ ft}^2$

Per Foot: $A_s = 0.182 \text{ ft}^2/\text{ft}$

Concrete:

I_g: $I_g = 48 \text{ in } (36 \text{ in})^3/12 = 186{,}624.0 \text{ in}^4 = 9.00 \text{ ft}^4$

Per Foot: $I_g = 9.00\ ft^4/4\ ft = 2.25\ ft^4/ft$

Transform to Steel Equivalent:

$I_{g(tr)} = [2.25\ ft^4/ft]/n = [2.25\ ft^4/ft]/6$

$I_{g(tr)} = 0.375\ ft^4/ft$

$A_c = 12\ ft^2 = 1728\ in^2 = 432\ in^2/ft$

$A_{c(tr)} = [432\ in^2/ft]/6 = 72.0\ in^2/ft$

$A_{c(tr)} = 0.5\ ft^2/ft$

Cracked Concrete Considered:

$M_{cr} = f_r\ I_g/Y_t$

$f_r = 7.5(7000)^{½} = 627.50\ psi$

$I_g = 2.25\ ft^4 = 186{,}624\ in^4$

$Y_t = 18$ in (½ of 36 inch wall thickness)

$$M_{cr} = \frac{(627.5\ psi)(186{,}624\ in^4)}{18\ in} = 6{,}505{,}868.37\ in\text{-}lb$$

$M_{cr} = 542.16$ ft-k

Per foot: $M_{cr} = 135.54$ ft-k/ft

M_{cr} is the bending moment required to crack the concrete. Consideration of the effective moment of inertia, I_{eff}, is required when bending moments exceed M_{cr}.

In Terms of Stress, Strain:

$$f_{cr} = M_{cr}c/I_g = \frac{(6{,}505{,}869 \text{ in-lb})(18 \text{ in})}{186{,}624 \text{ in}^4} = 627.5 \text{ psi}$$

$$\epsilon_{cr} = f_c/E_c = 627.5 \text{ psi}/4{,}770 \text{ ksi}$$

$$\epsilon_{cr} = 0.0001316 = 131.6 \ (10^{-6})$$

Whereas at the strain gages on the piles subjected to a proportional amount of strain:

ϵ @ y = 15.169 in (Distance from N.A. to the strain gages)

$$\epsilon_{15.69} = 131.6 \ (10^{-6})(15.69/18.0) = 114.7 \ (10^{-6})$$

$\epsilon_{15.69}$ = 114.7 Microstrain at strain gages

(Flexural strain only, axial strain not included.)

Wall Stiffness Input to CBEAMC

$E = E_s = 29{,}000.0$ ksi

$E = 4{,}176{,}000.0$ ksf

Steel Pile Only:

$I = I_s = 0.298$ ft^4/ft

$A_s = 0.182$ ft^2/ft

Composite Steel and Gross Concrete:

$I = I_s + I_{g(tr)} = 0.298 + 0.375 = 0.673$ ft^4/ft

% Stress in Steel = $0.298/0.673 = 0.446 = 44.6\% \Rightarrow 45\%$

% Stress in Gross Concrete = $55.4\% \Rightarrow 55\%$

$A = A_s + A_{c(tr)} = 0.182 + 0.5 = 0.7$ ft^2/ft

Detemine I_{cr}:

$M_{cr} = 135.54$ ft-k/ft

$A_s = 0.44$ in^2 (Rebar, not steel pile)

$n = 6$

$d = 29.625$ in

$A_{s(tr)} = A_s(n) = 0.44\ (6) = 2.64\ in^2$

(Transforms rebar to concrete)

$12x^2/2 = A_{s(tr)}(d\text{-}x)$

$6x^2 = 2.64\ (29.625 - x) = 78.21 - 2.64x$

$6x^2 + 2.64x - 78.21 = 0$

$x^2 + 0.44x - 13.04 = 0$

$x = 3.40$

$I_{cr} = \frac{1}{3}(12)(3.40)^3 + 2.64(29.625 - 3.40)^2$

$I_{cr} = 1{,}972.88\ in^4/ft$

$I_{cr} = 1{,}997.62\ in^4/ft = 0.095\ ft^4/ft$

Transform to Steel:

$I_{cr(tr)} = (0.095\ ft^4/ft)/n = (0.095\ ft^4/ft)/6$

$I_{cr(tr)} = 0.016\ ft^4/ft$

Recall $I_{g(tr)} = 0.375\ ft^4/ft$

Appendix B

Calculation of a Soil Spring

Example Soil Spring: Left Side, El.-29

RSD:

K_m = 36 pci (Dewatered)

K_m = (36 pci)(12 in)^3/ft^3 = 62,208 pcf

K_A = 0.333

K_o = 0.5

K_p = 3.0

Surcharge = 9 ft

ϕ = 30$^-$

y = 81-(-29) = 110 ft

γ_m = 118 pcf

Vertical Pressure:

@ El.+81: y = 0 ft

σ_v = (9ft)(118 pcf) = 1,062 psf

@ El.-29: y = 110 ft

σ_v = (110 ft)(118 pcf) + 1,062 psf

σ_v = 14,042 psf

Horizontal Pressures:

@ El.-29: $P_A = 0.333\ \sigma_v = 0.333(14{,}042\ psf) = 4{,}681\ psf$

$P_o = 0.5\ \sigma_v = 0.5\ (14{,}042\ psf) = 7{,}021\ psf$

$P_p = 3.0\ \sigma_v = 3.0\ (14{,}042\ psf) = 42{,}126\ psf$

X-Equivalent: (For a given soil unit weight at a particular elevation, X-Equivalent is an equivalent depth of soil based on the vertical pressure at that elevation as though all of the soil above that point had the same unit weight instead of layers of soil with various unit weights.)

@ El.-29: X-Equiv. $= \sigma_v/\gamma_m = 14{,}042\ psf/118\ pcf$

X-Equiv. = 119 ft

E_s:

D = 10 ft (Typical distance between anchors.)

$E_s = K_m$ (X-Equiv.)/D = 62,208 pcf (119 ft)/10 ft

E_s = 740,275 pcf

Displacement:

@ El.-29: $\delta_a = (P_o - P_A)/E_s$

$P_o = 7{,}021$ psf

$P_a = 4{,}681$ psf

$E_s = 740{,}275$ pcf

$\delta_a = (7{,}021 - 4{,}681)\text{psf}/740{,}275$ pcf

$\delta_a = 0.0032$ ft

$\delta_p = (P_o - P_p)/E_s$

$P_p = 42{,}126$ psf

$\delta_p = (7{,}021 - 42{,}126)\text{psf}/740{,}275$ pcf

$\delta_p = -0.0474$ ft

Spring Definition:

@ El.-29: @ $P_p = 42{,}126$ psf, $\delta_p = -0.0474$ ft

@ $P_a = 4{,}681$ psf, $\delta_a = 0.0032$ ft

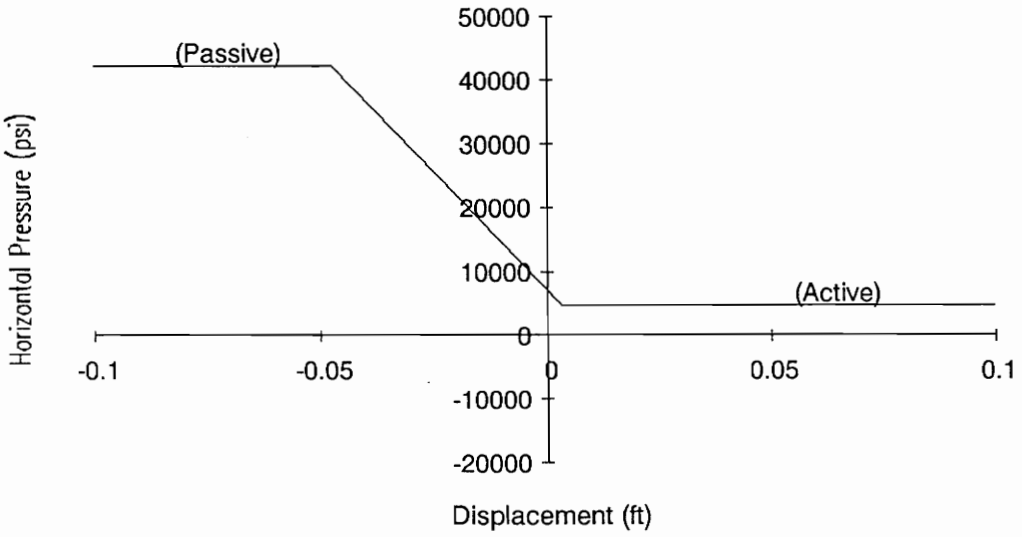

Figure B.1 Example Soil Spring.

Appendix C

Sample CBEAMC Computer Input and Results

```
101 'ANALYSIS OF GUARD WALL AT PANEL 178 AS A TIEBACK WALL, BASE @ EL.-37, (RSD & TW)
102 'SSI ANALYSIS OF CONSTRUCTION SEQUENCE, W 33 X 387, ** AS-CONSTRUCTED CONDITIONS **
103 'EXCAVATE TO EL. 20, PRIOR TO INSTALLATION OF TIE AT EL. 22, WATER AT TOP OF WEIGLE = EL. -29
104 'FILENAME = SQ6NE, NO PROOF LOAD, SOIL SPRINGS NOT "DOUBLED", WALL "EI" CORRECTED
110 BEAM F K
125 0 120 4176000 .500 .673
130 NODES F
140 0 120 2
150 FIX F
160 120 0 F F
170 NONLINEAR F P
171 (LEFT SIDE NONLINEAR SOIL SPRINGS)
180 DISTRIBUTED Y 0 2 1 1
190 -0.0948 0.0063
200 3186.0 354.0
210 CONTINUE 110 2 1 1
220 -0.0948 0.0063
230 42126.0 4680.7
240 CONTINUE 111 2 1 1
250 -0.0575 0.0057
260 47354.6 3044.6
294 CONTINUE 118 2 1 1
295 -0.0572 0.0056
296 49036.7 3231.5
298 CONTINUE 118.5 3 1 1000
299 -0.0042 0 1
300 1843 0 0
301 END 120 3 1 1000
302 -0.0042 0 1
303 1843 0 0
507 (RIGHT SIDE NONLINEAR SOIL SPRINGS)
509 DIST Y 62 2 1 1
510 -0.0190 0.2845
511 -39.3 -354.0
512 C 110 2 1 1
513 -0.0190 0.2845
514 -1927.3 -17346.0
516 C 111 2 1 1
517 -0.0272 0.2026
518 -291.3 -22574.6
525 CONTINUE 118 2 1 1
526 -0.0257 0.1981
527 -478.2 -24256.7
529 CONTINUE 118.5 3 1 1000
530 -1 0 0.0042
531 0 0 -1843
532 END 120 3 1 1000
533 -1 0 0.0042
534 0 0 -1843
564 (PERMANENT TIEBACK AT EL.+79)
590 CONCENTRATED 2 -70 3 1 1000
600 -.4629 0.0 0.7714
610 70.31 43.94 0.0
611 (TEMPORARY TIEBACKS)
612 CON 12 -70 3 1 1000
613 -0.4050 0.0 0.6750
614 62.92 39.33 0.0
615 CON 22 -70 3 1 1000
616 -0.3905 0.0 0.6509
617 62.92 39.33 0.0
618 CON 32 -70 3 1 1000
619 -0.3761 0.0 0.6268
620 62.92 39.33 0.0
621 CON 42 -70 3 1 1000
622 -0.3616 0.0 0.6027
623 62.92 39.33 0.0
624 CON 51 -70 3 1 1000
625 -0.3327 0.0 0.5545
626 62.92 39.33 0.0
750 LOADS NEW F P
815 (CRANE LOADING)
820 D Y 0 500 3
```

```
821 D Y 3 250 8
822 D Y 8 60 30
830 (ONE E-80 TRAIN)
840 D Y 0 40 21
850 D Y 21 70 87
860 D Y 87 45 141
1055 FINISH
```

'ANALYSIS OF GUARD WALL AT PANEL 178 AS A TIEBACK WALL, BASE @ EL.-37, (R
'SSI ANALYSIS OF CONSTRUCTION SEQUENCE, W 33 X 387, ** AS-CONSTRUCTED CON
'EXCAVATE TO EL. 20, PRIOR TO INSTALLATION OF TIE AT EL. 22, WATER AT TOP
'FILENAME = SQ6NE, NO PROOF LOAD, SOIL SPRINGS NOT "DOUBLED", WALL "EI" C

2.--BEAM CROSS SECTION DATA

X-COORDINATE			<---------SECTION PROPERTIES--------->			
			<----START----->		<-----STOP----->	
START (FT)	STOP (FT)	MODULUS OF ELASTICITY (KSF)	AREA (SQFT)	INERTIA (FT**4)	AREA (SQFT)	INERTIA (FT**4)
.00	120.00	4.18E+06	.50	.67	.50	.67

3.--NODE SPACING DATA

X-COORDINATE		MAXIMUM NODE SPACING
START (FT)	STOP (FT)	(FT)
.00	120.00	2.00

4.--LOAD DATA

4.A.--CONCENTRATED LOADS

NONE

4.B.--DISTRIBUTED LOADS

LOAD	<-----START----->		<------STOP----->	
DIRECT	X-COORD (FT)	LOAD (P/FT)	X-COORD (FT)	LOAD (P/FT)
Y	.00	500.00	3.00	500.00
Y	3.00	250.00	8.00	250.00
Y	8.00	60.00	30.00	60.00
Y	.00	40.00	21.00	40.00
Y	21.00	70.00	87.00	70.00
Y	87.00	45.00	141.00	45.00

5.--FIXED SUPPORT DATA

SUPPORT	SPECIFIED DISPLACEMENTS		
X-COORD (FT)	X-DISP. (FT)	Y-DISP. (FT)	ROTATION (RAD)
120.00	.00	FREE	FREE

6.--LINEAR SPRING DATA

NONE

7.--NONLINEAR SPRING DATA

7.A.--NONLINEAR CONCENTRATED SPRINGS

SPRING		CURVE COORD. MULTIPLIERS	
X-COORD (FT)	ANGLE (DEG)	DISPLACEMENT (FT)	FORCE (P)
2.00	-70.00	1.00E-02	1.00E+03

DISP. COORDS.	-46.29	.00	77.14
FORCE COORDS.	70.31	43.94	.00

SPRING		CURVE COORD. MULTIPLIERS	
X-COORD (FT)	ANGLE (DEG)	DISPLACEMENT (FT)	FORCE (P)
12.00	-70.00	1.00E-02	1.00E+03

DISP. COORDS.	-40.50	.00	67.50
FORCE COORDS.	62.92	39.33	.00

SPRING		CURVE COORD. MULTIPLIERS	
X-COORD	ANGLE	DISPLACEMENT	FORCE

```
      (FT)          (DEG)          (FT)             (P)
      22.00         -70.00         1.00E-02       1.00E+03

DISP. COORDS.    -39.05     .00  65.09
FORCE COORDS.     62.92   39.33    .00

     SPRING                     CURVE COORD. MULTIPLIERS
    X-COORD         ANGLE       DISPLACEMENT       FORCE
      (FT)          (DEG)          (FT)             (P)
      32.00         -70.00         1.00E-02       1.00E+03

DISP. COORDS.    -37.61     .00  62.68
FORCE COORDS.     62.92   39.33    .00

     SPRING                     CURVE COORD. MULTIPLIERS
    X-COORD         ANGLE       DISPLACEMENT       FORCE
      (FT)          (DEG)          (FT)             (P)
      42.00         -70.00         1.00E-02       1.00E+03

DISP. COORDS.    -36.16     .00  60.27
FORCE COORDS.     62.92   39.33    .00

     SPRING                     CURVE COORD. MULTIPLIERS
    X-COORD         ANGLE       DISPLACEMENT       FORCE
      (FT)          (DEG)          (FT)             (P)
      51.00         -70.00         1.00E-02       1.00E+03

DISP. COORDS.    -33.27     .00  55.45
FORCE COORDS.     62.92   39.33    .00
```

7.B.--NONLINEAR DISTRIBUTED SPRINGS

```
                    SPRING      SPRING     CURVE COORD. MULTIPLIERS
     DISTRIBUTION   DIRECTION   X-COORD     DISPLACEMENT       FORCE
                                  (FT)          (FT)            (P)
       STARTS          Y          .00       1.00E-03       1.00E+02

DISP. COORDS.    -94.80   6.30
FORCE COORDS.     31.86   3.54

                    SPRING      SPRING     CURVE COORD. MULTIPLIERS
     DISTRIBUTION   DIRECTION   X-COORD     DISPLACEMENT       FORCE
                                  (FT)          (FT)            (P)
       CONTINUES       Y        110.00       1.00E-03       1.00E+03

DISP. COORDS.    -94.80   6.30
FORCE COORDS.     42.13   4.68

                    SPRING      SPRING     CURVE COORD. MULTIPLIERS
     DISTRIBUTION   DIRECTION   X-COORD     DISPLACEMENT       FORCE
                                  (FT)          (FT)            (P)
       CONTINUES       Y        111.00       1.00E-03       1.00E+03

DISP. COORDS.    -57.50   5.70
FORCE COORDS.     47.35   3.04

                    SPRING      SPRING     CURVE COORD. MULTIPLIERS
     DISTRIBUTION   DIRECTION   X-COORD     DISPLACEMENT       FORCE
                                  (FT)          (FT)            (P)
       CONTINUES       Y        118.00       1.00E-03       1.00E+03

DISP. COORDS.    -57.20   5.60
FORCE COORDS.     49.04   3.23

                    SPRING      SPRING     CURVE COORD. MULTIPLIERS
     DISTRIBUTION   DIRECTION   X-COORD     DISPLACEMENT       FORCE
                                  (FT)          (FT)            (P)
       CONTINUES       Y        118.50       1.00E-01       1.00E+05

DISP. COORDS.      -.04     .00  10.00
FORCE COORDS.     18.43     .00    .00
```

DISTRIBUTION	SPRING DIRECTION	SPRING X-COORD (FT)	CURVE COORD. MULTIPLIERS DISPLACEMENT (FT)	FORCE (P)
ENDS	Y	120.00	1.00E-01	1.00E+05

DISP. COORDS.	-.04	.00	10.00
FORCE COORDS.	18.43	.00	.00

DISTRIBUTION	SPRING DIRECTION	SPRING X-COORD (FT)	CURVE COORD. MULTIPLIERS DISPLACEMENT (FT)	FORCE (P)
STARTS	Y	62.00	1.00E-02	1.00E+01

DISP. COORDS.	-1.90	28.45
FORCE COORDS.	-3.93	-35.40

DISTRIBUTION	SPRING DIRECTION	SPRING X-COORD (FT)	CURVE COORD. MULTIPLIERS DISPLACEMENT (FT)	FORCE (P)
CONTINUES	Y	110.00	1.00E-02	1.00E+03

DISP. COORDS.	-1.90	28.45
FORCE COORDS.	-1.93	-17.35

DISTRIBUTION	SPRING DIRECTION	SPRING X-COORD (FT)	CURVE COORD. MULTIPLIERS DISPLACEMENT (FT)	FORCE (P)
CONTINUES	Y	111.00	1.00E-02	1.00E+03

DISP. COORDS.	-2.72	20.26
FORCE COORDS.	-.29	-22.57

DISTRIBUTION	SPRING DIRECTION	SPRING X-COORD (FT)	CURVE COORD. MULTIPLIERS DISPLACEMENT (FT)	FORCE (P)
CONTINUES	Y	118.00	1.00E-02	1.00E+03

DISP. COORDS.	-2.57	19.81
FORCE COORDS.	-.48	-24.26

DISTRIBUTION	SPRING DIRECTION	SPRING X-COORD (FT)	CURVE COORD. MULTIPLIERS DISPLACEMENT (FT)	FORCE (P)
CONTINUES	Y	118.50	1.00E-01	1.00E+05

DISP. COORDS.	-10.00	.00	.04
FORCE COORDS.	.00	.00	-18.43

DISTRIBUTION	SPRING DIRECTION	SPRING X-COORD (FT)	CURVE COORD. MULTIPLIERS DISPLACEMENT (FT)	FORCE (P)
ENDS	Y	120.00	1.00E-01	1.00E+05

DISP. COORDS.	-10.00	.00	.04
FORCE COORDS.	.00	.00	-18.43

II.--SUMMARY OF RESULTS

II.A.--HEADING
'ANALYSIS OF GUARD WALL AT PANEL 178 AS A TIEBACK WALL, BASE @ EL.-37, (R
'SSI ANALYSIS OF CONSTRUCTION SEQUENCE, W 33 X 387, ** AS-CONSTRUCTED CON
'EXCAVATE TO EL. 20, PRIOR TO INSTALLATION OF TIE AT EL. 22, WATER AT TOP
'FILENAME = SQ6NE, NO PROOF LOAD, SOIL SPRINGS NOT "DOUBLED", WALL "EI" C

II.B.--MAXIMA

	MAXIMUM POSITIVE	X-COORD (FT)	MAXIMUM NEGATIVE	X-COORD (FT)
AXIAL DISPLACEMENT (FT) :	3.584E-03	.00	.000E+00	.00
LATERAL DISPLACEMENT (FT):	8.897E-02	73.54	-8.820E-02	.00
ROTATION (RAD) :	3.087E-03	2.00	-2.649E-03	102.33
AXIAL FORCE (K) :	.000E+00	.00	-8.087E+01	51.00
SHEAR (K) :	2.838E+01	32.00	-1.274E+02	118.50
BENDING MOMENT (K-FT) :	3.174E+02	118.00	-4.692E+02	69.69

II.C.--REACTIONS AT FIXED SUPPORTS

X-COORD (FT)	X-REACTION (K)	Y-REACTION (K)	MOM-REACTION (K-FT)
120.00	-8.09E+01	.00E+00	.00E+00

II.D.--FORCES IN CONCENTRATED NONLINEAR SPRINGS

X-COORD (FT)	ANGLE (DEG)	DEFORMATION (FT)	FORCE (K)
2.00	-70.00	7.831E-02	3.948E+01
12.00	-70.00	5.022E-02	3.640E+01
22.00	-70.00	2.515E-02	3.781E+01
32.00	-70.00	1.806E-03	3.922E+01
42.00	-70.00	-2.314E-02	4.084E+01
51.00	-70.00	-4.736E-02	4.269E+01

PROGRAM CBEAMC - ANALYSIS OF BEAM-COLUMNS WITH NONLINEAR SUPPORTS
DATE: 0/ 0/ 0 TIME: 0: 0: 0

III.--COMPLETE RESULTS

III.A.--HEADING

'ANALYSIS OF GUARD WALL AT PANEL 178 AS A TIEBACK WALL, BASE @ EL.-37, (R
'SSI ANALYSIS OF CONSTRUCTION SEQUENCE, W 33 X 387, ** AS-CONSTRUCTED CON
'EXCAVATE TO EL. 20, PRIOR TO INSTALLATION OF TIE AT EL. 22, WATER AT TOP
'FILENAME = SQ6NE, NO PROOF LOAD, SOIL SPRINGS NOT "DOUBLED", WALL "EI" C

III.B.--DISPLACEMENTS AND INTERNAL FORCES

	<---------DISPLACEMENTS-------->			<--------INTERNAL FORCES------->		
X-COORD (FT)	AXIAL (FT)	LATERAL (FT)	ROTATION (RAD)	AXIAL (K)	SHEAR (K)	MOMENT (K-FT)
.00	3.584E-03	-8.820E-02	3.085E-03	.000E+00	.000E+00	.000E+00
2.00	3.584E-03	-8.203E-02	3.087E-03	.000E+00	7.551E+00	7.399E+00
2.00	3.584E-03	-8.203E-02	3.087E-03	-1.350E+01	-2.955E+01	7.399E+00
3.00	3.577E-03	-7.895E-02	3.084E-03	-1.350E+01	-2.545E+01	-2.012E+01
4.67	3.566E-03	-7.382E-02	3.061E-03	-1.350E+01	-1.862E+01	-5.691E+01
6.33	3.556E-03	-6.875E-02	3.019E-03	-1.350E+01	-1.136E+01	-8.195E+01
8.00	3.545E-03	-6.377E-02	2.966E-03	-1.350E+01	-3.735E+00	-9.457E+01
10.00	3.532E-03	-5.790E-02	2.898E-03	-1.350E+01	5.396E+00	-9.297E+01
12.00	3.519E-03	-5.217E-02	2.838E-03	-1.350E+01	1.480E+01	-7.281E+01
12.00	3.519E-03	-5.217E-02	2.838E-03	-2.595E+01	-1.941E+01	-7.281E+01
13.80	3.497E-03	-4.711E-02	2.782E-03	-2.595E+01	-1.082E+01	-1.000E+02
15.60	3.474E-03	-4.216E-02	2.713E-03	-2.595E+01	-2.206E+00	-1.117E+02
17.40	3.452E-03	-3.734E-02	2.642E-03	-2.595E+01	6.352E+00	-1.080E+02
19.20	3.429E-03	-3.264E-02	2.578E-03	-2.595E+01	1.478E+01	-8.896E+01
21.00	3.407E-03	-2.805E-02	2.531E-03	-2.595E+01	2.298E+01	-5.494E+01
22.00	3.395E-03	-2.553E-02	2.516E-03	-2.595E+01	2.745E+01	-2.971E+01
22.00	3.395E-03	-2.553E-02	2.516E-03	-3.889E+01	-8.076E+00	-2.971E+01
24.00	3.357E-03	-2.052E-02	2.491E-03	-3.889E+01	5.362E-01	-3.717E+01
26.00	3.320E-03	-1.556E-02	2.467E-03	-3.889E+01	8.616E+00	-2.792E+01
28.00	3.283E-03	-1.064E-02	2.455E-03	-3.889E+01	1.605E+01	-3.135E+00
30.00	3.246E-03	-5.723E-03	2.466E-03	-3.889E+01	2.272E+01	3.577E+01
32.00	3.208E-03	-7.538E-04	2.509E-03	-3.889E+01	2.838E+01	8.703E+01
32.00	3.208E-03	-7.538E-04	2.509E-03	-5.230E+01	-8.473E+00	8.703E+01
34.00	3.158E-03	4.323E-03	2.566E-03	-5.230E+01	-3.852E+00	7.489E+01

36.00	3.108E-03	9.507E-03	2.618E-03	-5.230E+01	-2.158E-01	7.089E+01
38.00	3.058E-03	1.479E-02	2.669E-03	-5.230E+01	3.543E+00	7.419E+01
40.00	3.008E-03	2.019E-02	2.725E-03	-5.230E+01	7.459E+00	8.516E+01
42.00	2.958E-03	2.570E-02	2.792E-03	-5.230E+01	1.153E+01	1.041E+02
42.00	2.958E-03	2.570E-02	2.792E-03	-6.627E+01	-2.684E+01	1.041E+02
43.80	2.901E-03	3.078E-02	2.844E-03	-6.627E+01	-2.304E+01	5.921E+01
45.60	2.844E-03	3.592E-02	2.869E-03	-6.627E+01	-1.912E+01	2.125E+01
47.40	2.787E-03	4.109E-02	2.873E-03	-6.627E+01	-1.506E+01	-9.525E+00
49.20	2.729E-03	4.625E-02	2.859E-03	-6.627E+01	-1.088E+01	-3.289E+01
51.00	2.672E-03	5.138E-02	2.832E-03	-6.627E+01	-6.567E+00	-4.860E+01
51.00	2.672E-03	5.138E-02	2.832E-03	-8.087E+01	-4.668E+01	-4.860E+01
52.83	2.601E-03	5.652E-02	2.773E-03	-8.087E+01	-4.216E+01	-1.301E+02
54.67	2.530E-03	6.152E-02	2.664E-03	-8.087E+01	-3.751E+01	-2.031E+02
56.50	2.459E-03	6.627E-02	2.510E-03	-8.087E+01	-3.272E+01	-2.675E+02
58.33	2.388E-03	7.070E-02	2.317E-03	-8.087E+01	-2.780E+01	-3.230E+02
60.17	2.317E-03	7.474E-02	2.091E-03	-8.087E+01	-2.275E+01	-3.694E+02
62.00	2.246E-03	7.835E-02	1.837E-03	-8.087E+01	-1.757E+01	-4.064E+02
63.92	2.172E-03	8.161E-02	1.549E-03	-8.087E+01	-1.253E+01	-4.352E+02
65.85	2.097E-03	8.429E-02	1.244E-03	-8.087E+01	-7.891E+00	-4.548E+02
67.77	2.023E-03	8.638E-02	9.284E-04	-8.087E+01	-3.671E+00	-4.659E+02
69.69	1.948E-03	8.786E-02	6.081E-04	-8.087E+01	1.213E-01	-4.692E+02
71.62	1.874E-03	8.872E-02	2.879E-04	-8.087E+01	3.485E+00	-4.657E+02
73.54	1.799E-03	8.897E-02	-2.781E-05	-8.087E+01	6.423E+00	-4.561E+02
75.46	1.725E-03	8.862E-02	-3.351E-04	-8.087E+01	8.950E+00	-4.412E+02
77.38	1.650E-03	8.769E-02	-6.306E-04	-8.087E+01	1.108E+01	-4.219E+02
79.31	1.576E-03	8.620E-02	-9.116E-04	-8.087E+01	1.285E+01	-3.988E+02
81.23	1.502E-03	8.419E-02	-1.176E-03	-8.087E+01	1.427E+01	-3.727E+02
83.15	1.427E-03	8.169E-02	-1.421E-03	-8.087E+01	1.539E+01	-3.441E+02
85.08	1.353E-03	7.874E-02	-1.646E-03	-8.087E+01	1.625E+01	-3.137E+02
87.00	1.278E-03	7.538E-02	-1.850E-03	-8.087E+01	1.688E+01	-2.818E+02
88.92	1.204E-03	7.165E-02	-2.031E-03	-8.087E+01	1.729E+01	-2.490E+02
90.83	1.130E-03	6.760E-02	-2.189E-03	-8.087E+01	1.757E+01	-2.156E+02
92.75	1.055E-03	6.327E-02	-2.325E-03	-8.087E+01	1.777E+01	-1.817E+02
94.67	9.811E-04	5.871E-02	-2.437E-03	-8.087E+01	1.793E+01	-1.475E+02
96.58	9.069E-04	5.395E-02	-2.526E-03	-8.087E+01	1.811E+01	-1.130E+02
98.50	8.327E-04	4.904E-02	-2.591E-03	-8.087E+01	1.836E+01	-7.802E+01
100.42	7.584E-04	4.403E-02	-2.632E-03	-8.087E+01	1.871E+01	-4.251E+01
102.33	6.842E-04	3.896E-02	-2.649E-03	-8.087E+01	1.922E+01	-6.185E+00
104.25	6.100E-04	3.389E-02	-2.641E-03	-8.087E+01	1.993E+01	3.131E+01
106.17	5.358E-04	2.886E-02	-2.606E-03	-8.087E+01	2.087E+01	7.037E+01
108.08	4.615E-04	2.392E-02	-2.544E-03	-8.087E+01	2.208E+01	1.115E+02
110.00	3.873E-04	1.912E-02	-2.453E-03	-8.087E+01	2.358E+01	1.552E+02
111.00	3.486E-04	1.670E-02	-2.394E-03	-8.087E+01	2.326E+01	1.788E+02
112.75	2.808E-04	1.262E-02	-2.270E-03	-8.087E+01	2.101E+01	2.174E+02
114.50	2.130E-04	8.768E-03	-2.124E-03	-8.087E+01	1.935E+01	2.527E+02
116.25	1.452E-04	5.195E-03	-1.956E-03	-8.087E+01	1.782E+01	2.850E+02
118.00	7.746E-05	1.932E-03	-1.769E-03	-8.087E+01	1.995E+01	3.174E+02
118.50	5.809E-05	1.062E-03	-1.713E-03	-8.087E+01	-1.274E+02	3.003E+02
120.00	.000E+00	-1.431E-03	-1.641E-03	-8.087E+01	.000E+00	.000E+00

III.C.--FORCES IN DISTRIBUTED NONLINEAR SPRINGS

	DISTRIBUTED SPRING FORCES	
X-COORD (FT)	AXIAL (K/FT)	LATERAL (K/FT)
.00	.000E+00	3.001E+00
2.00	.000E+00	3.457E+00
3.00	.000E+00	3.656E+00
4.67	.000E+00	3.946E+00
6.33	.000E+00	4.185E+00
8.00	.000E+00	4.376E+00
10.00	.000E+00	4.544E+00
12.00	.000E+00	4.647E+00
13.80	.000E+00	4.687E+00
15.60	.000E+00	4.678E+00
17.40	.000E+00	4.624E+00
19.20	.000E+00	4.527E+00
21.00	.000E+00	4.387E+00
22.00	.000E+00	4.290E+00
24.00	.000E+00	4.052E+00
26.00	.000E+00	3.758E+00
28.00	.000E+00	3.406E+00

30.00	.000E+00	2.993E+00
32.00	.000E+00	2.513E+00
34.00	.000E+00	1.956E+00
36.00	.000E+00	1.770E+00
38.00	.000E+00	1.849E+00
40.00	.000E+00	1.927E+00
42.00	.000E+00	2.006E+00
43.80	.000E+00	2.077E+00
45.60	.000E+00	2.148E+00
47.40	.000E+00	2.218E+00
49.20	.000E+00	2.289E+00
51.00	.000E+00	2.360E+00
52.83	.000E+00	2.432E+00
54.67	.000E+00	2.504E+00
56.50	.000E+00	2.576E+00
58.33	.000E+00	2.648E+00
60.17	.000E+00	2.721E+00
62.00	.000E+00	2.793E+00
62.00	.000E+00	2.652E+00
63.92	.000E+00	2.448E+00
65.85	.000E+00	2.234E+00
67.77	.000E+00	2.014E+00
69.69	.000E+00	1.790E+00
71.62	.000E+00	1.568E+00
73.54	.000E+00	1.350E+00
75.46	.000E+00	1.140E+00
77.38	.000E+00	9.410E-01
79.31	.000E+00	7.565E-01
81.23	.000E+00	5.889E-01
83.15	.000E+00	4.405E-01
85.08	.000E+00	3.135E-01
87.00	.000E+00	2.093E-01
88.92	.000E+00	1.295E-01
90.83	.000E+00	7.462E-02
92.75	.000E+00	4.505E-02
94.67	.000E+00	4.099E-02
96.58	.000E+00	6.219E-02
98.50	.000E+00	1.081E-01
100.42	.000E+00	1.776E-01
102.33	.000E+00	2.694E-01
104.25	.000E+00	3.817E-01
106.17	.000E+00	5.123E-01
108.08	.000E+00	6.583E-01
110.00	.000E+00	8.166E-01
111.00	.000E+00	-1.504E+00
112.75	.000E+00	-1.160E+00
114.50	.000E+00	-8.216E-01
116.25	.000E+00	-1.835E-01
118.00	.000E+00	2.493E+00
118.50	.000E+00	-4.660E+02
120.00	.000E+00	6.279E+02

Appendix D

Calculation of Corrected Composite Moment of Inertia

Directory of As-Built Models

Initially, the first runs of As-Built Models were:

SQ6NE

SQ6DE

SQ6TE

The above 3 models were each refined to identify a "correct" composite moment of intertia by a trial and error method and graph.

Model	Refined Models	Final Model
SQ6NE	N_1 TO N_7	N_7
SQ6DE	D_1 TO D_7	D_7
SQ6TE	T_1 TO T_3	T_3

The results are summarized below.

Sumarized Results:

Model	Correct Composite Moment of Inertia, I	Effective Moment of Inertia $I_{e(tr)}$	Moment in Steel Pile, M_s	Deflection, d
	(ft^4)	(ft^4)	(ft-k/ft)	(in)
SQ6NE	0.493	0.195	258.6	1.137
SQ6DE	0.561	0.264	174.4	0.695
SQ6TE	0.612	0.314	137.2	0.510

Determining the Correct Composite Moment of Interia, I:

From CBEAMC run of files N_1 through N_6, using an "assumed I" ($I_{assumed}$), determine a "calculated I" (I_{calc}) for each run based on the computer results. Plot $I_{assumed}$ and I_{calc}, Figure D.1. Estimate a correct composite moment of inertia, I, from the graph where the curves of $I_{assumed}$ and I_{calc} cross. This will be the correct composite moment of inertia, I, and will be verified in N_7.

To model N_1 through N_6, assume values for $I_{assumed}$ by assuming the effective moment of inertia of the concrete, $I_{e(tr)assumed}$ (the portion of the total moment resisted by the concrete's effective moment of inertia). Let $I_{e(tr)}$

range from 55.7% of $I_{assumed}$ (where $I_e = I_g$) to 20% of $I_{assumed}$ (where $I_e \approx I_{cr}$) in increments of approximately 7%. $I_s = 0.298$ ft^4.

given $I = I_s + I_{e(tr)}$

let $I_{assumed} = I_s + I_{e(tr)assumed} = I_s + \%I_{assumed}$

where $I_{e(tr)assumed} = \%I_{assumed}$

$\therefore \quad I_{assumed} - \%I_{assumed} = I_s$

or $I_{assumed} = I_s/(1-\%)$

and $I_{e(tr)assumed} = I_{assumed} - I_s$

Model	Assumed %I	Assumed I $I_{assumed} = I_s/(1-\%)$	Assumed $I_{e(tr)}$ $I_{e(tr)assumed} = I_{assumed}-I_s$
	%	(ft^4)	(ft^4)
N_1	55.7	$I=0.298/(1-0.557)=0.673$	$I_{e(tr)}=0.673 - 0.298=0.375$
N_2	48.0	0.573	0.275
N_3	41.0	0.505	0.207
N_4	34.0	0.452	0.154
N_5	27.0	0.408	0.110
N_6	20.0	0.373	0.075
		Calculated Results Based on Figure D.1	
N_7	39.6	0.493	0.195

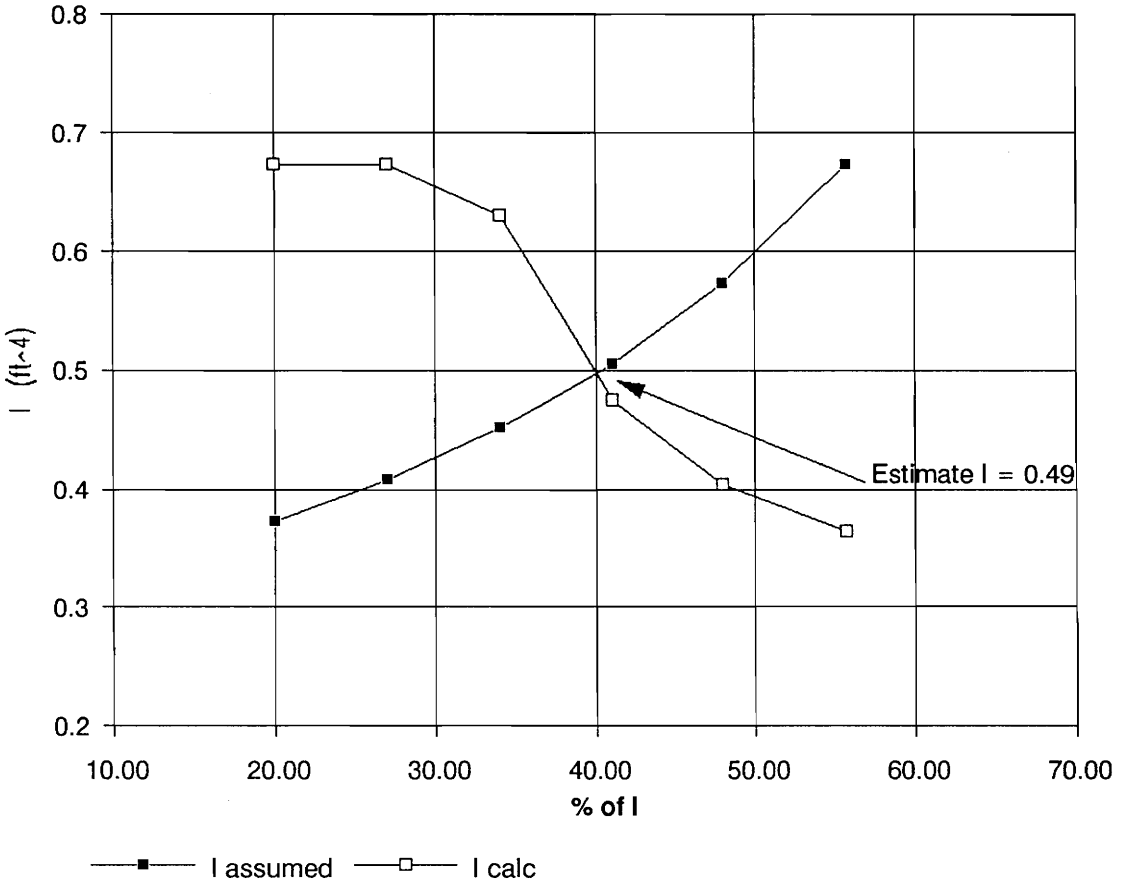

Figure D.1 Correct Composite Moment of Inertia, I.

Calculate I_{calc} Based on CBEAMC Results:

$$I_e = (M_{cr}/M_{conc})^3 I_g + [1 - (M_{cr}/M_{conc})^3] I_{cr}$$

From Appendix A:

M_{cr} = 135.5 ft-k, $I_g = 2.25\ ft^4$

$I_{cr} = 0.095\ ft^4$, n = 6

N_1: M_{max} = 469.2 ft-k @ $I_{assumed}$ = 0.673

M_{conc} = % M_{max} = 0.557 (469.2) = 261.3 ft-k

$M_s = M_{max} - M_{conc}$ 207.9 ft-k

$I_e = (135.5/261.3)^3\ 2.25 + [1-(135.5/261.3)^3]\ 0.095$

I_e = 0.397

$I_{e(tr)calc} = 0.397/6 = 0.066$

$I_{calc} = I_s + I_{e(tr)calc} = 0.298 + 0.066 = 0.364$

N_2: M_{max} = 448.6 ft-k @ $I_{assumed}$ = 0.573

$M_{conc} = 0.48\ (448.6) = 215.3$ ft-k

M_s = 233.3 ft-k

$I_e = (135.5/215.3)^3\ 2.25 + [1 - (135.5/215.3)^3]\ 0.095$

I_e = 0.633

$I_{e(tr)calc} = 0.633/6 = 0.106$

$I_{calc} = 0.298 + 0.106 = 0.404$

N_3: $M_{max} = 431.5$ ft-k @ $I_{assumed} = 0.505$

$M_{conc} = 0.41\ (431.5) = 176.9$ ft-k

$M_s = 254.6$ ft-k

$I_e = (135.5/176.9)^3\ 2.25 + [1-(135.5/176.9)^3]\ 0.095$

$I_e = 1.064$

$I_{e(tr)calc} = 1.064/6 = 0.177$

$I_{calc} = .0298 + 0.177 = 0.475$

N_4: $M_{max} = 415.9$ ft-k @ $I_{assumed} = 0.452$

$M_{conc} = 0.34\ (415.9) = 141.4$ ft-k

$M_s = 274.5$ ft-k

$I_e = (135.5/141.4)^3\ 2.25 + [1 - (135.5/141.4)^3]\ 0.095$

$I_e = 1.992$

$I_{e(tr)calc} = 1.992/6 = 0.332$

$I_{calc} = 0.298 + 0.332 = 0.630$

N_5: $M_{max} = 401.0$ ft-k @ $I_{assumed} = 0.408$

$M_{conc} = 0.27\,(401.0) = 108.3$ ft-k

$M_s = 292.7$ ft-k

$I_e = 135.5/108.3)^3\ 2.25 = [1 - (135.5/108.3)^3]\ 0.095$

$I_e = 4.31 > I_g = 2.25$

$\therefore$ use $I_e = I_g = 2.25$

$I_{e(tr)calc} = 2.25/6 = 0.375$

$I_{calc} = 0.298 + 0.375 = 0.673$

N_6: $M_{max} = 387.7$ ft-k @ $I_{assumed} = 0.373$

$M_{conc} = 0.20\,(387.7) = 77.54$ ft-k

$M_s = 310.16$ ft-k

$I_e = (135.5/77.54)^3\ 2.25 + [1 - (135.5/77.54)^3]\ 0.095$

$I_e = 11.59 \Rightarrow$ use 2.25

$I_e = I_g = 2.25$

$I_{e(tr)calc} = 2.25/6 = 0.375$

$I_{calc} = 0.298 + 0.375 = 0.673$

N_7: $M_{max} = 428.1$ ft-k, where from Figure D.1, estimate $I_{assumed} = 0.493$

$\therefore I_{e(tr)assumed} = 39.6\ \%$ of $I_{assumed}$

M_{conc} = 0.396 (428.1) = 169.5 ft-k

M_s = 258.6 ft-k

$I_e = (135.5/169.5)^3\ 2.25 + [1 - (135.5/169.5)^3]\ 0.095$

$I_e = 1.197 < I_g = 2.25$

$I_{e(tr)calc} = 1.197/6 = 0.199$

$I_{calc} = 0.298 + 0.199 = 0.497$

Check difference between I_{calc} and $I_{assumed}$:

$$100\ [(0.497/0.493) - 1] = 0.81\%\ \text{O.K.}$$

$\therefore$ I = 0.493, the Correct Composite Moment of Inertia

I_s = 0.298

$I_{e(tr)}$ = 0.195

M_{max} = 428.1 ft-k

M_{conc} = 169.5 ft-k

M_s = 258.6 ft-k

d_{max} = 1.137 in

Appendix E

Calculation of Moment Based on Measured Strains in Steel Pile

Example calculation of Stress, Axial Force, and Bending Moment in a steel pile based on measured strain:

Known: $I_s = 24{,}722\ in^4$

$A = 104.9\ in^2$

$y = 15.69$ in (to strain gage)

$c = 18.09$ in

Select 20 Sept 90 Data, @ El.+ 67.2:

Note: R.S. = River Side

S.S. = Soil Side

		R.S.	S.S.
Cumulative Strain:	$\epsilon =$	$67(10^{-6})$,	$-69(10^{6})$
Since $f_s = \epsilon E_s$,			
and $E_s = 29{,}000$ ksi,	$f_s =$	1.943 ksi,	-2.001 ksi

The total stress in the pile, f_s, can be represented by the equation:

$$f = f_s = P/A + My/I$$

The first term represents the axial stress in the pile and the second term represents the flexural stress in the pile.

Axial Stress: (from the measured stress in the pile)

$P/A = [1.943 + (-2.001)]/2 = -0.029$ ksi (compression)

Flexural Stress:

River Side:

$f_s = P/A + My/I$

$f_s = -0.029 + My/I = 1.943$ ksi

$\therefore My/I = 1.972$ ksi

$M = 1.972\ I/y$

$M = 1.972$ ksi)(24,722 in^4)]/15.69 in

$M = 3107$ in-k

$M = 258.9$ ft-k

Soil Side:

$f = -0.029 + My/I = -2.001$ ksi

$\therefore My/I = -1.972$ ksi

$M = -1.972\ I/y = -3{,}107$ in-k ✓

$M = -258.9$ ft-k ✓

Per foot basis (for comparison with CBEAMC results):

$M = -258.9$ ft-k/4 ft $= -64.7$ ft-k/ft

(Use soil side for sign convention of + = Tension, and - = Compression)

SEQ3: (to compare the same excavation stage model with results of 20 Sept 90 measured data)

Flexural Bending:

@ El.+67.2: M = -75.06 ft-k/ft

Axial Force:

$P/A = -0.029$ ksi @ $A = 104.9$ in^2

$P = -0.029\ (104.9) = -3.0$ k (compression)

Appendix F

Calculation of Wall Stiffnesses for Sensitivity Study

Calculate Wall Stiffnesses, EI's, for the Sensitivity Study:

(Assumes concrete not cracked)

b = 1.0 ft

h = 3.0 ft

$I = bh^3/12 = 1(3)^3/12 = 2.25\ ft^4/ft$

Concrete only:

@ f'c = 3000 psi

$I = I_g = 2.25\ ft^4/ft$

$E = E_c = 57{,}000(3{,}000)^{1/2}/1{,}000 = 3{,}122\ ksi$

E = 449,570 ksf

EI = 449,570 ksf (2.25 ft^4/ft)

EI = 1,011,534 $k\text{-}ft^2/ft$

use EI = 1,012,000 $k\text{-}ft^2/ft$

@f'c = 10,000 psi

$E = E_c = 57{,}000(10{,}000)^{1/2}/1{,}000 = 5{,}700\ ksi$

E = 820,000 ksf

EI = 820,800 ksf (2.25 ft^4/ft)

EI = 1,846,800 $k\text{-}ft^2/ft$

use EI = 1,847,000 $k\text{-}ft^2/ft$

With Steel Piles:

No Concrete:

$I = I_s = 0.298\ ft^4/ft$

$E = E_s = 29{,}000\ ksi = 4{,}176{,}000\ ksf$

$EI = 4{,}176{,}000\ ksf\ (0.0298\ ft^4/ft)$

$EI = 1{,}244{,}448\ k\text{-}ft^2/ft$

use $EI = 1{,}244{,}000\ k\text{-}ft^2/ft$

With Concrete @ f'c = 7,000 psi:

$I = I_s + I_{g(tr)} = 0.298 + 0.375 = 0.673$

$E = E_s = 29{,}000\ ksi = 4{,}176{,}000\ ksf$

$EI = 4{,}176{,}000\ ksf\ (0.673\ ft^4/ft)$

$EI = 2{,}789{,}568\ k\text{-}ft^2/ft$

Use $2{,}790{,}000\ k\text{-}ft^2/ft$

Consider the lower end size diaphragm wall for stiffness considerations: h = 2.5 ft

f'c = 3000 psi

$E_c = 449{,}570\ ksf$

Stiffness:

$I = bh^3/12 = 1(2.5)^3/12 = 1.3\ ft^4/ft$

$EI = 449{,}570\ ksf\ (1.3\ ft^4/ft) = 585{,}378\ k\text{-}ft^2/ft$

use EI = 585,000 k-ft^2/ft

Cracking Moment:

$M_{cr} = f_r I_g / y_t$ $\quad f_r = 7.5(3000)^{½} = 410.8$ psi

$I_g = 1.3$ ft^4 = 26,998.3 in^4

$y_t = 2.5$ ft/2 = 30 in/2 = 15 in

$M_{cr} = [(410.8)(26,998.3)]/15 = 739,378.1$ in-lb

$M_{cr} = 61.6$ k-ft

Per foot:

$M_{cr} = 15.4$ k-ft/ft

Wall Type	EI	% Increase in total wall stiffness
	(k-ft^2/ft)	(%)
2.5 ft concrete @f'c = 3,000	585,000	
		73.0
3.0 ft concrete @f'c = 3,000	1,012,000	
		22.9
Steel, no concrete	1,244,000	
		48.5
2.5 concrete @f'c = 10,000	1,847,000	
		51.1
Steel, with concrete	2,790,000	

Files for Concrete Runs:

Filename	f'c	ℓ_h	E	I	Thickness
	(psi)	(x 18 pci)	(ksf/ft)	(ft^4/ft)	(ft)
SQ6N3	3,000	1	449,570	2.25	3.0
SQ6D3	3,000	2	449,570	2.25	3.0
SQ6T3	3,000	3	449,570	2.25	3.0
SQ6N10	10,000	1	820,800	2.25	3.0
SQ6D10	10,000	2	820,800	2.25	3.0
SQ6T10	10,000	3	820,800	2.25	3.0
SQ6N32	3,000	1	449,570	1.30	2.5
SQ6D32	3,000	2	449,570	1.30	2.5
SQ6T32	3,000	3	449,570	1.30	2.5

Appendix G
Calculations Based on Beams on Elastic Foundation Theory

Sensitivity Study: timo1.xls

Beams on Elastic Foundations per Timoshenko

For Maximum Moments and Deflections, for Concentrated Loads :

y = Kd [PB/k]

M = Km[P/B]

where : B = [k/4EI]^.25

Kd & Km = Non-Dimensional Constants, assume equal to 1

			y = B / k	M = 1 / B
EI	k	B	y	M
1	1	0.71	0.71	1.41
1	2	0.84	0.42	1.19
1	3	0.93	0.31	1.07
2	1	0.59	0.59	1.68
2	2	0.71	0.35	1.41
2	3	0.78	0.26	1.28
3	1	0.54	0.54	1.86
3	2	0.64	0.32	1.57
3	3	0.71	0.24	1.41
4.77	1	0.48	0.48	2.09
4.77	2	0.57	0.28	1.76
4.77	3	0.63	0.21	1.59

EI and k values representative of stiffness values used in CBEAMC :

let k = Es = Km(X-Equiv.)/D see Appendix B

585000	218000	0.55	2.53E-06	1.81
585000	436000	0.66	1.51E-06	1.52
585000	654000	0.73	1.11E-06	1.38
2790000	218000	0.37	1.71E-06	2.67
2790000	436000	0.44	1.02E-06	2.25
2790000	654000	0.49	7.52E-07	2.03

% Change in deflection, y, and Moment, M with changes to Soil Stiffness, k, and Beam Stiffness, EI.

Concentreated Load :

Defl:	k = 1	2	3	Moments:	k = 1	2	3
EI =				EI =			
1	0.71	0.42	0.31	1	1.41	1.19	1.07
2	0.59	0.35	0.26	2	1.68	1.41	1.28
% =	-15.9	-15.9	-15.9	% =	18.9	18.9	18.9
3	0.54	0.32	0.24	3	1.86	1.57	1.41
% =	-24.0	-24.0	-24.0	% =	31.6	31.6	31.6
4.77	0.48	0.28	0.21	4.77	2.09	1.76	1.59
% =	-32.3	-32.3	-32.3	% =	47.8	47.8	47.8
585000	2.5E-06	1.50689E-06	1.11E-06	585000	1.81	1.52	1.38
2790000	1.7E-06	1.01969E-06	7.52E-07	2790000	2.67	2.25	2.03
% =	-32.3	-32.3	-32.3	% =	47.8	47.8	47.8

Defl:	k = 1	2	% =	Moments:	k = 2	1	% =
EI =				EI =			
1	0.71	0.42	-40.5	1	1.19	1.41	18.9
2	0.59	0.35	-40.5	2	1.41	1.68	18.9
% =	-15.9	-15.9		% =	18.9	18.9	

Defl:	k = 1	3	% =	Moments:	k = 3	1	% =
EI =				EI =			
1	0.71	0.31	-56.1	1	1.07	1.41	31.6
3	0.54	0.24	-56.1	3	1.41	1.86	31.6
% =	-24.0	-24.0		% =	31.6	31.6	

VITA

Jeffrey S. Sedey was born in Medford, Oregon on May 27, 1955. He attended public schools in Medford graduating in 1973. Jeff attended college for a year then chose to serve four years in the U.S. Coast Guard prior to returning to college. In 1979 he enrolled at Oregon State University where in June 1983, he received a Bachelor of Science degree in Civil Engineering. From 1983 to 1990, he worked for the U.S. Army Corps of Engineers, earning his registration as a Professional Engineer in 1987. In 1990, under sponsorship from the U.S. Army Corps of Engineers, he entered the graduate program in the Civil Engineering Department at Virginia Polytechnic Institute and State University in Blacksburg, Virginia.